

Learning Clique Forests

Guido Previde Massara

GUIDO.MASSARA.12@UCL.AC.UK

Tomaso Aste

T.ASTE@UCL.AC.UK

Department of Computer Science

University College London

Gower Street, London, WC1E 6B

UCL Centre for Blockchain Technologies, UCL, London, UK.

Systemic Risk Centre, London School of Economics, London UK.

Editor: TBD

Abstract

We propose a new algorithm for learning complex networks from data, named Maximally Filtered Clique Forest (MFCF). The MFCF is a preferential attachment scheme where new nodes are added to a growing forest of cliques by means of a *clique expansion operator*. The clique expansion operator is topologically invariant and always transforms clique forests into clique forests. Nodes are added recursively and the selection of the next node and of the attachment points is driven by the increase in a given score (gain function). We show that the clique forests produced by the MFCF are chordal. This makes an associated graphical model decomposable and it makes it easy to construct an associated sparse inverse covariance matrix. The clique expansion operator can be customized so as to control the size of the cliques and the multiplicity of their separators. The algorithm is general, and can be constructed with gain functions suited to diverse applications. In this paper we provide examples for the problem of covariance selection for Gaussian graphical models and compare the results obtained by the MFCF with the Graphical Lasso.

Keywords: Clique forest, topological learning, structure learning, TMFG, LoGo, chordal graphs, DAG, Topological Data Analysis, network sparsification, Markov Random Fields,

1. Introduction

In this paper we introduce a novel algorithm, the Maximally Filtered Clique Forest (MFCF) which produces *clique forests* representative of the structure of input data sets. Clique forests are acyclic graphs that span the set of the cliques of a base graph. The nodes of a clique forest are the maximal complete subsets of the graph (the cliques) and the edge, which we will call *separator*, joining two cliques is made of the elements in the intersection of the two cliques¹.

The clique forest, as a data structure, enjoys a number of useful properties.

1. There is a further technical requirement, the *clique intersection property* that will be described in section 2.2

1. The graph underlying a clique forest is a *chordal*, or *triangulated* graph². Chordal graphs are a particular case of *perfect graphs* (Golumbic, 2004), for which there are known polynomial time solutions for many problems that are much harder for general graphs such as graph coloring, maximum clique, maximum independent set (Grötschel et al., 2012; Vandenberghe et al., 2015).
2. The structure of the cliques and separators is such that the clique forest is also an example of an *abstract simplicial complex* (Munkres, 2018). We believe this fact (although not exploited in the current paper) might add the tools of Topological Data Analysis (Wasserman, 2018) to the analysis of networks modelled as clique forests.
3. The maximum clique size allowed in the forest is in direct correspondence with the *treewidth* of the graph and the treewidth is linked to the computational complexity of the most common inference tasks (Bach and Jordan, 2001). Limiting the treewidth (or equivalently the maximum size of a clique in the forest) is both a way to limit the complexity of inference and the number of parameters associated to a graphical model, see Bach and Jordan (2001). Decomposable models associated with clique forests are particularly suitable for inference (Koller and Friedman, 2009, Chap. 10), since in this case inference can be carried out exactly and efficiently using variable elimination, belief propagation and the junction-tree algorithm (Shafer and Shenoy, 1990; Koller and Friedman, 2009). In the case of clique forests, the complexity of inference is defined by the size of the maximal cliques in the model, hence the interest in producing “thin junction trees” (Bach and Jordan, 2001; Chechetka and Guestrin, 2008), that are graphs where the maximal size of the cliques is small. Conversely, if the underlying graph is not a junction forest, exact inference is infeasible since it is NP-hard (see Chandrasekaran et al. (2012)) and has to be carried out using a number of approximate inference procedures based on sampling (e.g. Gibbs, Markov Chain Monte Carlo, importance sampling) or on deterministic approximate inference (variational approximation, loopy belief propagation, expectation propagation, see Wainwright and Jordan (2008); Koller and Friedman (2009); Barber (2012)).

When the problem is to infer the *sparse* dependency structure of the dataset, the MFCF clique-forest structure yields to a *decomposable* Markov random field (MRF). MRFs are (Lauritzen, 1996; Drton and Maathuis, 2017; Scutari and Strimmer, 2011) multivariate probability distributions associated with an undirected graph $G(V, E)$ (and are therefore also called undirected graphical models, UGM). The vertices $v \in V$ are in a one to one relationship with a collection of random variables $X_v, v \in V$; the edges in E join the conditionally dependent random variables. In MRFs the absence of an edge between two variables represents conditional independence. Structure learning is the process of inferring from the data the pattern of missing edges.

The problem of finding the dependency structure that allows to carry out inference in a system of variables is, in general, NP-complete (Karger and Srebro, 2001; Bogdanov et al., 2008; Chickering, 1996; Chickering et al., 1994), and some simplifying assumptions are required in practice.

2. See, for instance, the excellent reference Blair and Peyton (1992, Theorem 3.1) for a proof. Note that the authors refer to *clique trees*, rather than clique forests, with the understanding that all the arguments and demonstration can be repeated separately for all of the connected components of a clique forest.

When a clique forest is the underlying graph of a graphical model (Lauritzen, 1996) the cliques represent a completely interdependent set of random variables, and the separator is the conditioning set that mediates the interaction between two cliques. The graphical model is *decomposable* and has many desirable properties: the maximum likelihood estimators of the parameters are known in closed form for a number of probability distributions (Lauritzen, 1996); the calculation of the probability density can be expressed in closed form without the need to perform a demanding calculation of the partition function; and, finally, the clique forest readily supports the application of the *junction tree* algorithm (see, for instance, Koller and Friedman (2009)). As it is common in many types of probabilistic graphical models (Koller and Friedman, 2009) we make the assumption that the global dependence structure is *sparse* and therefore the number of edges in the graph G is small with respect to the total possible number of edges, $|E| \sim \mathcal{O}(|V|) \ll \frac{1}{2}|V|(|V| - 1)$. The presence of noise and the low number of samples makes it difficult to establish whether a conditional dependency between two variables is significant, and therefore it should be represented with an edge in the MRF, or whether it is due to spurious effects, in which case the associated edge should not be present in the MRF. Structure learning in the context of this paper is the problem of identifying and estimating significant structural links while filtering spurious interactions. There are many upsides to the use of sparse graphical models (Hastie et al., 2015):

1. from the end user point of view they display meaningful relationships and provide interpretable predictive models;
2. from a computational point of view they require less storage and computing resources than the dense counterparts and are tractable for exact inference or sampling;
3. If the dependency network is sparse, then the cliques in the network are of small sizes with respect to the total number of variables and such a joint probability distribution can be calibrated from data even when the number of samples is much lower than the number of variables overcoming the “curse of dimensionality” issue (Lauritzen, 1996; Barfuss et al., 2016; Gross et al., 2018).
4. finally, from a modelling point of view there is the consideration that goes under the name of “bet on sparsity” (Hastie et al., 2015, p. 2): “Use a procedure that does well in sparse problems, since no procedure does well in dense problems”. In other words, when the number of samples is low compared to the number of parameters and the problem is not sparse, no estimation of a large number of parameters is feasible (see also Barfuss et al. (2016)).

In this paper we provide examples for decomposable Gaussian graphical models constructed on MFCE addressing the problem of covariance selection and we compare the results with the L_1 -norm regularization via Graphical Lasso. The same machinery introduced for Gaussian graphical models can be directly used for the more general covariance selection problem. Indeed, MFCE can be used as L_0 -seminorm regularization tools which generate sparse inverse covariances with direct application to modeling with the whole multivariate elliptical family distribution (Aste, 2020). We chose the problem of covariance selection, and specifically a comparison with the Glasso, because of the combination of extensive and successful practical use, exhaustive literature and availability of reliable software implementations; therefore the comparison between Glasso and MFCE can benefit from the many different contexts, papers, and software.

1.1 Contributions

Structure learning has been studied extensively, however, to the best of our knowledge, the emphasis has been so far on testing pairwise relationships represented by a single edge, rather than on the detection of higher order topological structures³. In this paper we propose a methodology we name *Maximally Filtered Clique Forest* (MFCF) that exploits the equivalence between decomposable graphs and clique forests (see Lauritzen (1996, Par. 2.2.3) and Koller and Friedman (2009, Th. 4.12)) and models the clique forest directly, rather than the underlying collection of edges.

The MFCF works by recursively adding vertices to the cliques of a clique forest using a local topological move, *clique expansion*, that involves a clique and a vertex (see Section 3.1); at each step the algorithm adds the vertex whose addition maximises the gain of a given score function. The vertex can be added to the clique, effectively extending it, or can be added to a subset of the clique, creating two cliques separated by the subset; consistently with the terminology of graphical models, we call such a subset the *separator*. The algorithm is generic, in the sense that it does not rely on a specific score function but it assumes that there is a function that takes in input a clique and a vertex and returns a gain in score and the resulting separator, but, in principle, it can take into account the existing graph structure (the assumption of chordality for the underlying graph is extremely helpful in controlling the dependency structure). In this paper we provide some examples related to graphical models and covariance selection problem and we specify what requirements must be fulfilled by a score function to fit into the MFCF algorithm. The MFCF has broad applicability beyond graphical modeling as a general methodology to construct clique forests.

1.2 Organisation

The structure of this paper is as follows: in Section 2 we briefly review some essential background literature and introduce notations and definitions. In Section 3 we describe the clique expansion operator, the ideas underlying the gain function and the MFCF algorithm. In Section 4 we describe a specific application to covariance selection models and compare the results against alternative methods. Section 5 provides discussion and conclusions. We provide a vast Appendix (Section 7) containing some additional theorems that are useful, if not strictly required for the problem at hand, as well as a detailed description of the experiments performed and some extra results.

2. Background literature, notations and definitions

2.1 Information filtering with networks: a brief review

Let us briefly review four approaches to associate, from data, a meaningful network structure to a multivariate system of random variables. Specifically here we briefly introduce five important topics: (1) structure learning algorithms for graphical models; (2) sparse graphical models and covariance selection; (3) information filtering networks; (4) the Triangulated Maximally Filtered Graph algorithm, which the present paper generalises; (5) other miscellaneous approaches.

3. Some exceptions are based on frequent itemsets (Huang et al., 2002) and t-cherry trees (Szántai and Kovács, 2013).

2.1.1 STRUCTURE LEARNING IN GRAPHICAL MODELS

General approaches to structure learning in Graphical Models can be classified into three main categories (Zhou, 2011; Lauritzen, 2012; Scutari and Strimmer, 2011; Koller and Friedman, 2009): *score based*, *constraint based*, and *Bayesian methods*. Let us here briefly introduce and comment them one by one.

Score based algorithms perform structure learning by detecting edges or other structures that optimize some global function such as likelihood, Kullback-Leibler divergence (Kullback and Leibler, 1951), Bayesian Information Criterion (BIC) (Schwarz et al., 1978), Minimum Description Length (Rissanen, 1978) or the likelihood ratio test statistics (Petitjean et al., 2013). In general, the identification of the structure that optimises the score function results in a difficult combinatorial optimization problem (Koller and Friedman, 2009, Ch. 20) and some sort of greedy approach should be implemented to produce a sequence of steps that optimize a limited space of solutions.

One of the leading methods in the score based sparse representation of joint probability distributions is the *Chow-Liu* trees (CLT). In the original paper, Chow and Liu (1968) proposed a mechanism where a p -order discrete distribution is approximated by the product of a number of second-order distributions. The second order distributions are specified by using the minimum spanning tree algorithm (MST) by maximizing the total mutual information of the $p - 1$ edges. For the MST this maximization coincides with the maximum-likelihood estimation for a tree inference structure. Ku and Kullback (1969) extended the CLT for discrete probability distributions by allowing the use of marginal probabilities of order greater than two. They used the Kullback-Leibler divergence as a scoring function. To control the complexity of the resulting model they did not use full marginal distributions, but the marginals of small sets of variables (that is probabilities defined on small cliques of variables). Huang et al. (2002) built a Chow-Liu Tree and successively refined it by adding frequent-itemset in large vertices (Large vertex Chow-Liu Tree – LNCLT), which are set of vertices that occur frequently together. The statistical learning theory of Chow-Liu trees is presented in detail in Koski (2010).

When the goal is to learn a decomposable model, the score based algorithms need to fulfil the additional chordality constraint: in this area there are a number of methods that efficiently explore the graphical structure (directed, in the case of Bayesian networks, or undirected in the case of log-linear or multivariate Gaussian models) with the help of suitable graph algorithms based on the manipulation of data structures representing junction trees or clique graphs (Giudici and Green, 1999; Deshpande et al., 2001; Petitjean et al., 2013). Kovács and Szántai (2013) describe a “pruning” approach for multivariate discrete distributions which removes links iteratively refining a junction-tree, optimising the total correlation (“information content”). Szántai and Kovács (2013) developed an algorithm specialised for a particular clique tree (the “t-cherry” junction tree) and used it to approximate a multivariate discrete distribution. To the best of our knowledge all structure learning methods⁴ for decomposable models deal with the chordality constraint on an edge-by-edge basis and, differently from the proposed MFCE approach, do not model the clique forest as an aggregation of cliques.

Constraint based algorithms often start from a complete model and adopt a *backward selection* approach by testing the independence of vertices conditioned on subsets of the remaining vertices (e.g. in the Spirtes-Glymour-Scheines (SGS) and Peter-Clark (PC)

4. With the exception of Szántai and Kovács (2013).

(Spirtes et al., 2000; Zhou, 2011) algorithms) and removing edges associated to vertices that are conditionally independent. Conversely *forward selection* algorithms start from a sparse model and add edges associated to vertices that are discovered to be conditionally dependent. An hybrid model is the Grow-Shrinkage (GS) algorithm where a number of candidate edges is added to the model (the “grow” step) in a forward selection phase and subsequently reduced using a backward selection step (the “shrinkage” step) (Margaritis and Thrun, 2000; Zhou, 2011). The complexity of checking a large number of conditional independence statements makes these methods unsuitable for graphs with a large number of vertices. Furthermore, aside from the complexity of measuring conditional independence, these methods do not generally optimize a global function, such as likelihood or the Akaike Information Criterion (Akaike, 1974, 1998), but they rather try to exhaustively test all the conditional independence properties of a set of data and therefore are difficult to use in a probabilistic framework.

Bayesian methods consider the presence or absence of an edge in the inference network structure as a random variable. More precisely (Madigan et al., 1995; Eaton and Murphy, 2012; Scutari et al., 2013) the likelihood of a model result from the product of a discrete probability distribution over the space of all graphs ($P(G)$) and a continuous distribution of the random variables conditional on the graph structure $P(X, G) = P(X|G)P(G)$. Applying Bayes rule, the posterior probability of a graph can be taken as $P(G|X) \propto P(X|G)P(G)$. Therefore, if the probability on all graphs is the same optimising the probability of the graph is equivalent to optimising the marginal likelihood $P(X|G)$ (see for instance Madigan et al. (1995); Eaton and Murphy (2012) and references therein). Usually the probability over the graph structure is indeed taken as uniform, meaning that each graph is equally probable. Conversely, in the present perspective, the MFCCF approach introduces a non-uniform prior which is recursively updated after every clique expansion.

2.1.2 SPARSE GRAPHICAL GAUSSIAN MODELS

When the variables X_v follow a multivariate Gaussian distribution the conditional independence of two variables X_a and X_b is directly reflected in the inverse of the covariance matrix (or *precision matrix*) J : $X_a \perp\!\!\!\perp X_b \mid (X_r, r \in V \setminus \{a, b\}) \iff J_{ab} = 0$. The pattern of missing edges corresponds to conditionally independent variables and it is exactly the same as the zero elements in the precision matrix. The problem of estimating a precision matrix is called “Covariance selection” (Dempster, 1972) and the associated graphical models are called Gaussian Graphical Models (GGM) or Gaussian Markov Random Fields (GMRF). In the field of GMRFs there are several approaches (d’Aspremont et al., 2008; Banerjee et al., 2008b, 2006) that exploit the link between edges and zero-elements of the precision matrix: the general idea is to maximise the likelihood of the multivariate normal distribution (which can be expressed in terms of the sparse inverse covariance matrix) penalised by a non-decreasing function of the number and weight of the non-zero elements in the precision matrix. Specifically, ridge regression uses a ℓ_2 -norm penalty; instead the *lasso* method (Tibshirani, 1996) uses an ℓ_1 -norm penalty and the elastic-net approach uses a convex combination of ℓ_2 and ℓ_1 penalties (Zou and Hastie, 2005). These approaches are among the best performing regularization methodologies presently available. The ℓ_1 -norm penalty term favours solutions with parameters with zero value leading to models with sparse inverse covariances. Sparsity is controlled by regularization parameters $\lambda_{ij} > 0$; the larger the value of the parameters the more sparse

the solution becomes. This approach is extremely popular and around the original idea a large body of literature has been published with several novel algorithmic techniques that are continuously advancing this method (Tibshirani, 1996; Meinshausen and Bühlmann, 2006; Banerjee et al., 2008a; Ravikumar et al., 2011; Hsieh et al., 2011; Oztoprak et al., 2012) among these the popular implementation *Glasso* (Graphical-lasso) (Friedman et al., 2008) which uses lasso to compute sparse graphical models. However, Glasso methods are computationally intensive and the selection of the penalisation parameter is often difficult to justify as it does not have an immediate link to the data. Within this framework, the MFCCF approach introduced in this paper is a L_0 -seminorm regularization. Compared to Glasso it is computationally more efficient and it has the advantage of returning the maximum likelihood solution of the sparse problem instead of a shrunken solution (Aste, 2020).

2.1.3 INFORMATION FILTERING NETWORKS

With Information Filtering Networks we refer to a set of network-based approaches aimed at extracting information about the dependency structure from correlation (or, more broadly, similarity) matrices by retaining a sparse network from the most relevant correlations only. This methodology originated in the Econophysics community where the interest in modelling dependence stems from studies on the spectral properties of the correlation matrix of financial portfolios (Laloux et al., 1999), focusing on cleaning methodologies inspired by Random Matrix Theory (RMT) (Bun et al., 2017). An alternative approach has been to use tools from topology to investigate the structure of financial markets. One seminal idea (Mantegna, 1999) was to use the Minimum Spanning Tree algorithm to build a hierarchical tree structure that retains the largest correlations. In further developments other topological constraints have been investigated, notably imposing the planarity of the filtered network (Tumminello et al., 2005) and studying hyperbolic embeddings (Aste et al., 2005; Tumminello et al., 2007). These methodologies have enabled the study of several properties of financial portfolios with applications to portfolio diversification (Pozzi et al., 2013; Musmeci et al., 2015b), clustering (Musmeci et al., 2015a; Song et al., 2012) and dynamics of correlation structure in markets (Aste et al., 2010).

2.1.4 TRIANGULATED MAXIMALLY FILTERED GRAPHS

In Massara et al. (2016) we proposed a greedy algorithm that builds a Triangulated Maximally Filtered Graph by recursively adding vertices to a k -width tree while minimising a given score function (which in a particular probabilistic application is the Kullback-Leibler divergence). In Barfuss et al. (2016) this general algorithm was applied to the approximation of multivariate normal distributions by using the multivariate normal Kullback-Leibler divergence as a scoring function; in the same paper some basic results on Gaussian Markov random fields are used to provide applications to financial portfolio modelling. The TMFG produces planar and chordal networks by restricting the size of the cliques and clique-intersections and by constraining the topology of the clique tree. Christensen et al. (2018b) carry out a comparison of Glasso and information filtering networks based on TMFG from the point of view of psychometric networks showing that TMFG have better interpretability. The work in the present paper is a radical generalisation of the TMFG algorithm where the size of the clique is no longer a constraint but an adjustable parameter that can be tuned to the data, and the size and use of separators is driven by the gain in a score function.

2.1.5 OTHER APPROACHES

Of course, there are many more approaches to the problem of structure learning, and we can only hope to hint at a few alternative methods that present less similarities with ours. One reasearch direction is towards spectral sparsification using the concept of *effective resistance* (Batson et al., 2013; Spielman and Srivastava, 2011). Other approaches are formulated, and make extensive use of, numeric tensor analysis to produce reduces-rank representation of large data represented as tensors (Cichocki, 2018, 2014; Cichocki et al., 2015; Kolda and Bader, 2009). Finally, many methods in topological data analysis aim at producing a simplified view of clouds of data points where the persistent topological features represent a version of the data where the noise has been removed (Wang and Wei, 2016; Edelsbrunner et al., 2000; Edelsbrunner and Harer, 2008; Wasserman, 2018; Guskov and Wood, 2001).

2.2 Notation and Definitions

In this section we provide the minimum amount of notation and results required by the paper, Lauritzen (1996, Chap. 2) provides the full notation and proofs.

2.2.1 GRAPHS AND CHORDAL GRAPHS

A Markov random field is a collection $X_i, i \in \{1, \dots, p\}$ of random variables together with an undirected graph $G = G(V, E)$ with a vertex set V and a edge set E . We call *vertices* the elements of V and *edges* the elements of E . The variables X_i are in a one-to-one correspondence with the vertices V so that $|V| = p$. E is a collection of unordered pairs of elements of V , e.g. $e \in E \Rightarrow e = \{a, b\}$ with $a \in V, b \in V$. A graph is chordal when every cycle of length ≥ 4 has a “chord”, that is an edge between two non-adjacent vertices in the cycle. Graphical models whose underlying graph is chordal are *decomposable models* (Lauritzen, 1996, chap. 2).

We use the notation $\mathbf{X} = \{X_1, \dots, X_p\}$ to indicate the multivariate random variable. When we examine the realisations of the variables X_i , we will use the hat symbol on top of the variable (e.g. $\hat{\mathbf{X}}$) and will use n to refer to the total number of realisations, so that: $\hat{X}_i^t, i \in \{1, \dots, p\}, t \in \{1, \dots, n\}$ is the t -th realisation of the i -th variable, and $\hat{\mathbf{X}}^t = \{\hat{X}_1^t, \dots, \hat{X}_p^t\}$. For a given subset $C \subset \{1, \dots, p\}$ we use the shorthand notation $\hat{\mathbf{X}}_C = \{\hat{X}_i, i \in C\}$.

2.2.2 CLIQUE FOREST

A *clique* is a maximal complete subset of vertices, that is, where any pair of vertices is joined by an edge, and it is not included in a larger complete set. We indicate with \mathcal{C}_G (or \mathcal{C} when there is no ambiguity) the set of cliques of G .

Similarly we introduce the separator set, \mathcal{S} , made of intersections of the elements of \mathcal{C} . For two cliques C_a and C_b the separator is $S_{ab} = C_a \cap C_b$. Given a graph $G(V, E)$ with set of cliques $\mathcal{C} = \{C_1, C_2, \dots, C_m\}$ of G , we say that there is separator between C_i and C_j if $C_i \cap C_j$ is not empty and we denote the set of separators with $\mathcal{S} = \{S_1, S_2, \dots, S_k\}$. The graph $\mathcal{K}(\mathcal{C}, \mathcal{S})$ where the vertices are the cliques of G and the edges are the not-empty intersections of the cliques is called the *clique graph or intersection graph* of $G(V, E)$.

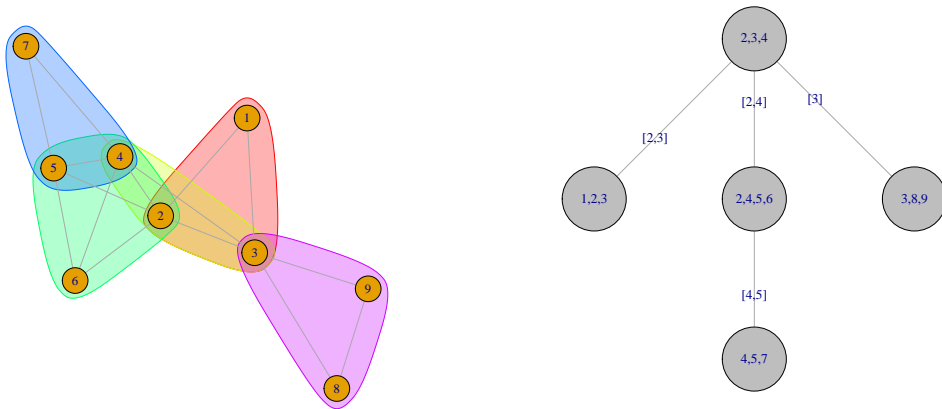
Definition 1 (Clique intersection property and clique forest) *A clique forest for $G(V, E)$ is a clique graph with no cycles that includes all the cliques of G and that additionally fulfils the clique-intersection property (CIP)(Blair and Peyton, 1992):*

For any two cliques $C_i, C_j \in \mathcal{C}$ the set $C_i \cap C_j$ is contained in every clique on the path between C_i and C_j in the tree. We will denote a clique forest with $\mathcal{F}(\mathcal{C}, \mathcal{S})$.

When a graph $G = G(V, E)$ has a clique forest we say that the graph has the CF-property.

Example 1 (Clique forest) Figure 1 shows an example of a chordal graph with its associated representation as a clique forest. (A single clique tree in this case.)

Example 2 (The four-cycle does not have the CF-property) The four cycle graph, shown in Figure 2 is a negative example. Any tree spanning the nodes of the clique graph does not enjoy the running intersection property. The picture should provide an intuitive appreciation of the definition of a clique forest; there should be no “holes” in the graph whose boundary is made of cliques.



(a) A chordal graph with the maximal cliques highlighted.

(b) The same graph represented as a clique tree. The edges of the tree are labelled with the elements of the intersection.

Figure 1: Illustration of the relationship between a chordal graph and the associated clique forest.

Definition 2 (CF-property, CF-invariance) We will say that a graph that has a clique forest enjoys the CF-property. We will also say that any transformation of a graph that conserves the CF-property is CF-invariant

The following theorem 3 establishes the equivalence between chordality and CF-property for a graph. We will not make use of this theorem directly as we will provide direct demonstrations of the CF-property (see Corollary 10) and of the chordality for the networks produced by the MFCF (see Theorem 16).

Theorem 3 A graph G has a clique forest $\mathcal{T}(\mathcal{C}, \mathcal{S})$ if and only if G is chordal.

Proof See Blair and Peyton (1992, Th. 3.1) or Koller and Friedman (2009, Th. 4.3) for a proof. ■

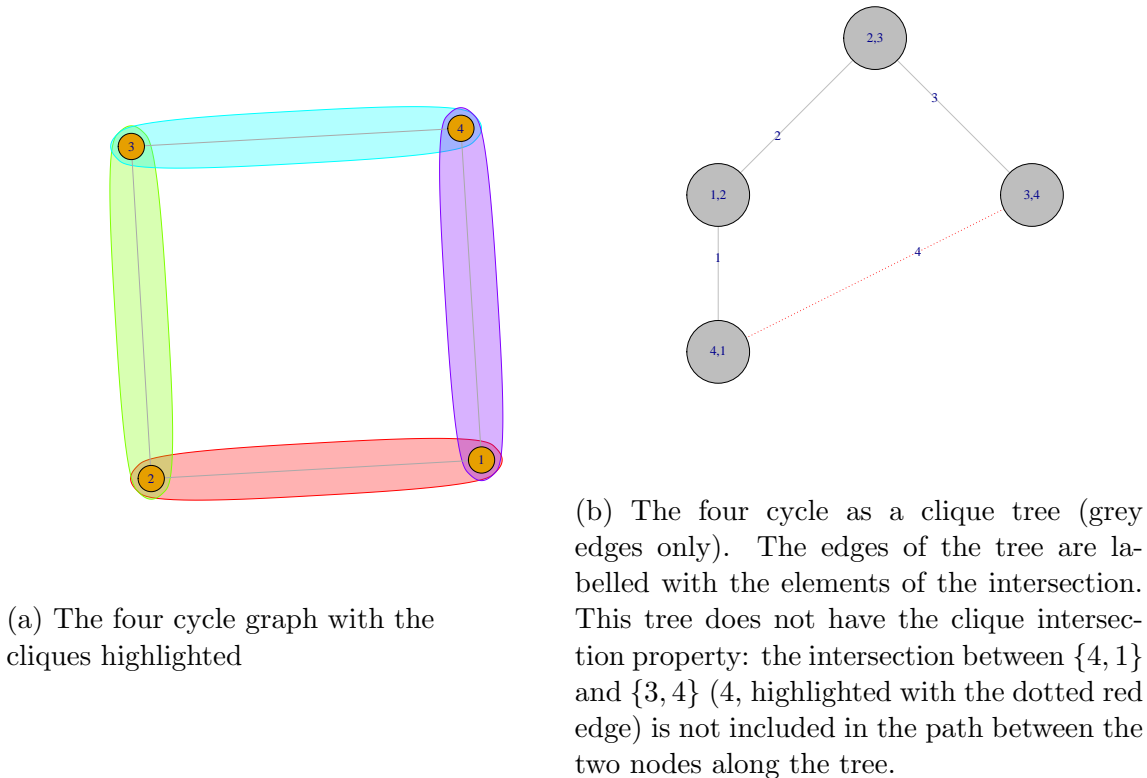


Figure 2: The four cycle graph is the simplest graph that does not have a clique forest.

2.2.3 DECOMPOSABLE GRAPHICAL MODELS

Definition 4 Let $A \subset V$, $B \subset V$, $C \subset V$ be three subsets of vertices of a graph G . We say that the triple (A, B, C) decomposes $G(V, E)$ if $V = A \cup B \cup C$ and the following conditions hold: C separates A and B ; C is a complete graph.

Let us assume that (A, B, C) decomposes $G(V, E)$. We associate the random variables $\mathbf{X}_A = \mathbf{X}_{v \in A}$, $\mathbf{X}_B = \mathbf{X}_{v \in B}$, $\mathbf{X}_C = \mathbf{X}_{v \in C}$ if \mathbf{X}_A and \mathbf{X}_B are independent given \mathbf{X}_C :

$$\mathbf{X}_A \perp\!\!\!\perp \mathbf{X}_B | \mathbf{X}_C \tag{1}$$

we state that the joint distribution of the variables $\mathbf{X}_{v \in V}$ has the *Global Markov Property*

In this case, where $C = A \cap B$, (as depicted in Figure 10 in the Appendix) the joint probability distribution can be shown (Lauritzen, 1996, Prop. 3.17) to follow a generalisation of Bayes' rule⁵:

$$P(\mathbf{X}_A, \mathbf{X}_B) = \frac{P(\mathbf{X}_A)P(\mathbf{X}_B)}{P(\mathbf{X}_{A \cap B})} \tag{2}$$

Equation 2 and Figure 10 are equivalent to a tree decomposition of the set V where the tree has two vertices A and B joined by the edge $C = A \cap B$.

In case A and B are in turn decomposable (or fully connected cliques) it can be shown (Lauritzen, 1996, Chap. 3) that the joint probability distribution can be further

5. Provided that the probability measure is positive in the product space.

recursively factored into finer decomposable components until we get to the clique set (\mathcal{C}) and separator set (\mathcal{S}) of G :

$$P(\mathbf{X}) = \frac{\prod_{c \in \mathcal{C}} P(\mathbf{X}_c)}{\prod_{s \in \mathcal{S}} P(\mathbf{X}_s)} \quad (3)$$

Remark 5 *Note that in case two sets of variables are disjoint (unconditionally independent) the corresponding separator is the empty set and the tree structure is a forest.*

Remark 6 *It is possible that a separator appears more than once in a clique forest, for example when it separates more than two cliques. In such a case in our notation the separator set reports the separator more than once, so that the separator multiplicity is automatically taken into account.*

3. Methodology

3.1 Generation of Clique Forests: the clique expansion operator

In this section we describe the tool for building clique forests that is originally introduced with this paper.

The *clique expansion* procedure takes as input a clique C_a and an isolated vertex v and produces a new clique C_b and a separator S . In general, $S \subseteq C_a$ contains the vertices that produce the largest gain when combined with v and the new clique is $C_b = S \cup v$.

Figure 3 describes the *clique expansion* operation. The inputs of the operation are: the clique $C_1 = \{1, 2, 3, 4\}$ and the isolated vertex $\{5\}$. Figure 3b shows the output of the clique expansion in the general case: two cliques C_1 and $C_2 = \{1, 2, 5\}$ and the separator $S = C_1 \cap C_2 = \{1, 2\}$. There are two special cases.

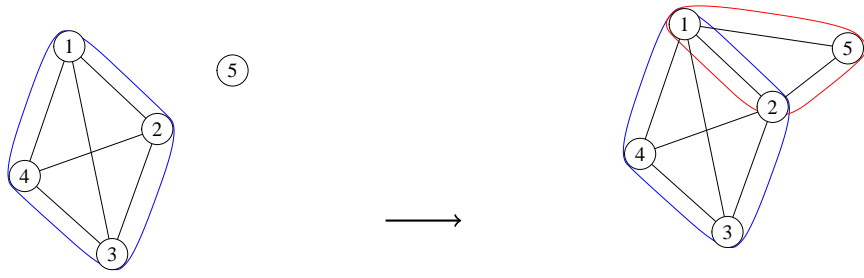
1. If none of the elements of C_a have a strong relationship with v , then vertex v is not attached and $C_b = \{v\}$ and $S = \emptyset$ (see Figure 3d).
2. If all the elements in C_a have a strong relationship with the isolated vertex then C_a is extended with v ($C_a \leftarrow C_a \cup v$) and both the separator S and the new clique C_b are empty (see Figure 3f).

We note that S , being a subset of a complete graph, is complete, and also that it separates $C_1 \setminus S$ and $C_2 \setminus S$.

Theorem 7 (CF-invariance of the clique expansion operator) *The clique expansion operator is CF-invariant.*

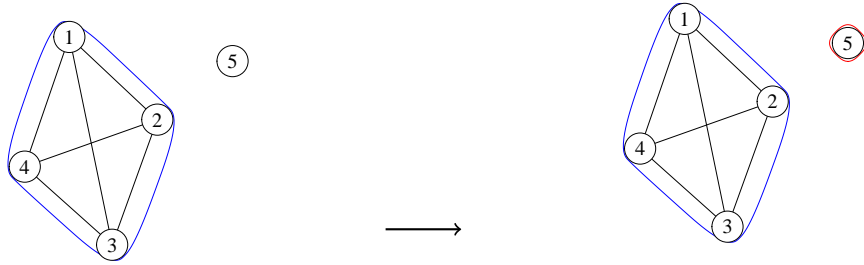
Proof Let \mathcal{F}_{n-1} be a clique forest: in particular, this means that \mathcal{F}_{n-1} has the CIP (as per Definition 1). We build a new clique forest \mathcal{F}_n applying the clique expansion operator and adding a new node n to a clique $C_m \in \mathcal{F}_{n-1}$. We want to show that \mathcal{F}_n has the CIP. Let us denote with C_n the new clique created by the clique expansion operator.

In the general case (figure 3b) a new clique $C_n \subset C_m \cup \{n\}$ is introduced and the new node n does not belong to any clique intersection, therefore any node belonging to the intersection of C_n with any other clique $C_{m'}$ must belong to C_m as well. Due to the inductive hypothesis, given any other clique $C_{m'} \in \mathcal{F}_{n-1}$, there is a path $C_m - C_{m_1} - \dots - C_{m_k} - C_{m'}$ that contains all the nodes in $C_m \cap C_{m'}$. The path $C_n - C_m - C_{m_1} - \dots - C_{m_k} - C_{m'}$ therefore connects C_n to $C_{m'}$ in \mathcal{F}_n and fulfills the CIP.



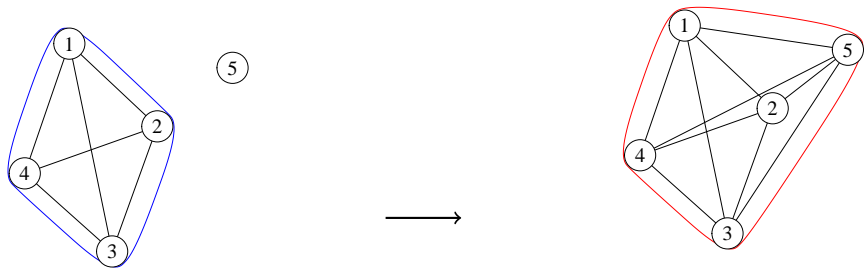
(a) Before clique expansion (general case)
 $P(X = x \mid G_a) = \phi_{1234}(X_1, X_2, X_3, X_4)\phi_5(X_5)$

(b) After clique expansion (general case),
 $P(X = x \mid G_b) = \frac{\phi_{1234}(X_1, X_2, X_3, X_4)\phi_{125}(X_1, X_2, X_5)}{\phi_{12}(X_1, X_2)}$
 $S = \{1, 2\}$



(c) Before clique expansion (isolated vertex case)
 $P(X = x \mid G_a) = \phi_{1234}(X_1, X_2, X_3, X_4)\phi_5(X_5)$

(d) After clique expansion (isolated vertex case),
 $P(X = x \mid G_b) = \phi_{1234}(X_1, X_2, X_3, X_4)\phi_5(X_5)$
 $S = \emptyset$



(e) Before clique expansion (full expansion)
 $P(X = x \mid G_a) = \phi_{1234}(X_1, X_2, X_3, X_4)\phi_5(X_5)$

(f) After clique expansion (full expansion),
 $P(X = x \mid G_b) = \phi_{12345}(X_1, X_2, X_3, X_4, X_5)$
 $S = \emptyset$

Figure 3: Illustration of the clique expansion operator. If S is a proper subset of C_1 the operation produces two cliques and a separator; if $S = \emptyset$ the result produces two disconnected cliques C_1 and $C_2 = \{5\}$ and the separator is the empty set if $S = C_1$ the operation purely expands the original clique with the new vertex and does not introduce a new clique or separator.

In the case (figure 3d) when n is added as new disconnected clique there is nothing to prove as the CIP follows from the inductive hypothesis.

In the case of full expansion (figure 3f) the clique $C_n = C_m \cup \{n\}$ replaces C_m and the new node n does not belong to any clique intersection, therefore any node belonging to the intersection of C_n with any other clique $C_{m'}$ must belong to C_m as well. Due to the inductive hypothesis, given any other clique $C_{m'} \in \mathcal{F}_{n-1}$, there is a path $C_m - C_{m_1} - \dots - C_{m_k} - C_{m'}$ that contains all the nodes in $C_m \cap C_{m'}$. The path $C_n - C_{m_1} - \dots - C_{m_k} - C_{m'}$, obtained by replacing C_m with C_n , *a fortiori* connects C_n to $C_{m'}$ in \mathcal{F}_n and fulfills the CIP. ■

Theorem 8 (Decomposibility invariance of the clique expansion operator) *Let \mathcal{F}_{n-1} be a clique forest underlying a graphical model with associated random variables X_1, \dots, X_{n-1} with underlying density $\phi_{X_1, \dots, X_{n-1}}(X_1, \dots, X_{n-1})$. If we add one random variable X_n to the graphical model and use the clique expansion operator to attach the associated node to the graph, the density of the updated graphical model is*

$$\phi_{X_1, \dots, X_n}(X_1, \dots, X_n) = \phi_{X_1, \dots, X_{n-1}}(X_1, \dots, X_{n-1}) \frac{\phi_{X_{C_n}}(X_{C_n})}{\phi_{X_S}(X_S)}$$

where C_n and S are respectively the clique and separator introduced by the clique expansion operator.

Proof The proof is immediate since the separator S is complete by construction and separates the graph. In cases where the network is fully built using the clique expansion operator decomposition shown in Equation 3 follows by induction. ■

3.2 The MFCE algorithm

The MFCE algorithm that we introduce in this paper is a generalisation to clique forests of Prim's minimum spanning tree algorithm (Prim (1957)). Prim's algorithm constructs the Minimum Spanning Tree tree starting with an arbitrary vertex and adds the closest (i.e. with minimal edge weight) unconnected vertex. In case the graph is not connected, for instance when some subsets are at infinite distance, the algorithm can be applied to the distinct connected components to produce a minimum spanning forest. (Blair and Peyton, 1992, Ch. 4) illustrates the connection between Prim's algorithm and the maximum cardinality search algorithm (MCS, Tarjan (1976)), used to test graph chordality.

In our generalisation the vertices are replaced by cliques and we optimise a gain function, rather than an edge weight; depending on the function we might look for the minimum (e.g. minimum cost) or the maximum (e.g. maximum gain). The algorithm starts by selecting one or more cliques and, at each stage, one of the unconnected vertices is added to the clique forest by performing an edge expansion. The vertex is chosen so as to optimise the scoring function. The initial clique(s) can be chosen with an heuristic (as in the variant of the algorithm presented here) or they could be assumed as given from previous knowledge or expert judgement. For instance in genetic regulatory networks there is interest in incorporating certain topological *motifs* that are known to appear frequently in this kind of networks (Fiori et al., 2012). In this case the cliques provided must be a clique forest.

Algorithm 1 *MFCF*: Builds a clique forest with given clique size range.

Description: Builds a clique forest by applying the clique expansion operator repeatedly until there are no more outstanding vertices. For performance reasons, the algorithm maintains a gain table that holds the possible scores for any combination of cliques already added to the forest and the outstanding vertices.

Input:

W [mandatory]: Either a data matrix with n rows of p -variate observations (e.g. time series of stock market returns) or a p -by- p similarity matrix (e.g. correlation matrix of returns).

gain_function [mandatory]: a function that calculates the gain of a clique expansion based on **W** .

max_cl_size [optional]: size of maximal clique (default value: 4, range = $[2, p]$).

min_cl_size [optional]: size of minimal clique (default value: 4, range = $[1, max_clique_size]$).

reuse_separators [optional]: whether to use separators more than once (default value: TRUE).

C_I, S_I [optional]: Initial list of cliques and separators.

Output:

cliques: list of cliques of the clique forest, ordered as a perfect sequence of sets.

separators: list of separators of the clique forest.

tree: topological description of the clique forest.

Algorithm:

- S1. [Initialize] $p \leftarrow$ number of variables. $cliques \leftarrow \emptyset$. $separators \leftarrow \emptyset$. $outstanding_vertices \leftarrow \{1, \dots, p\}$
- S2. [Initialize list of cliques]
 - If C_I is empty
 - $C_1 \leftarrow FirstClique()$
 - $cliques \leftarrow C_1$
 - $outstanding_vertices \leftarrow outstanding_vertices \setminus \{v, v \in C_1\}$.
 - Else
 - $cliques \leftarrow C_I$,
 - $separators \leftarrow S_I$,
 - $outstanding_vertices \leftarrow outstanding_vertices \setminus \{v, v \in C_I\}$.
- S3. [Init Gain Table]. For every $v \in outstanding_vertices$ and every $C \in cliques$, calculate score and optimal separator for C and v and add to gain table.
- S4. [Check for termination]. If $outstanding_vertices = \emptyset$ then return $cliques, separators, tree$.
- S5. [Get best possible expansion]. Select from gain table the clique $C_a \in cliques$, separator $S \subset C_a$ and vertex $v \in outstanding_vertices$ corresponding to the entry with the highest score.

- S6. [Create new clique / separator].
- If S is a proper subset of C_a then
 - $C_b \leftarrow S \cup v$
 - $cliques \leftarrow cliques \cup C_b$
 - $separators \leftarrow separators \cup S$.
 - If $S = C_a$ (extension without new separators) then
 - $C_a \leftarrow C_a \cup v$.
 - If $S = \emptyset$ (disconnected cliques) then
 - $C_b \leftarrow v$
 - $cliques \leftarrow cliques \cup C_b$.
- S7. [Update outstanding vertices, tree]. $outstanding_vertices = outstanding_vertices \setminus v$.
 Set the edge between C_a and C_b to be the separator: $tree(C_a, C_b) \leftarrow S$
- S8. [Update gain table]. Delete from gain table all entries where the vertex is v .
 Add to gain table entries with gains for C_b .
 If $reuse_separators$ is false, delete from the gain table where the separator is S .
 Update gains for C_a .
- S9. [Close loop]. Return to [S4].

Remark 9 *The function $FirstClique()$ provides an estimate of the best first clique. It can be obtained by starting with a clique made of the two vertices (or a larger clique) with the largest gain and growing it using the clique expansion operator until it reaches the minimum size required.*

The MFCE algorithm is a radical extension of the TMFG algorithm proposed in Massara et al. (2016) which build a planar graph applying a special case of clique expansion operator (T_2 in that paper) with the following constraints: (a) the maximum clique size is 4, (b) the minimum clique size is also 4, and (c) a separator are triangles and they can be used only once. Note that the MST is also retrievable with the MFCE algorithm by setting the maximum clique size to 2, the minimum clique size also at 2, and separators can be used more than once. Interestingly, there is another class of networks, which lies between the MST and the TMFG, which is constituted of triangular cliques and edge separators and has not been explored yet in the literature.

A straightforward application of Theorem 7 shows that the cliques produced by the MFCE are clique forests.

Corollary 10 (The MFCE produces clique forests) *The networks produced by the MFCE have the CF-property.*

Proof This results from the fact that the MFCE applies the clique expansion operator, which is CF-invariant by virtue of Theorem 7. ■

3.3 Gain Functions

An advantage of the formulation in terms of clique trees is that we can use any multivariate function as a scoring function. Specifically, we aim for a function that, given a set of random variables \mathbf{X}_c produces a score which is a measure of the strength of association between the variables, taking into account local interactions through the separator.

Definition 11 *The gain is the increase in score that results from a clique expansion.*

We also want to require the score to have a validation procedure, so that we can test significance. Significance can be validated both through a parametric statistical test under some assumptions or non-parametrically via permutation test. Further, cross-validation can be implemented by computing the gain on the validation sample using the function estimated on the train sample. In many cases the contribution to the score is made up of a positive contribution due to the introduction of a new clique and a negative correction from the separator. The meaning of the negative correction is sometimes related to double counting and sometimes related to conditioning.

Let us here exemplify the above by introducing two gain functions: one based on scores from a similarity matrix, and a second one based on log-likelihood with an explicit formulation for the gaussian case.

3.3.1 GAIN FUNCTION FROM SIMILARITY MATRIX

As discussed in Massara et al. (2016) there are applications where it is required to build a network that maximises the sum of the weights of a similarity matrix subject to some constraint. Examples are the correlation networks mentioned in Section 2.1.3 (Mantegna, 1999; Di Matteo and Aste, 2002; Di Matteo et al., 2005; Tumminello et al., 2005; Aste et al., 2005; Tumminello et al., 2007; Aste et al., 2010; Song et al., 2012; Pozzi et al., 2013; Musmeci et al., 2015b,a).

Let us define a symmetric matrix of weights W , where w_{ij} quantifies the “similarity” of elements i and j and $w_{i,i} = 0$. If C is a subset of the row indices of W we define $Score(C) = \sum_{i \in C, j \in C} W_{ij}$.

The gain function returns the best available separator that, joined with a vertex, gives the highest possible sum of the weights. In this case the total score is the sum of the weights of the cliques minus the sum of the weights of the separators. The total score is given by

$$Score = \sum_{c \in \mathcal{C}} \sum_{i \in c, j \in c} W_{ij} - \sum_{s \in \mathcal{S}} \sum_{i \in s, j \in s} W_{ij} \quad (4)$$

When we perform a clique expansion and introduce a new clique \tilde{c} and a new separator \tilde{s} the corresponding gain in score is:

$$G(\tilde{c}, \tilde{s}) = \sum_{i \in \tilde{c}, j \in \tilde{c}} W_{ij} - \sum_{i \in \tilde{s}, j \in \tilde{s}} W_{ij} \quad (5)$$

In the special case when the clique expansion results in the extension of a previous clique, such that $\tilde{C} = C \cup v$, the gain is the difference in score between the new clique and the old one (the separator is obviously zero):

$$G(\tilde{c}, c) = \sum_{i \in \tilde{c}, j \in \tilde{c}} W_{ij} - \sum_{i \in c, j \in c} W_{ij} = \sum_{i \in \tilde{c}} W_{iv} \quad (6)$$

One might also add a form of validation to this gain function and add only the edges with weights that are significantly larger than zero and exceed a given threshold either in-sample or off-sample (cross validation).

3.3.2 GAIN FUNCTION FROM LOG-LIKELIHOOD

Equation 3 is a likelihood for a given realisation $\mathbf{X} = \hat{\mathbf{x}}$:

$$\mathcal{L}(\mathbf{X} = \hat{\mathbf{x}} | \{c \in \mathcal{C}\}, \{s \in \mathcal{S}\}) = \frac{\prod_{c \in \mathcal{C}} P(\mathbf{X}_c = \hat{\mathbf{x}}_c)}{\prod_{s \in \mathcal{S}} P(\mathbf{X}_s = \hat{\mathbf{x}}_s)} \quad (7)$$

and accordingly the log-likelihood is:

$$\ell(\mathbf{X} = \hat{\mathbf{x}} | \{c \in \mathcal{C}\}, \{s \in \mathcal{S}\}) = \sum_{c \in \mathcal{C}} \log P(\mathbf{X}_c = \hat{\mathbf{x}}_c) - \sum_{s \in \mathcal{S}} \log P(\mathbf{X}_s = \hat{\mathbf{x}}_s) \quad (8)$$

When we add a new clique \tilde{c} and a new separator \tilde{s} the gain in log-likelihood is:

$$G(\tilde{c}, \tilde{s}) = \log P(\mathbf{X}_{\tilde{c}} = \hat{\mathbf{x}}_{\tilde{c}}) - \log P(\mathbf{X}_{\tilde{s}} = \hat{\mathbf{x}}_{\tilde{s}}) . \quad (9)$$

Instead, when we add a new clique \tilde{c} by expanding an existing one c the gain in log-likelihood is:

$$G(\tilde{c}, c) = \log P(\mathbf{X}_{\tilde{c}} = \hat{\mathbf{x}}_{\tilde{c}}) - \log P(\mathbf{X}_c = \hat{\mathbf{x}}_c) . \quad (10)$$

It is possible to add a significance test to this gain function since the model with the additional clique and separator are nested and the difference in log-likelihood is one-half of the *deviance* (Wasserman, 2010). Under some relatively mild assumptions the deviance is asymptotically distributed as a chi-squared variable with k degrees of freedom, where k is the number of edges added to the model with the clique expansion (Lauritzen, 1996, Ch. 5.2.2). Other possible significance tests could be a cross-validation on a different set or an information criteria such as AIC or BIC (Akaike (1974); Schwarz et al. (1978)).

When a test statistic is available it is conceivable to use the p -value as a gain function. The intuitive meaning is to build a network where the links of greatest statistical significance are added first.

From a Bayesian perspective, here we are maximizing posterior probability $P(G|X)$ updating recursively the graph G with the clique expansion move. In this framework, one starts with a model which assumes independent variables except for the initial clique C_I . Then, the gain table allows to chose the clique expansion operation which maximizes posterior probability by including one extra variable into the dependency structure. Given the greedy, recursive nature of the algorithm there is no guarantee to end at the global maxima. Nonetheless, this is an effective way to estimate inference structures with high posterior probabilities solving efficiently a problem which is otherwise NP-complete.

3.3.3 GAIN FUNCTION FROM LOG-LIKELIHOOD FOR THE MULTIVARIATE NORMAL DISTRIBUTION

In the important specific case of a p -variate normal distribution the log-likelihood function for a given clique forest structure \mathcal{T} can be written, using Equation 8:

$$\begin{aligned}
 \ell(\mathbf{X} = \hat{\mathbf{x}} | \{c \in \mathcal{C}\}, \{s \in \mathcal{S}\}) &= -\frac{p}{2} \ln(2\pi) \\
 &\quad + \frac{1}{2} \sum_{c \in \mathcal{C}} (\ln |J_c| - (\hat{\mathbf{x}}_c - \mu_c)^t J_c (\hat{\mathbf{x}}_c - \mu_c)) \\
 &\quad - \frac{1}{2} \sum_{s \in \mathcal{S}} (\ln |J_s| - (\hat{\mathbf{x}}_s - \mu_s)^t J_s (\hat{\mathbf{x}}_s - \mu_s)) \\
 &= -\frac{p}{2} \ln(2\pi) + \frac{1}{2} \sum_{c \in \mathcal{C}} \left(\ln |J_c| - \text{Tr}(\hat{\Sigma}_c J_c) \right) - \frac{1}{2} \sum_{s \in \mathcal{S}} \left(\ln |J_s| - \text{Tr}(\hat{\Sigma}_s J_s) \right) \quad (11)
 \end{aligned}$$

where

1. $\hat{\Sigma}_c$ (resp. $\hat{\Sigma}_s$) is the sample covariance matrix of the variables \mathbf{X}_c (resp. \mathbf{X}_s), and
2. J_s (resp. J_c) is the inverse covariance matrix (precision matrix).

For a given clique forest structure the likelihood is maximised by $J_c = \hat{J}_c = \hat{\Sigma}_c^{-1}$ and $J_s = \hat{J}_s = \hat{\Sigma}_s^{-1}$. In this case we have $\sum_{c \in \mathcal{C}} \text{Tr}(\hat{\Sigma}_c \hat{J}_c) - \sum_{s \in \mathcal{S}} \text{Tr}(\hat{\Sigma}_s \hat{J}_s) = p$ and do not change with the application of the clique expansion operator and therefore Equation 11 can be simplified to:

$$\ell(\mathbf{X} = \hat{\mathbf{x}} | \{c \in \mathcal{C}\}, \{s \in \mathcal{S}\}) = -\frac{p}{2} \ln(2\pi) + \sum_{c \in \mathcal{C}} \frac{1}{2} \ln |\hat{J}_c| - \sum_{s \in \mathcal{S}} \frac{1}{2} \ln |\hat{J}_s| + \frac{p}{2} \quad (12)$$

where the maximum likelihood estimations of the matrices \hat{J}_c and \hat{J}_s depend on the observations $\hat{\mathbf{x}}$ for both the structure and their values.

When we perform a clique expansion and introduce a new clique \tilde{c} and a new separator \tilde{s} the corresponding gain in score is:

$$G(\tilde{c}, \tilde{s}) = \frac{1}{2} \left(\ln |\hat{J}_{\tilde{c}}| - \ln |\hat{J}_{\tilde{s}}| \right) = \frac{1}{2} \left(-\ln |\hat{\Sigma}_{\tilde{c}}| + \ln |\hat{\Sigma}_{\tilde{s}}| \right) \quad (13)$$

Instead, when a clique is expanded ($\tilde{c} = c \cup v$) the corresponding gain in score can be expressed as:

$$G(\tilde{c}, c) = \frac{1}{2} \left(\ln |\hat{J}_{\tilde{c}}| - \ln |\hat{J}_c| \right) = \frac{1}{2} \left(-\ln |\hat{\Sigma}_{\tilde{c}}| + \ln |\hat{\Sigma}_c| \right) \quad (14)$$

Note that this can be interpreted as an increase in likelihood or as a decrease in *entropy*. In this case beside the asymptotic tests of the log-likelihood ratio, there are also several small sample tests that work in the ‘‘big data’’ cases where $p \gg n$ (with n the number of data observations for \mathbf{X}).

It is possible to apply a significance test to the gain expressed in Equations 13 and 14 by using a variant of the likelihood ratio test (Rencher, 2003, Par. 7.1). Indeed, if we have two alternative covariance matrices called for instance $\hat{\Sigma}_1$ and $\hat{\Sigma}_0$ it is possible to test whether they are significantly different by using the following statistics:

$$u = \nu \left(\log |\hat{\Sigma}_0| - \log |\hat{\Sigma}_1| + \text{Tr} \left(\hat{\Sigma}_1^{-1} \hat{\Sigma}_0 \right) - p \right). \quad (15)$$

Where ν is, in the case of un-pooled data, the number of observation in the time series minus one⁶, $(n - 1)$.

In general u is χ^2 distributed with the number of degrees of freedom equal to $\frac{1}{2}p(p+1)$, with p the dimension of the matrix. However, if the two matrices are nested, the number of degrees of freedom is the number of additional parameters in the nested model, with respect to the external model. In the case of the clique expansion operator the degrees of freedom are therefore $p - 1$.

4. Experiments

We performed a set of experiments to analyse the performances of the MFCF methodology by comparing the results against two methodologies for covariance or correlation matrices estimation that are widely accepted in the literature (Fan et al., 2011): the Graphical Lasso (Friedman et al., 2008) and a shrinkage estimator.

Since the Graphical Lasso optimises a penalised version of Gaussian log-likelihood, we have used two score functions that are closely related to it, so that the results are effectively comparable:

- Gaussian log-likelihood, described in Section 4.3.1, where we fix the size of the cliques to the same value and evaluate the results for a range of clique sizes.
- Gaussian log-likelihood statistically validated, described in Section 4.3.2, where we allow cliques of any size up to a maximum value.

4.1 Construction of the precision matrix in the multivariate Gaussian case

In the Gaussian case, once the clique forest structure is known, the maximum likelihood estimate of the precision matrix is given in explicit form (see Lauritzen (1996, Prop. 5.9) or Barfuss et al. (2016)):

$$\hat{J} = \sum_{c \in \mathcal{C}} \left[\left(\hat{\Sigma}_c \right)^{-1} \right]^V - \sum_{s \in \mathcal{S}} \left[\left(\hat{\Sigma}_s \right)^{-1} \right]^V \quad (16)$$

where the notation $[M_c]^V$ in Equation 16 means a matrix of dimension $p = |V|$ where all the elements are zero, excepting for the ones with the indices in the clique c ; that is $[M_c]_{ij}^V = M_{ij}$ if $i \in c$ and $j \in c$, $[M_c]_{ij}^V = 0$ otherwise.

4.2 MFCF shrinkage procedures

In all the experiments we have applied some shrinkage to the maximum likelihood estimate. The shrinkage parameter has been calibrated to the validation data set by looking for the best likelihood and performing a grid search. We have used two shrinkage targets: the commonly used identity matrix (Ledoit and Wolf, 2003, Sec. 3.3), and a new shrinkage target we call “the clique tree target”, described in 7.2.

6. It is also possible to apply a small sample correction to the statistics u , see Rencher (2003, Eq. 7.2) for the details.

4.3 Gain Functions Used

4.3.1 GAUSSIAN LOG-LIKELIHOOD

For the gain function we use Equations 13 and 14 to compute the increase in log-likelihood for a clique expansion in the multivariate gaussian case. Let C_a denote a clique and v_0 an isolated vertex. The number of elements in C_a is equal to the clique size (k). Given a vertex outside C_a , the gain function must return both the gain and a subset of the vertices in C_a yielding the highest statistically significant gain relative to v_0 . The construction of the separator is performed in the gain function in a greedy way, first by selecting from C_a the vertex v_1 with the highest gain relative to with v_0 , so that $S \leftarrow v_1$. The next best vertex v_2 is the one that added to S increases the most the log-likelihood (Equation 14), and we put $S \leftarrow S \cup v_2$, and so on until the clique size is reached.

4.3.2 GAUSSIAN LOG-LIKELIHOOD STATISTICALLY VALIDATED

This scoring function is also based on the increase of the log-likelihood in the multivariate Gaussian case. However, in this case we perform the clique expansion only if the gain is significantly greater than zero using Equation 15 to test the hypothesis within a given confidence level. If it is not statistically different from zero the corresponding score is set to zero. This results in sparser networks than the ones obtained using the score function in 4.3.1, especially when the number of data points is low.

The selection of the separator is also performed in a greedy way similar to process described in 4.3.1, with the difference that the process might stop before the maximum clique size is reached if the increase in log-likelihood is not statistically significant.

4.4 Data

We test the performance of the algorithm on three types of synthetic data and on a real dataset of stocks returns. The synthetic data are multivariate Gaussian generated using respectively: (1) a sparse chordal inverse matrix with known sparsity pattern; (2) a factor model; (3) a random positive definite matrix generated from random eigenvalues and a random rotation. The real example is taken from a long-return series of stock prices. All the datasets used in the experiments have been produced for 100 variables ($p = 100$) and varying time series lengths ($n \in \{25, 50, 75, 100, 200, 300, 400, 500, 750, 1000, 1500\}$). The details about the data generation process are described in Appendix, sub-Sections 8.1.1, 8.1.2, 8.1.3 and 8.1.4.

For every type of data we generate the following datasets:

1. The *train data set* which is used to learn the model parameters, such as the MFCCF network and the elements of the precision matrix. For every type of data we generate 5 distinct training data sets to test reproducibility.
2. The *validation data set* is used to select the model hyper-parameters: these are the L_1 penalty for the graphical lasso, the shrinkage parameter for the shrinkage method, and the maximum clique size and shrinkage parameter for the MFCCF. For all methods we perform a grid search over the hyper-parameters and select the model that achieves the best likelihood on the validation dataset. In analogy with the train data we generate 5 distinct validation data sets.

3. The *test data set* is used to assess the performance of the models. We use 10 distinct test datasets for every training/validation data set and therefore for every data type we have 50 test datasets.

The full description of the methods used to generate the dataset is in the Appendix (7).

4.5 Algorithms and methodologies

We have generated sparse inverse correlation⁷ estimates with different constructions of the MFCF algorithm and compared their performances with the Glasso and shrinkage estimators, the real benchmark and the null hypothesis.

1. **GLASSO_XVAL**: the Graphical Lasso (Friedman et al., 2008); we use the implementation provided by the R package *huge* (Zhao et al., 2015). The penalty parameter is estimated through cross-validation using an adaptive grid search in the interval $[0.01, 1]$. The precision matrix is estimated, for a given penalty parameter, on the training data set; the penalty parameter selected is the one that produces the estimate with the highest log-likelihood on the validation data set⁸. Performances are assessed on the test data sets.
2. **SHRINKAGE**: a shrinkage estimator with target the identity matrix. We produce shrunk correlation matrices estimators from the training dataset using a grid search for the shrinkage parameter associated with the highest likelihood on the validation data set. Performances are assessed on the test data sets. Recall that this method does not produce sparse precision matrices.
3. **MFCF_FIX**: the MFCF algorithm with fixed clique size, the shrinkage target is the clique tree target described in 4.2, and the gain function described in 4.3.1. We proceed in two steps: initially the correlation matrix built from the training set is shrunk by a small parameter $\epsilon = 0.05$ using the identity matrix as a target⁹. Then we produce a set of models with clique sizes between 2 and 20.¹⁰ The precision matrix estimates are produced using the training datasets and the shrinkage procedure described in Section 4.2. The shrinkage parameter is the one that achieves the best likelihood on the validation data set, estimated with a grid search as we do for the graphical lasso and the shrinkage estimators.
4. **MFCF_FIX_ID**: same as **MFCF_FIX**, excepting for the shrinkage target where we use the identity matrix.
5. **MFCF_VAR**: same as **MFCF_FIX** (in particular using the clique tree target as a shrinkage target) but with variable clique sizes between 2 and 20 and the gain function described in 4.3.2. The p-value used (in 4.3.2) for the likelihood ratio test was 0.05.

7. Although the problem is *covariance* estimation, we have used correlation matrices in all of the test cases, since the problem is equivalent.

8. The minimum penalty of 0.01 has been used because for smaller values we have encountered convergence problems with some of the test cases.

9. This step is performed to stabilise numerically the algorithm; otherwise the matrices for some cliques might be near singular numerically and lead to problems in the calculation of the gains. The parameter 0.05 has not been tuned but just used as a reasonably small number.

10. Larger values would lead to essentially dense models.

6. `MFCF_VAR_ID`: same as `MFCF_VAR` excepting the shrinkage target where we use the identity matrix.
7. `REAL_OR_ML`: the benchmark ‘real’ precision matrix. For synthetic data, when the structure of the correlation matrix is known exactly, we use the exact inverse; in the case of real data, for which we do not know the real correlation matrix, we use the inverse of the sample correlation matrix computed on the entire time series.
8. NULL hypothesis: the identity matrix as the inverse precision matrix.

4.6 Performance indicators

For every test set we collect the following performance indicators:

1. Log likelihood;
2. Accuracy;
3. Sensitivity;
4. Specificity;
5. The *correlation* of the estimated precision matrix with the true precision matrix;
6. *Eigenvalue distance*; and
7. *Eigenvalue inverse distance*.

The definition for these performance indicators can be found in the Appendix (8.2).

4.7 Results

The full set of results for all the dataset is reported in the Appendix (4.7). In this section we wish to draw the attention to the main highlights of the method and some interesting features of the solution.

4.7.1 SPARSE DECOMPOSABLE SYSTEMS

Figure 4 (and Figure 11 in the Appendix) provide a box plot representing the mean, the confidence interval and the extreme values of the log-likelihood achieved by the algorithms over the test data sets, broken down by the length of the series¹¹. We observe that, in all cases, the MFCF algorithms outperform both the graphical lasso and the shrinkage estimator. The graphical lasso improves performances as the length increases but does not exceed MFCFs. The same results are presented in tabular form in Table 1. The dispersion around the mean is similar for all methods and it has been computed by repeating the experiments on 50 independent datasets (10 testing sets for each 5 training and validating sets, as explained in section 8.1 in the appendix).

11. The boxplots in this paper have been produced with the R (R Core Team, 2016) package GGLOT2 (Wickham, 2009). According to the package documentation the first lower and upper hinges correspond to the first and third quartile, the upper whisker covers the values from the third quartile hinge to 1.5 times the inter-quartile range away from the hinge, and similarly the lower whisker covers the values between the first quartile hinge and 1.5 times the interquartile range below the hinge. The remaining points are considered outliers and plotted individually.

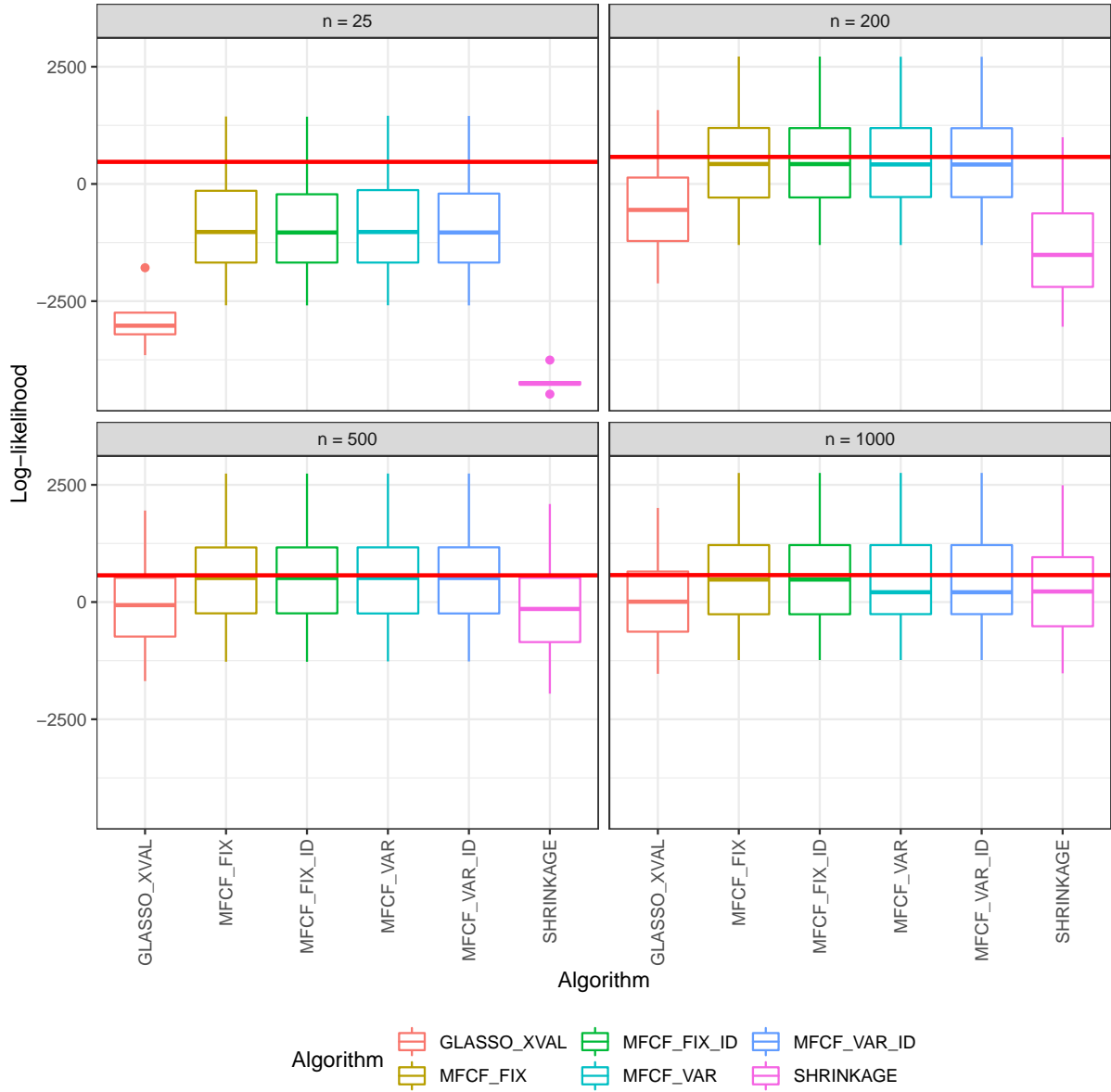


Figure 4: Box plot for the log-likelihood of the algorithms on synthetic data (sparse decomposable precision matrix) for different lengths of the series. The statistics is based on a total of 50 test sets (10 test sets for each of 5 different training / validation sets). The red horizontal line shows the average log-likelihood achieved by the real model, which is seen as an upper limit.

Series length	GLASSO XVAL	MFCF FIX	MFCF FIX ID	MFCF VAR	MFCF VAR ID	REAL OR ML	SHRINKAGE
25	-2882.80	-799.43	-817.47	-793.26	-811.31	701.03	-4200.59
50	-2232.17	241.89	238.47	229.19	229.28	768.55	-3590.65
75	-1804.68	400.90	400.83	410.29	410.23	696.69	-3117.99
100	-1231.09	468.27	468.24	472.50	472.18	690.84	-2643.30
200	-436.25	548.88	548.13	547.93	546.42	659.23	-1277.56
300	-145.02	594.35	595.46	596.03	597.04	662.61	-566.08
400	-34.19	598.96	599.91	601.84	602.07	653.18	-295.88
500	-3.83	580.88	580.91	582.46	582.45	620.99	-69.26
750	66.79	587.58	587.52	586.60	586.60	615.98	204.10
1000	100.79	590.33	590.33	537.03	537.03	612.48	327.54
1500	130.50	596.72	596.72	598.33	598.33	612.41	431.36

Table 1: Log-likelihood of the models. Mean values over 5 distinct training / validation sets and for 10 test set each. (Underscore removed from the name of the algorithms to allow line breaks.)

Figure 5 shows a summary of the performance measures. We observe that the MFCF family is better, overall, than the graphical lasso especially for what concerns accuracy and specificity (the two measures are very close in this example, due to the high sparsity of the model). While the graphical lasso is more sensitive picking up more true positives. However, it is also less selective and produces denser precision matrices with a much higher number of false negatives. We observe that the performance of the graphical lasso improves in all measures for time series of length greater than 200, when the penalty parameter is essentially fixed at 0.01. The MFCF exhibit better log-likelihood, as already observed, and also larger correlations with the true precision matrix.

Figure 6 (and Figure 15 in the Appendix) shows the number of cliques of different size produced by the MFCF_VAR algorithm as a function of the maximum allowed clique size and of the time series length. We note that as the time series length increases the test becomes less stringent with a higher number of large cliques in the model; conversely, when the time series is shorter ($n < p$), the models produced are more parsimonious. The number of cliques of size smaller than the maximum is linked to the degree of sparsity of the model. We will see in Section 8.3.3 that in the case of systems that are inherently dense the vast majority of the cliques will have the maximum allowed clique size.

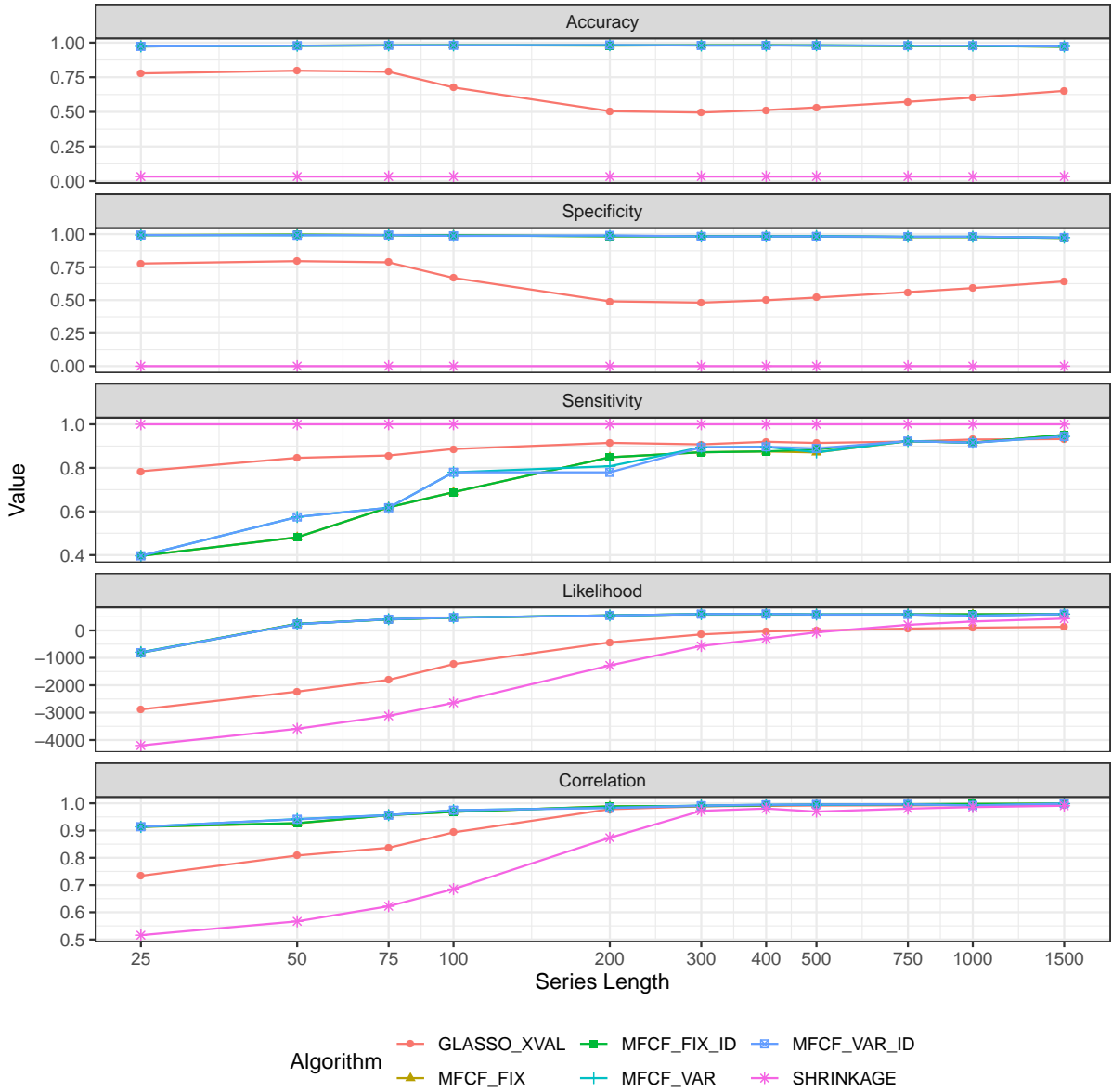


Figure 5: Performance measures of the algorithms on synthetic data (sparse decomposable precision matrix) for different lengths of the series. The statistics is based on a total of 50 test sets (10 test sets for each of 5 different training / validation sets).

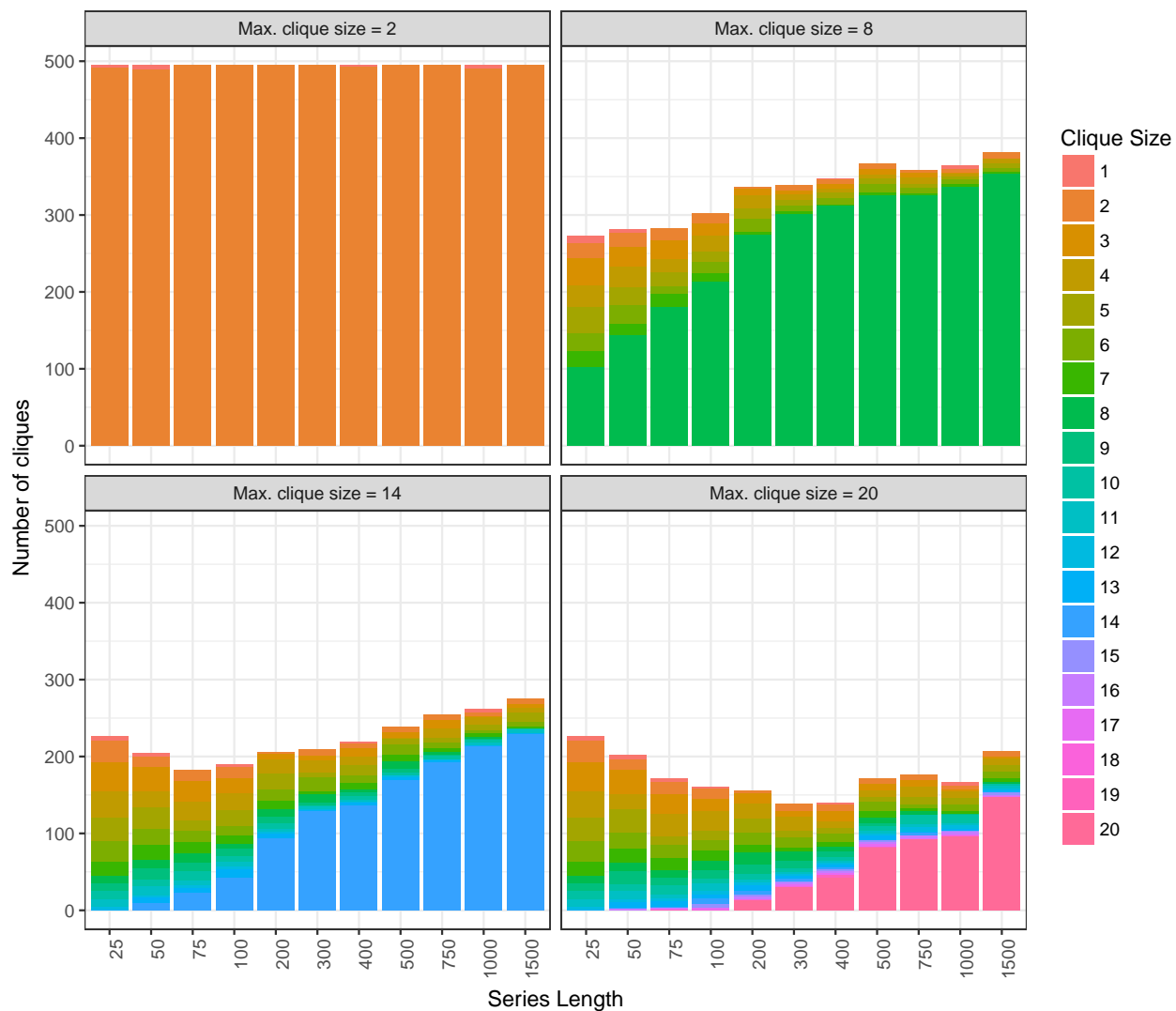


Figure 6: Composition of cliques from MFCF_VAR for synthetic data (sparse decomposable precision matrix). The statistics is based on a total of 5 different training / validation sets.

4.7.2 REAL DATA

Performance measures are reported in Figures 7-9. Please note that this model is essentially non-sparse and therefore there are no true negatives; for this reason we do not report specificity and accuracy and sensitivity are essentially the same measure (see 8.2 for the definition of the performance indicators used. For the same reason the SHRINKAGE model performs better in terms of accuracy than the other models, but not significantly so in terms of log-likelihood. We see from the inspection of Figures 7 and 8 that with real data the log-likelihood is comparable across all models, with slight better values for MFCF_FIX and MFCF_VAR for shorter time series. It is worth noting that, in the family of the MFCF algorithms, the two that use the clique tree shrinkage target described in Equation 19 (MFCF_FIX and MFCF_VAR) perform significantly better, for short time series, than the models with the same structure but the simpler identity matrix (MFCF_FIX_ID and MFCF_VAR_ID) as a shrinkage target. However, as Table 10 shows, in the case of long time series Glasso uses a significantly higher number of parameters than the MFCF. The same results are shown in tabular form in Table 2.

Series length	GLASSO XVAL	MFCF FIX	MFCF FIX ID	MFCF VAR	MFCF VAR ID	REAL OR ML	SHRINKAGE
25	-2463.20	-2172.21	-2550.56	-2243.48	-2559.13	-1280.20	-2558.49
50	-2528.49	-2427.37	-2670.42	-2438.69	-2674.56	-1461.33	-2725.01
75	-2618.80	-2621.05	-2761.78	-2619.53	-2759.37	-1836.75	-2821.22
100	-2610.36	-2578.57	-2684.32	-2572.94	-2699.43	-1822.45	-2799.69
200	-2605.54	-2495.72	-2555.83	-2506.77	-2561.94	-1958.70	-2664.73
300	-2613.91	-2527.65	-2556.48	-2524.18	-2553.71	-2089.36	-2662.54
400	-2618.82	-2606.22	-2628.84	-2607.56	-2630.98	-2185.06	-2705.29
500	-2583.27	-2551.57	-2571.16	-2554.57	-2572.88	-2171.48	-2628.21
750	-2450.17	-2521.73	-2531.22	-2516.58	-2527.05	-2205.35	-2563.06
1000	-2493.24	-2563.27	-2569.82	-2563.31	-2569.77	-2311.93	-2568.76
1500	-2467.06	-2549.02	-2553.15	-2552.45	-2556.22	-2340.61	-2519.63

Table 2: Log-likelihood of the models. Mean values over 5 distinct training / validation sets and for 10 test set each. (Underscore character removed from the names of the algorithms to allow for line breaks.

Figure 9 shows that, excepting for the shortest time series, the MFCF_VAR algorithms almost always use the largest allowed clique size.

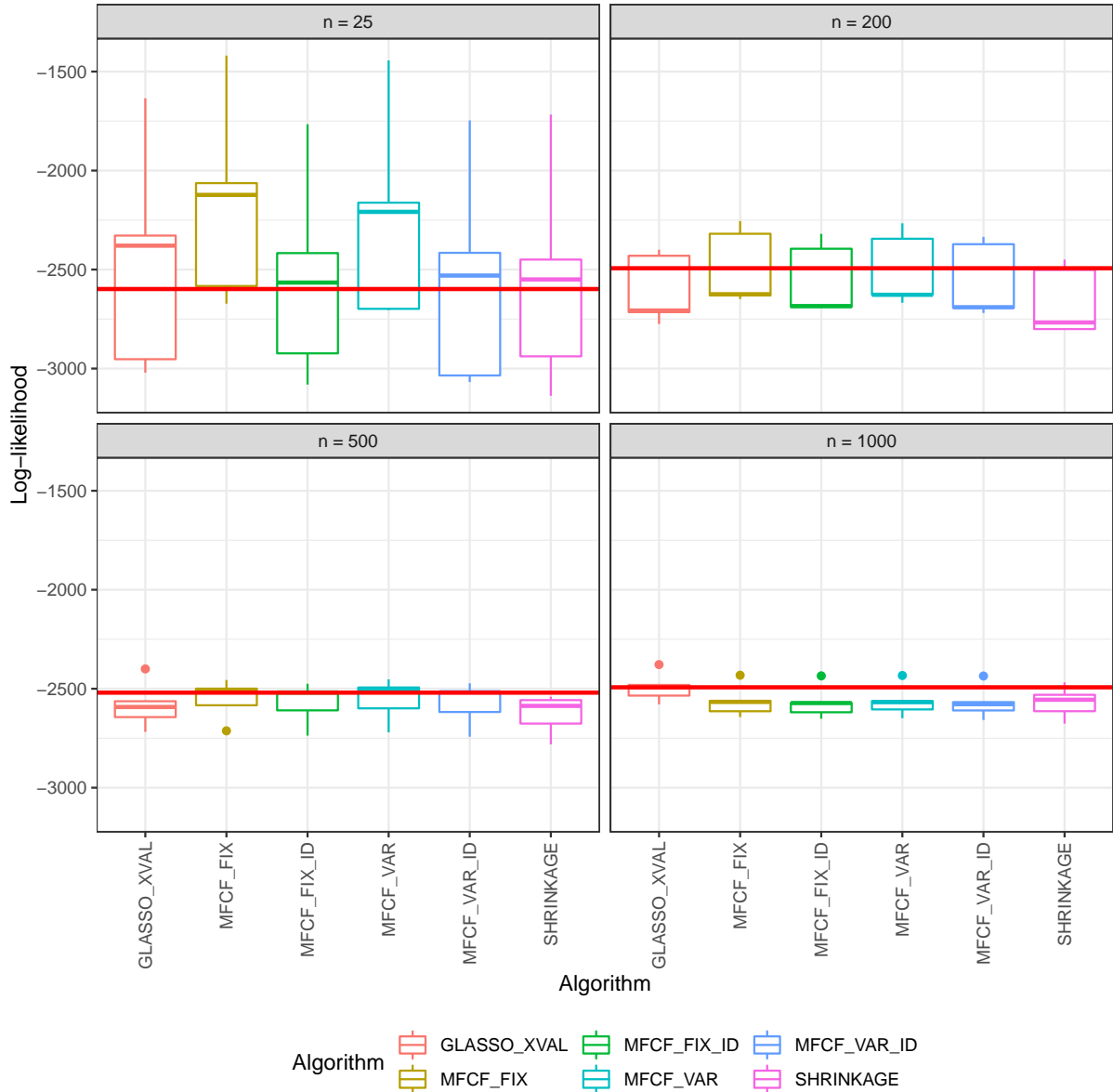


Figure 7: Log-likelihood of the algorithms on real data (stock returns) for different length of the series. The statistics is based on a total of 50 test sets (10 test sets for each of 5 different training / validation sets) per length of the time series. The red horizontal line shows the average log-likelihood achieved by the “maximum likelihood” model, the one where the correlation matrix is estimated from the full data set, i.e. using the longest possible time series.

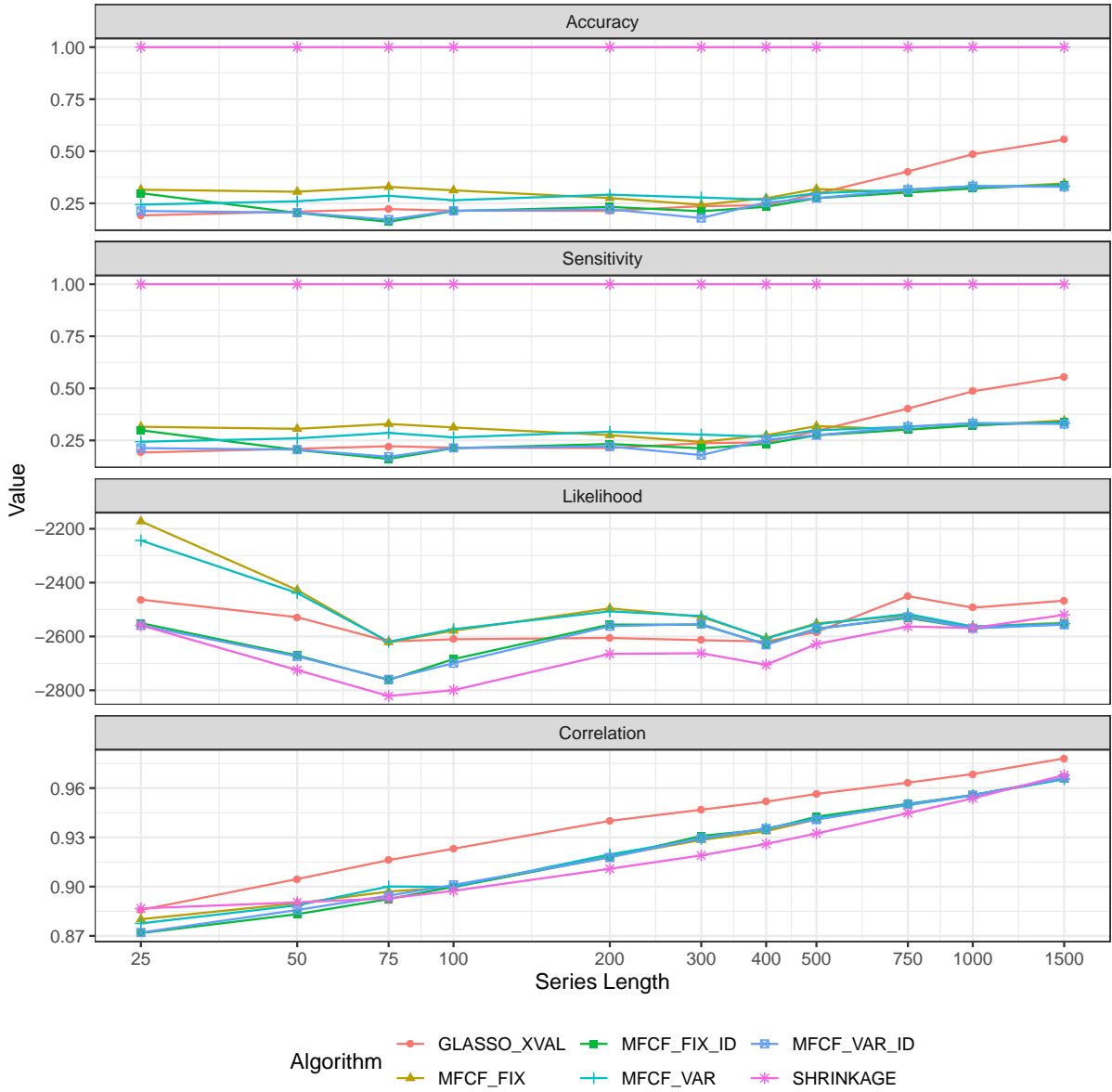


Figure 8: Performance of the algorithms on real data (stock returns) for different lengths of the series. The statistics is based on a total of 50 test sets (10 test sets for each of 5 different training / validation sets) per length of the time series.

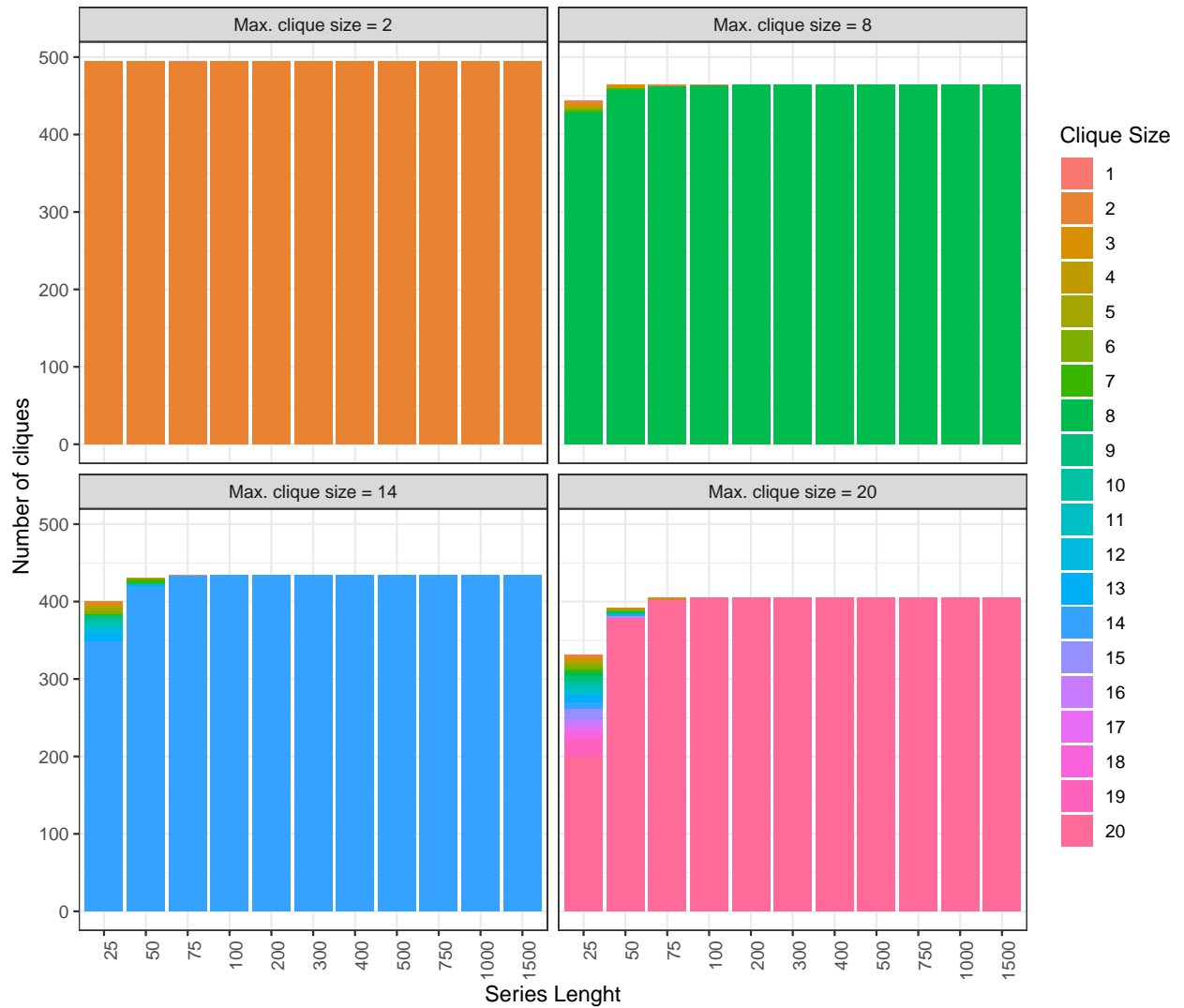


Figure 9: Composition of cliques from MFCF_VAR for real data (stock returns). The statistics is based on a total of 5 different training / validation sets per length of the time series.

5. Conclusions

In this paper we have introduced the MFCE algorithm which generates chordal graphs (clique forests) through a local elementary move named clique expansion. The clique expansion move preserves chordality so it can be applied freely to local configurations without the need to check if the global graph structure is chordal. The MFCE is a topological learning algorithm. In this paper it is used to estimate the inference structure of a system of random variables from data. The clique expansion move can be conditioned to various kinds of gain functions and statistical validations. This methodology can be directly compared with well-established regularization techniques such as Shrinkage (Margaretis and Thrun, 2000; Zhou, 2011) and Lasso (Tibshirani, 1996; Friedman et al., 2008). For this purpose, in this paper, we discuss a set of experiments for covariance selection using log-likelihood gain functions with both synthetic data and real financial time series. Results reveal that MFCE can outperform both Shrinkage and Lasso in several cases with better relative performances particularly when the number of observations is small.

We discovered that the structure of validated clique forests provides important insights on the sparsity and locality of the data. The geometric approach advocated by the MFCE methodology provides, in our view, several benefits over other approaches.

- The MFCE calculates the clique-separator structure, as well as a perfect elimination ordering, and this can help with variable elimination and execution of the junction tree algorithm.
- The proposed methodology allows to seed the algorithm with a given clique tree, and this will help when incorporating previous established knowledge or expert judgement.
- The clique forest structure allows also to identify which edges could be “pruned” without compromising the clique forest geometry (Lauritzen, 1996, Lemma 2.19). We have not made use of this possibility here but it is a possible direction of investigation for future works where the clique forest could be updated dynamically as the data changes.
- Finally we have also described a possible shrinkage target (the “clique tree target”) that exploits the geometry of the clique forest and seems to provide encouraging results especially with small samples.

This work is a radical generalization of the TMFG methodology previously introduced by the authors in Massara et al. (2016). As for the TMFG case, the MFCE generates a chordal graph associated to a multivariate system of variables where the network structure reflects the degree of conditional independence between the variables. TMFG structure was demonstrated to be useful across domains from psychology Christensen et al. (2018b,a) to finance Barfuss et al. (2016). The main limitation in the TMFG approach was the rigidity of its structural construction that allowed 4-cliques with triangular separators between couples of cliques only. MFCE allows instead cliques of arbitrary sizes and the separators can be between multiple cliques. This, combined with the possibility to use different gain functions, greatly generalizes the construction of chordal graphs from data. This also lifts the overall topology of the generated chordal graphs beyond planarity opening the way for the use of MFCE in the field of topological data analytics and, in particular, in the domain of persistent homology (Edelsbrunner and Harer, 2008). Indeed,

the local and the step-by-step nature of the MFCE construction makes it easy to keep track of all topological and hierarchical properties of the network.

Since the MFCE is a generalisation of Prim’s MST algorithm, a legitimate question would be what is, if possible, a generalisation of Kruskal’s algorithm (Kruskal Jr., 1956). It turns out that it is possible to produce an analogue of the MFCE based upon Kruskal’s algorithm. This requires the introduction of a “bridge” operator based upon the direct join of two clique trees (Lauritzen, 1996, pagg. 22-23). However, preliminary investigations reveal that the Kruskal version of the algorithm tends to privilege the creation of very tightly linked small cliques in the first steps which are difficult to join in later steps while keeping the decomposability of the system and a good performance.

The main purpose of this paper was to introduce the MFCE algorithm and the clique expansion elementary move demonstrating their effectiveness with a set of experiments. The experiments were limited to the covariance selection problem because this is a domain of particular interest and there are well-established alternative methods which can be used for comparison. Results shows that the MFCE approach outperforms state-of-the-art Glasso and shrinkage methods.

The methodologies introduced in this paper open many possibilities and have great potentials that will be explored in following works. For instance, we would like to explore a larger range of gain functions and validations beyond likelihood. Preliminary results (see, Savu (2019)) show that gain functions resulting from the application of local, non-linear regressions can be very powerful especially for the analytics of datasets with data at different frequencies (i.e. the combination of daily and quarterly time series) and of different kinds (i.e. the combination of continuous, discrete and categorical variables).

6. Code

The original R code used to carry out the experiments, as well as the code used to generate all the graphs and tables in this paper, is stored in project “Learnig Clique Forests (Code)” hosted in the Open Science Framework repository (Massara, 2021).

An implementation of the MFCE algorithm is also present in Alex Christensen’s NetworkToolbox (Christensen, 2018).

Finally, there is a GitHub repository (Previde Massara and Aste, 2021) that contains ongoing developments and algorithms related to the MFCE in Matlab (MATLAB, 2012) and Octave (Eaton et al., 2020).

Acknowledgments

We thank Daniel Savu for exploring complementary aspects of this algorithm that helped us to contextualise the value and potentials of the present approach. Many thanks to the UCL-FCA group for help with discussions and proof reading. Finally, we are grateful to the ESRC for funding the Systemic Risk Centre (ES/K002309/1), the EPSRC for funding the BARAC project (EP/P031730/1) and to EC for funding the FinTech project (H2020-ICT-2018-2 825215), that partially support this work.

References

Hirotoyu Akaike. Information theory and an extension of the maximum likelihood principle. In *Selected Papers of Hirotoyu Akaike*, pages 199–213. Springer, 1998.

- Hirotsugu Akaike. A new look at the statistical model identification. *Automatic Control, IEEE Transactions on*, 19(6):716–723, 1974.
- T Aste, T Di Matteo, and ST Hyde. Complex networks on hyperbolic surfaces. *Physica A: Statistical Mechanics and its Applications*, 346(1):20–26, 2005.
- Tomaso Aste. Topological regularization with information filtering networks. *arXiv preprint arXiv:2005.04692*, 2020.
- Tomaso Aste, W Shaw, and T Di Matteo. Correlation structure and dynamics in volatile markets. *New Journal of Physics*, 12(8):085009, 2010.
- Francis R Bach and Michael I Jordan. Thin junction trees. In *Advances in Neural Information Processing Systems*, pages 569–576, 2001.
- Jushan Bai, Serena Ng, et al. Large dimensional factor analysis. *Foundations and Trends® in Econometrics*, 3(2):89–163, 2008.
- Onureena Banerjee, Laurent El Ghaoui, Alexandre d’Aspremont, and Georges Natsoulis. Convex optimization techniques for fitting sparse gaussian graphical models. In *Proceedings of the 23rd international conference on Machine learning*, pages 89–96. ACM, 2006.
- Onureena Banerjee, Laurent El Ghaoui, and Alexandre d’Aspremont. Model selection through sparse maximum likelihood estimation for multivariate gaussian or binary data. *J. Mach. Learn. Res.*, 9:485–516, June 2008a. ISSN 1532-4435. URL <http://dl.acm.org/citation.cfm?id=1390681.1390696>.
- Onureena Banerjee, Laurent El Ghaoui, and Alexandre d’Aspremont. Model selection through sparse maximum likelihood estimation for multivariate gaussian or binary data. *The Journal of Machine Learning Research*, 9:485–516, 2008b.
- David Barber. *Bayesian reasoning and machine learning*. Cambridge University Press, 2012.
- Wolfram Barfuss, Guido Previde Massara, Tiziana Di Matteo, and Tomaso Aste. Parsimonious modeling with information filtering networks. *Physical Review E*, 94(6):062306, 2016.
- Joshua Batson, Daniel A Spielman, Nikhil Srivastava, and Shang-Hua Teng. Spectral sparsification of graphs: theory and algorithms. *Communications of the ACM*, 56(8): 87–94, 2013.
- Jean RS Blair and Barry Peyton. An introduction to chordal graphs and clique trees. In *Graph theory and sparse matrix computation*, pages 1–29. Springer, 1992.
- Andrej Bogdanov, Elchanan Mossel, and Salil Vadhan. The complexity of distinguishing markov random fields. In *Approximation, Randomization and Combinatorial Optimization. Algorithms and Techniques*, pages 331–342. Springer, 2008.
- Joël Bun, Jean-Philippe Bouchaud, and Marc Potters. Cleaning large correlation matrices: tools from random matrix theory. *Physics Reports*, 666:1–109, 2017.

- Venkat Chandrasekaran, Nathan Srebro, and Prahladh Harsha. Complexity of inference in graphical models. *arXiv preprint arXiv:1206.3240*, 2012.
- Anton Checheta and Carlos Guestrin. Efficient principled learning of thin junction trees. In *Advances in Neural Information Processing Systems*, pages 273–280, 2008.
- David M Chickering, Dan Geiger, David Heckerman, et al. Learning bayesian networks is np-hard. Technical report, Citeseer, 1994.
- David Maxwell Chickering. Learning bayesian networks is np-complete. In *Learning from data*, pages 121–130. Springer, 1996.
- C. Chow and C. Liu. Approximating discrete probability distributions with dependence trees. *IEEE Transactions on Information Theory*, 14(3):462–467, May 1968. ISSN 0018-9448. doi: 10.1109/TIT.1968.1054142.
- Alexander P. Christensen. NetworkToolbox: Methods and Measures for Brain, Cognitive, and Psychometric Network Analysis in R. *The R Journal*, 10(2):422–439, 2018. doi: 10.32614/RJ-2018-065. URL <https://doi.org/10.32614/RJ-2018-065>.
- Alexander P Christensen, Katherine N Cotter, and Paul J Silvia. Reopening openness to experience: A network analysis of four openness to experience inventories. *Journal of personality assessment*, pages 1–15, 2018a.
- Alexander P Christensen, Yoed N Kenett, Tomaso Aste, Paul J Silvia, and Thomas R Kwapil. Network structure of the wisconsin schizotypy scales–short forms: Examining psychometric network filtering approaches. *Behavior research methods*, 50(6):2531–2550, 2018b.
- Andrzej Cichocki. Era of big data processing: A new approach via tensor networks and tensor decompositions. *arXiv preprint arXiv:1403.2048*, 2014.
- Andrzej Cichocki. Tensor networks for dimensionality reduction, big data and deep learning. In *Advances in data analysis with computational intelligence methods*, pages 3–49. Springer, 2018.
- Andrzej Cichocki, Danilo Mandic, Lieven De Lathauwer, Guoxu Zhou, Qibin Zhao, Cesar Caiafa, and Huy Anh Phan. Tensor decompositions for signal processing applications: From two-way to multiway component analysis. *IEEE signal processing magazine*, 32(2):145–163, 2015.
- Alexandre d’Aspremont, Onureena Banerjee, and Laurent El Ghaoui. First-order methods for sparse covariance selection. *SIAM Journal on Matrix Analysis and Applications*, 30(1):56–66, 2008.
- A. P. Dempster. Covariance selection. *Biometrics*, 28(1):157–175, 1972.
- Amol Deshpande, Minos Garofalakis, and Michael I Jordan. Efficient stepwise selection in decomposable models. In *Proceedings of the Seventeenth conference on Uncertainty in artificial intelligence*, pages 128–135. Morgan Kaufmann Publishers Inc., 2001.

- T Di Matteo, T Aste, ST Hyde, and S Ramsden. Interest rates hierarchical structure. *PHYSICA A-STATISTICAL MECHANICS AND ITS APPLICATIONS*, 355(1):21–33, SEP 1 2005. ISSN 0378-4371. doi: {10.1016/j.physa.2005.02.063}. 1st Bonzenfreies Colloquium on Market Dynamics and Quantitative Economics, Alessandria, ITALY, SEP 09-10, 2004.
- Tiziana Di Matteo and Tomaso Aste. How does the eurodollar interest rate behave? *International Journal of Theoretical and Applied Finance*, 5(01):107–122, 2002.
- M. Drton and M. H. Maathuis. Structure Learning in Graphical Modeling. *Annual Review of Statistics and Its Application*, 4:365–393, March 2017. doi: 10.1146/annurev-statistics-060116-053803.
- Daniel Eaton and Kevin Murphy. Bayesian structure learning using dynamic programming and mcmc. *arXiv preprint arXiv:1206.5247*, 2012.
- John W. Eaton, David Bateman, Søren Hauberg, and Rik Wehbring. *GNU Octave version 6.1.0 manual: a high-level interactive language for numerical computations*, 2020. URL <https://www.gnu.org/software/octave/doc/v6.1.0/>.
- Herbert Edelsbrunner and John Harer. Persistent homology—a survey. *Contemporary mathematics*, 453:257–282, 2008.
- Herbert Edelsbrunner, David Letscher, and Afra Zomorodian. Topological persistence and simplification. In *Proceedings 41st annual symposium on foundations of computer science*, pages 454–463. IEEE, 2000.
- Jianqing Fan, Jinchi Lv, and Lei Qi. Sparse high-dimensional models in economics. *Annu. Rev. Econ.*, 3(1):291–317, 2011.
- Marcelo Fiori, Pablo Musé, and Guillermo Sapiro. Topology constraints in graphical models. In *Advances in Neural Information Processing Systems*, pages 791–799, 2012.
- Jerome Friedman, Trevor Hastie, and Robert Tibshirani. Sparse inverse covariance estimation with the graphical lasso. *Biostatistics (Oxford, England)*, 9(3):432–441, 2008.
- Paolo Giudici and PJ Green. Decomposable graphical gaussian model determination. *Biometrika*, 86(4):785–801, 1999.
- Martin Charles Golumbic. *Algorithmic graph theory and perfect graphs*, volume 57. Elsevier, 2004.
- Elizabeth Gross, Seth Sullivant, et al. The maximum likelihood threshold of a graph. *Bernoulli*, 24(1):386–407, 2018.
- Martin Grötschel, László Lovász, and Alexander Schrijver. *Geometric algorithms and combinatorial optimization*, volume 2. Springer Science & Business Media, 2012.
- Igor Guskov and Zoë J Wood. Topological noise removal. *2001 Graphics Interface Proceedings: Ottawa, Canada*, page 19, 2001.
- Trevor Hastie, Robert Tibshirani, and Martin Wainwright. *Statistical learning with sparsity: the lasso and generalizations*. CRC press, 2015.

- Cho-jui Hsieh, Inderjit S. Dhillon, Pradeep K. Ravikumar, and Mátyás A. Sustik. Sparse inverse covariance matrix estimation using quadratic approximation. In J. Shawe-Taylor, R.S. Zemel, P.L. Bartlett, F. Pereira, and K.Q. Weinberger, editors, *Advances in Neural Information Processing Systems 24*, pages 2330–2338. Curran Associates, Inc., 2011. URL <http://papers.nips.cc/paper/4266-sparse-inverse-covariance-matrix-estimation-using-quadratic-approximation.pdf>.
- Kaizhu Huang, Irwin King, and Michael R Lyu. Constructing a large node chow-liu tree based on frequent itemsets. In *Neural Information Processing, 2002. ICONIP'02. Proceedings of the 9th International Conference on*, volume 1, pages 498–502. IEEE, 2002.
- David Karger and Nathan Srebro. Learning markov networks: Maximum bounded tree-width graphs. In *Proceedings of the twelfth annual ACM-SIAM symposium on Discrete algorithms*, pages 392–401. Society for Industrial and Applied Mathematics, 2001.
- Tamara G Kolda and Brett W Bader. Tensor decompositions and applications. *SIAM review*, 51(3):455–500, 2009.
- Daphne Koller and Nir Friedman. *Probabilistic graphical models: principles and techniques*. MIT press, 2009.
- Timo Koski. Lectures on statistical learning theory for chow-liu trees. 2010.
- Edith Kovács and Tamás Szántai. Discovering the markov network structure. *CoRR*, abs/1307.0643, 2013. URL <http://arxiv.org/abs/1307.0643>.
- Joseph B. Kruskal Jr. On the shortest spanning subtree of a graph and the traveling salesman problem. *Proceedings of the American Mathematical Society*, 7(1):48–50, February 1956.
- H Ku and Solomon Kullback. Approximating discrete probability distributions. *IEEE Transactions on Information Theory*, 15(4):444–447, 1969.
- Solomon Kullback and Richard A Leibler. On information and sufficiency. *The annals of mathematical statistics*, 22(1):79–86, 1951.
- Laurent Laloux, Pierre Cizeau, Jean-Philippe Bouchaud, and Marc Potters. Noise dressing of financial correlation matrices. *Physical review letters*, 83(7):1467, 1999.
- Steffen Lauritzen. Structure estimation in graphical models. Wald Lecture, World Meeting on Probability and Statistics, 2012.
- Steffen L. Lauritzen. *Graphical Models*. Oxford:Clarendon, 1996.
- Olivier Ledoit and Michael Wolf. Improved estimation of the covariance matrix of stock returns with an application to portfolio selection. *Journal of empirical finance*, 10(5): 603–621, 2003.
- Olivier Ledoit and Michael Wolf. Honey, i shrunk the sample covariance matrix. *The Journal of Portfolio Management*, 30(4):110–119, 2004. ISSN 0095-4918. doi: 10.3905/jpm.2004.110. URL <http://jpm.ijournals.com/content/30/4/110>.

- David Madigan, Jeremy York, and Denis Allard. Bayesian graphical models for discrete data. *International Statistical Review/Revue Internationale de Statistique*, pages 215–232, 1995.
- Rosario Nunzio Mantegna. Hierarchical structure in financial markets. *The European Physical Journal B - Condensed Matter and Complex Systems*, 11(1):193–197, 1999. URL <http://EconPapers.repec.org/RePEc:spr:eurphb:v:11:y:1999:i:1:p:193-197>.
- Dimitris Margaritis and Sebastian Thrun. Bayesian network induction via local neighborhoods. In *Advances in neural information processing systems*, pages 505–511, 2000.
- Guido P Massara. Learning clique forests (code), Apr 2021. URL osf.io/w4t69.
- Guido Previde Massara, Tiziana Di Matteo, and Tomaso Aste. Network filtering for big data: triangulated maximally filtered graph. *Journal of complex Networks*, 5(2):161–178, 2016.
- MATLAB. (*R2012a*). The MathWorks Inc., Natick, Massachusetts, 2012.
- Nicolai Meinshausen and Peter Bühlmann. High dimensional graphs and variable selection with the lasso. *Annals of Statistics*, 34(3):1436–1462, 2006.
- James R Munkres. *Elements of algebraic topology*. CRC Press, 2018.
- N Musmeci, T Aste, and T Di Matteo. Relation between financial market structure and the real economy: Comparison between clustering methods. *PLoS ONE*, 10(3):e0116201, 2015a.
- Nicoló Musmeci, Tomaso Aste, and T Di Matteo. Risk diversification: a study of persistence with a filtered correlation-network approach. *Network Theory in Finance*, 1(1):77–98, 2015b.
- Figen Oztoprak, Jorge Nocedal, Steven Rennie, and Peder A. Olsen. Newton-like methods for sparse inverse covariance estimation. In P. Bartlett, F.c.n. Pereira, C.j.c. Burges, L. Bottou, and K.q. Weinberger, editors, *Advances in Neural Information Processing Systems 25*, pages 755–763, 2012. URL http://books.nips.cc/papers/files/nips25/NIPS2012_0344.pdf.
- François Petitjean, Geoffrey Webb, Ann E Nicholson, et al. Scaling log-linear analysis to high-dimensional data. In *Data Mining (ICDM), 2013 IEEE 13th International Conference on*, pages 597–606. IEEE, 2013.
- F Pozzi, T Di Matteo, and T Aste. Spread of risk across financial markets: better to invest in the peripheries. *Scientific Reports*, 3:1665, 2013.
- G. Previde Massara and T. Aste. Mfcf matlab. <https://github.com/gprevide/MFCF-Matlab>, 2021.
- R.C. Prim. Shortest connection networks and some generalizations. *Bell System Technical Journal, The*, 36(6):1389–1401, Nov 1957. ISSN 0005-8580. doi: 10.1002/j.1538-7305.1957.tb01515.x.

- Weiliang Qiu and Harry Joe. *clusterGeneration: Random Cluster Generation (with Specified Degree of Separation)*, 2015. URL <https://CRAN.R-project.org/package=clusterGeneration>. R package version 1.3.4.
- R Core Team. *R: A Language and Environment for Statistical Computing*. R Foundation for Statistical Computing, Vienna, Austria, 2016. URL <https://www.R-project.org/>.
- Pradeep Ravikumar, Martin J. Wainwright, Garvesh Raskutti, and Bin Yu. High-dimensional covariance estimation by minimizing ℓ_1 -penalized log-determinant divergence. *Electronic Journal of Statistics*, 5:935–980, 2011. doi: 10.1214/11-EJS631. URL <http://dx.doi.org/10.1214/11-EJS631>.
- Alvin C Rencher. *Methods of multivariate analysis*, volume 492. John Wiley & Sons, 2003.
- Jorma Rissanen. Modeling by shortest data description. *Automatica*, 14(5):465–471, 1978.
- Daniel Savu. Developing sparse probabilistic models from real data by means of complex networks. Master’s thesis, UCL, Computer Science, 2019.
- Gideon Schwarz et al. Estimating the dimension of a model. *The annals of statistics*, 6(2):461–464, 1978.
- Marco Scutari and Korbinian Strimmer. *Introduction to Graphical Modelling*, chapter 11, pages 235–254. Wiley-Blackwell, 2011. ISBN 9781119970606. doi: 10.1002/9781119970606.ch11. URL <https://onlinelibrary.wiley.com/doi/abs/10.1002/9781119970606.ch11>.
- Marco Scutari et al. On the prior and posterior distributions used in graphical modelling. *Bayesian Analysis*, 8(3):505–532, 2013.
- Glenn R Shafer and Prakash P Shenoy. Probability propagation. *Annals of Mathematics and Artificial Intelligence*, 2(1-4):327–351, 1990.
- W.-M. Song, T. Di Matteo, and T. Aste. Hierarchical information clustering by means of topologically embedded graphs. *PLoS ONE*, 7:e31929, 2012.
- Won-Min Song, T. Di Matteo, and Tomaso Aste. Nested hierarchies in planar graphs. *DISCRETE APPLIED MATHEMATICS*, 159(17):2135–2146, OCT 28 2011. ISSN 0166-218X. doi: {10.1016/j.dam.2011.07.018}.
- Daniel A Spielman and Nikhil Srivastava. Graph sparsification by effective resistances. *SIAM Journal on Computing*, 40(6):1913–1926, 2011.
- Peter Spirtes, Clark N Glymour, Richard Scheines, David Heckerman, Christopher Meek, Gregory Cooper, and Thomas Richardson. *Causation, prediction, and search*. MIT press, 2000.
- Tamás Szántai and Edith Kovács. Discovering a junction tree behind a markov network by a greedy algorithm. *Optimization and Engineering*, 14(4):503–518, 2013.
- Robert Endre Tarjan. Maximum cardinality search and chordal graphs. *Unpublished Lecture Notes CS*, 259, 1976.

- Robert Tibshirani. Regression shrinkage and selection via the lasso. *Journal of the Royal Statistical Society, Series B*, 58(1):267–288, 1996.
- M. Tumminello, T. Aste, T. Di Matteo, and R. N. Mantegna. A tool for filtering information in complex systems. *Proceedings of the National Academy of Sciences of the United States of America*, 102(30):10421–10426, 2005. doi: 10.1073/pnas.0500298102.
- MICHELE Tumminello, T Di Matteo, T Aste, and Rosario Nunzio Mantegna. Correlation based networks of equity returns sampled at different time horizons. *The European Physical Journal B-Condensed Matter and Complex Systems*, 55(2):209–217, 2007.
- Lieven Vandenbergh, Martin S Andersen, et al. Chordal graphs and semidefinite optimization. *Foundations and Trends® in Optimization*, 1(4):241–433, 2015.
- W. N. Venables and B. D. Ripley. *Modern Applied Statistics with S*. Springer, New York, fourth edition, 2002. URL <http://www.stats.ox.ac.uk/pub/MASS4>. ISBN 0-387-95457-0.
- Martin J. Wainwright and Michael I. Jordan. Graphical models, exponential families, and variational inference. *Foundations and Trends® in Machine Learning*, 1(1–2):1–305, 2008. ISSN 1935-8237. doi: 10.1561/22000000001. URL <http://dx.doi.org/10.1561/22000000001>.
- Bao Wang and Guo-Wei Wei. Object-oriented persistent homology. *Journal of computational physics*, 305:276–299, 2016.
- Larry Wasserman. *All of Statistics: A Concise Course in Statistical Inference*. Springer Publishing Company, Incorporated, 2010. ISBN 1441923225, 9781441923226.
- Larry Wasserman. Topological data analysis. *Annual Review of Statistics and Its Application*, 5:501–532, 2018.
- Hadley Wickham. *ggplot2: Elegant Graphics for Data Analysis*. Springer-Verlag New York, 2009. ISBN 978-0-387-98140-6. URL <http://ggplot2.org>.
- Tuo Zhao, Xingguo Li, Han Liu, Kathryn Roeder, John Lafferty, and Larry Wasserman. *huge: High-Dimensional Undirected Graph Estimation*, 2015. URL <https://CRAN.R-project.org/package=huge>. R package version 1.2.7.
- Yang Zhou. Structure learning of probabilistic graphical models: a comprehensive survey. *arXiv preprint arXiv:1111.6925*, 2011.
- Hui Zou and Trevor Hastie. Regularization and variable selection via the elastic net. *Journal of the Royal Statistical Society: Series B (Statistical Methodology)*, 67(2):301–320, 2005.

7. Appendix

In this section we include some additional definitions and theorems related to the MFCF that highlight important characteristics of the algorithm, but that are not used in the specific application to the Covariance Selection problem.

7.0.1 THE RUNNING INTERSECTION PROPERTY AND PERFECT SEQUENCES OF SETS

Definition 12 An ordering of the cliques of a graph is a bijective application σ from the first m natural numbers (where m is the cardinality of \mathcal{C} , the number of maximal cliques) into \mathcal{C} , $\sigma : \{1, \dots, m\} \rightarrow \mathcal{C}$. The cliques in \mathcal{C} are ordered as $C_{\sigma(1)} < \dots < C_{\sigma(m)}$. As a shorthand notation we will also write $\sigma = [C_1, \dots, C_m]$ meaning that the cliques are ordered according to σ .

Definition 13 Let $G(V, E)$ be a graph, \mathcal{C} the set of cliques of G and $\sigma = [C_1, C_2, \dots, C_m]$ an ordering of \mathcal{C} . We say that σ has the running intersection property if for every clique C_i with $2 \leq i \leq m$ there is a clique C_j , with $2 \leq j < i$ such that:

$$C_i \cap (C_1 \cup C_2 \cup \dots \cup C_{i-1}) \subset C_j \quad (17)$$

In graphical models the terms $H_i = (C_1 \cup C_2 \cup \dots \cup C_i)$ are called the “histories”, whereas $S_i = C_i \cap (C_1 \cup C_2 \cup \dots \cup C_{i-1})$ are called the separators and $R_i = C_i \setminus H_{i-1}$ the residuals. C_j is called the *parent* of C_i .

Definition 14 If all the separators are complete, the sequence of cliques in that order is called a perfect sequence of subsets. As the use of the term “parent” hints, a graph that has a perfect sequence of sets has also a clique forest (see Blair and Peyton (1992, Th. 3.4)).

This means in practice that, as we add cliques such as C_i following the ordering of a perfect sequence of subsets, the intersection with the previous cliques is always contained in a single predecessor clique at most, which means that every clique has at most one “parent” clique in the ordering. This gives an heuristic illustration to the following result, formally proved in (Blair and Peyton, 1992, Th. 3.4): any connected graph has a clique tree if and only if the cliques have the running intersection property¹². This also introduces the concept of nested hierarchies with separators forming a poset as described in Song et al. (2011). A property that can be used for clustering (Song et al., 2012).

In summary the three following conditions are equivalent:

1. G is chordal,
2. G has a clique forest \mathcal{T} , or
3. there is an ordering of \mathcal{C} $\sigma = [C_1, \dots, C_m]$ that has the running intersection property.

7.0.2 PERFECT ELIMINATION ORDER

Let $G(V, E)$ be a graph. Let $Adj(v_i)$ be the vertices that are adjacent to v_i in G . Let $\sigma = [v_1, v_2, \dots, v_n]$ be an ordering of the vertices of $G(V, E)$. We define $V_{[i,n]}$ as the set of vertices $\{v_i, v_{i+1}, \dots, v_n\}$ and G_i as the graph induced by $V_{[i,n]}$.

Definition 15 We say that the ordering σ is a perfect elimination order if $Adj(v_i) \cap G_{i+1}$ is a clique in G_{i+1} .

This is the same as saying that v_i is a *simplicial vertex* in G_i . The underlying idea is that v_i can be eliminated from the G_i using the process of variable elimination without introducing any additional link; this is a fundamental property in recursive algorithms where variables are eliminated one at a time and allows to maintain the sparsity of the graph, see Golombic (2004, Ch. 12) for applications to Gaussian Elimination.

12. For non connected graphs the same result applies to the connected components

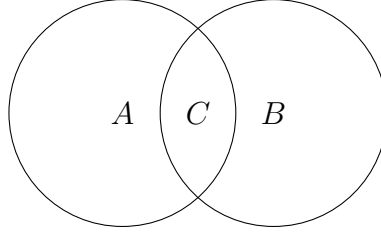


Figure 10: Set-theoretic representation of a decomposable system, with $C = A \cap B$.

7.1 Additional theorems

Theorem 16 *Let $G(V, E)$ a chordal graph with $|V| \geq 2$ and at least an isolated vertex v_i . Then expanding one clique of G with v_i does not introduce a chordless cycle of length ≥ 4 .*

Proof Let us call C_a any clique of G . We choose any subset $S \subset C_a$ as a separator of the clique expansion. If $|S| > 0$ we have that S does not have any chordless cycle of length ≥ 4 because S is a complete induced subgraph of C_a and the clique expansion adds all the edges between v_i and any vertex of S , resulting in a clique $C_b = S \cup v_i$ which is complete and therefore free from chordless cycles of length ≥ 4 . If $S = C_a$ the expansion generates a larger clique $C_b = C_a \cup v_i$ which is complete. If S is empty then the expansion trivially does not add any chordless cycle of length ≥ 4 . ■

Theorem 17 *The MFCF algorithm produces cliques in a perfect order, provided that the initial cliques C_I are arranged in a perfect order.*

Proof The demonstration can be performed by induction on the number of vertices added. Let's assume that the algorithm has added $m - 1$ vertices, and by definition there are cliques C_1, \dots, C_j that are perfectly ordered. When adding the next v_m vertex there are three possibilities:

- a) The algorithm selects a clique $C_i, 1 \leq i < j$ with a non empty separator S_i and therefore a new clique $C_k = S_i \cup v_m$ is created. The separator is clearly complete and by construction we have that $S_i \subset C_i$.
- b) The algorithm selects a clique $C_i, 1 \leq i < j$ and the separator $S_i = C_i$ (extension of clique C_i). By hypothesis there is a clique C_h with $1 \leq h < i$ such that $S_i \subset C_h$ and S_i is complete. Since v_m was disconnected from all the cliques it was in particular disconnected from C_h and therefore it does not change the intersection $C_h \cup S_i$, and therefore C_h still fulfils the requirements that $S_i \subset C_h$.
- c) The algorithm does not select a clique and adds a new clique made only of the vertex v_m . The intersection with any clique is the empty set and the result follows trivially.

■

7.2 The clique tree shrinkage target

The clique tree target is a generalisation of the constant correlation target (Ledoit and Wolf, 2004) where the target matrix is created gluing together smaller correlation target matrices that represent the cliques of a clique tree. The matrix is built in steps, starting from the calculation of the average correlation between elements in every clique c in the clique tree.

$$\hat{\rho}_c = \frac{\sum_{i \in c, j \in c, j > i} (\Sigma_c)_{ij}}{\sum_{i \in c, j \in c, j > i} 1} \quad (18)$$

Next we build a clique level correlation matrix for every clique c using the following rules:

- If $i \in c, j \in c, i = j$ then $(\hat{\Sigma}_c)_{ij} = 1$
- If $i \in c, j \in c, i \neq j$ then $(\hat{\Sigma}_c)_{ij} = \frac{\sum_{c' \in \mathcal{C}, i \in c', j \in c'} \hat{\rho}_{c'}}{\sum_{c' \in \mathcal{C}, i \in c', j \in c'} 1}$, that is we calculate average correlation as the mean of the average correlations of all the cliques the element belongs to.

And finally we build the estimate for the inverse applying the ‘‘Lauritzen formula’’ (16)

$$\hat{J} = \sum_{c \in \mathcal{C}} \left[\left((1 - \theta) \hat{\Sigma}_c + \theta \hat{\Sigma}_c \right)^{-1} \right]^V - \sum_{s \in \mathcal{S}} \left[\left((1 - \theta) \hat{\Sigma}_s + \theta \hat{\Sigma}_s \right)^{-1} \right]^V \quad (19)$$

Remark 18 *The constant correlation estimates $\hat{\Sigma}$ are positive definite because every $\hat{\Sigma}_c$ ($\hat{\Sigma}_s$) is the normalized sum of positive definite matrices.*

Theorem 19 *The MFCE algorithm adds vertices in reverse perfect elimination order, provided that the vertices in the initial cliques C_I are arranged in a reverse perfect order.*

Proof By induction on the number of vertices, let us assume that the total number of vertices is k and that j have been added by the MFCE and that they are ordered in reverse perfect order $\{v_k, v_{k-1}, \dots, v_j\}$. When adding the next vertex v_i it is by construction added to a separator S_i which is complete, and therefore $adj(i) \cap G_j = S_i$ is trivially complete. ■

8. Experiments

8.1 Data

We test the performance of the algorithm on three types of synthetic data and on a real dataset of stocks returns. The synthetic data are multivariate Gaussian generated using respectively: (1) a sparse chordal inverse matrix with known sparsity pattern; (2) a factor model; (3) a random positive definite matrix generated from random eigenvalues and a random rotation. The real example is taken from a long-return series of stock prices. All the datasets used in the experiments have been produced for 100 variables ($p = 100$) and varying time series lengths ($n \in \{25, 50, 75, 100, 200, 300, 400, 500, 750, 1000, 1500\}$). The details about the data generation process are described in the sub-Sections 8.1.1, 8.1.2, 8.1.3 and 8.1.4.

For every type of data we generate the following datasets:

1. The *train data set* which is used to learn the model parameters, such as the MFCE network and the elements of the precision matrix. For every type of data we generate 5 distinct training data sets to test reproducibility.
2. The *validation data set* is used to select the model hyper-parameters: these are the L_1 penalty for the graphical lasso, the shrinkage parameter for the shrinkage method, and the maximum clique size and shrinkage parameter for the MFCE. For all methods we perform a grid search over the hyper-parameters and select the model that achieves the best likelihood on the validation dataset. In analogy with the train data we generate 5 distinct validation data sets.
3. The *test data set* is used to assess the performance of the models. We use 10 distinct test datasets for every training/validation data set and therefore for every data type we have 50 test datasets.

8.1.1 SYNTHETIC DATA: SPARSE DECOMPOSABLE PRECISION MATRIX

This data has been produced with a multivariate model from a sparse inverse covariance matrix (the benchmark precision matrix) where the non-zero structure pattern is a clique forest. The clique forest was generated by applying repeatedly the clique expansion operator with a random choice of the vertices, cliques and separators that were available at any steps.

For every clique $c \in \mathcal{C}$ we have defined a factor F_c distributed as $\mathcal{N}(1, 1)$. Next we add up the factor contributions at the variable level: $X_i = \sum_{\{c \in \mathcal{C} | i \in c\}} F_c + \epsilon_{i,c}$, where $\epsilon_{i,c} \sim \mathcal{N}(0, 0.1)$ is a small noise factor to avoid perfect correlation between the variables in the clique c . Finally we assemble the sparse inverse covariance matrix by using the familiar sum over cliques and separators (see the description of Eq. 16 for the explanation of the notation): $J = \sum_{c \in \mathcal{C}} [(\Sigma_c)^{-1}]^V - \sum_{s \in \mathcal{S}} [(\Sigma_s)^{-1}]^V$.

As an example to help with the intuition, let us consider two cliques c_A and c_B with non empty intersection $S = c_A \cap c_B$. In this case the structure of the precision matrix consists of two blocks that overlap on the variables X_S . This means that the partial correlations of the variables X_A and X_B , controlling for X_S , are all zero, and this in turn means that $X_A \perp\!\!\!\perp X_B | X_S$. In the particular case where $S = \emptyset$, the variables X_A and X_B are unconditionally independent.

The exact inverse of the precision matrix has been used to generate the training, validation and test data sets, using the function `mvrnorm` of the package MASS (Venables and Ripley, 2002) developed for the R language (R Core Team, 2016).

8.1.2 SYNTHETIC DATA: FULL POSITIVE DEFINITE MATRIX FROM PACKAGE “CLUSTERGENERATION”

This data has been generated using the R package “clusterGeneration” (Qiu and Joe, (2015)). The methodology is to produce a vector of random eigenvalues ($p = 100$ values in the range $[0.01, 100]$ in this experiment) and to rotate the diagonal matrix of eigenvalues with a random orthogonal matrix to produce a dense positive definite matrix that is used as the benchmark reference covariance. As in the previous example the generation of the data sets has been carried out using the package ‘MASS’ as described in 8.1.1.

8.1.3 RANDOM FACTOR MODEL WITH NOISE

This data set has been generated by building a factor model with 5 factors. For a review of factor models, with particular regards to large factor models see Bai et al. (2008); here we follow their conventions and model the variables \mathbf{X} as $\mathbf{X} = \mathbf{\Lambda}\mathbf{F} + \epsilon$ where: \mathbf{F} is an $f \times n$ matrix, with $f < p$ the number of factors, $\mathbf{\Lambda}$ is the $p \times f$ matrix of *factor loadings* and ϵ is the $p \times n$ idiosyncratic term.

Accordingly, the correlation matrix breaks down in two parts: $\mathbf{\Sigma} = \mathbf{\Lambda}\mathbf{\Lambda}' + \mathbf{\Omega}$, where $\mathbf{\Lambda}\mathbf{\Lambda}'$ is the systematic component and $\mathbf{\Omega}$ is the idiosyncratic component .

The training, validation and test matrices have been generated using $f = 5$. The factor loadings have been randomly generated from independent normal distribution and the factors have been generated as independent normal variates. As the factor loadings are in general different from zero, this model is dense.

8.1.4 REAL DATA

This data set contains a set of stock returns for 342 companies over 4025 trading days, as described in Barfuss et al. (2016). For every training, validation and test execution we have sampled randomly without replacement $p = 100$ time series. The training, validation and testing datasets have been sampled taking days, with replacement, from the total time series of 4025 trading days.

The estimate of the ‘real’ reference covariance matrix has been produced using the full dataset, and this has been used as a benchmark for the estimates produced by the models.

8.2 Performances indicators

For every test set we collect the following performance indicators: ¹³

1. Log likelihood, which is $\frac{p}{2} \left(\log |J| - \text{Tr} \left(\hat{\Sigma} \cdot J \right) \right)$ (consistently with the definition of the objective function used in the R package glasso we omit the constant). Please note that J is the precision matrix estimated using the training dataset, while $\hat{\Sigma}$ is the sample correlation estimated on the test dataset.
2. *Accuracy* = $\frac{TP+TN}{TP+TN+FP+FN}$, which is the fraction of entries in the precision matrix J that are correctly predicted as zero or non-zero.
3. *Sensitivity* = $\frac{TP}{TP+FN}$, which is the fraction of non-zero entries in the precision matrix J that are correctly predicted by the models.
4. *Specificity* = $\frac{TN}{TN+FP}$, which is the fraction of zero entries in the precision matrix J that are correctly predicted by the model.
5. The *correlation* of the estimated precision matrix with the true precision matrix (which is known in the case of synthetic data) or with the maximum likelihood estimate of the precision matrix computed on the longest possible data set (in the

13. We define: TP (True Positives) as the count of elements in the precision matrix that are correctly predicted as different from zero, TN (True Negatives) as the count of elements in the precision matrix that are correctly predicted as zero, and FP (False Positives) and FN (False Negatives) in analogous fashion. This is possible only when the ‘true’ precision matrix is known (synthetic data) and these measures are meaningful only when it is sparse.

case of real data). The correlation is calculated as if the two matrices were vectors in \mathbb{R}^{p^2} .

6. *Eigenvalue distance* is the \mathbb{R}^2 norm of the vector of differences of the eigenvalues of the real or maximum-likelihood estimate precision matrix and the estimated precision matrix $\left(\sum_{i=1}^p (\hat{\lambda}_i - \lambda_i)^2\right)^{\frac{1}{2}}$.
7. *Eigenvalue inverse distance* is the \mathbb{R}^2 norm of the the vector of differences of the reciprocal of the eigenvalues of the real or maximum-likelihood estimate precision matrix and the estimated precision matrix $\left(\sum_{i=1}^p (\hat{\lambda}_i^{-1} - \lambda_i^{-1})^2\right)^{\frac{1}{2}}$.

8.3 Results

8.3.1 SYNTHETIC DATA: SPARSE DECOMPOSABLE PRECISION MATRIX

Figure 11 provides a box plot representing the mean the confidence interval and the extreme values of the log-likelihood achieved by the algorithms over the test data sets, broken down by the length of the series¹⁴. We observe that, in all cases, the MFCF algorithms outperform both the graphical lasso and the shrinkage estimator. The graphical lasso improves performances as the length increases but does not exceeds MFCFs. The dispersion around the mean is similar for all methods and it has been computed by repeating the experiments on 50 independent datasets (10 testing sets for each 5 training and validating sets, as explained in 8.1).

Table 3 reports the average value of the graphical lasso penalty parameter and of the shrinkage parameter as selected by the grid search. As expected, the parameters become smaller as the series length grows, with MFCFs requiring less shrinkage/penalisation than the other methodologies¹⁵, especially with short time series. We believe that this is a desirable feature of the MFCF algorithm: the topological constraint allows to estimate with good accuracy the cliques with high likelihood, and excludes edges with low likelihood with the end effect of requiring less shrinking.

Table 4 reports the number of non zero elements in the precision matrix for every length of the time series. One can observe that the MFCF algorithms are much more parsimonious than the graphical lasso (the shrinkage method produces always a full precision matrix).

Figure 12 shows a summary of the performance measures. We observe that that the MFCF family is better, overall, than the graphical lasso especially for what concerns accuracy and specificity. While the graphical lasso is more sensitive picking up more true positives. However, it is also less selective and produces denser precision matrices with a much higher number of false negatives. We observe that the performance of the graphical lasso improves in all measures for time series of length greater than 200, when the penalty parameter is essentially fixed at 0.01. The MFCF exhibit better log-likelihood, as already observed, and also larger correlations with the true precision matrix.

Figure 13 shows the distance between the spectra of the precision matrix produced by the models and the true precision matrix. The measure is normalised so that the identity matrix has distance one. We observe that the MFCF algorithms always perform better

14. The boxplots in this paper have been produced with the R (R Core Team, 2016) package GGPlot2 (Wickham, 2009). According to the package documentation the first lower and upper hinges correspond to the first and third quantile, the upper whisker covers the values form the third quartile hinge to 1.5 times the inter-quartile range away from the hinge, and similarly the lower whisker covers the

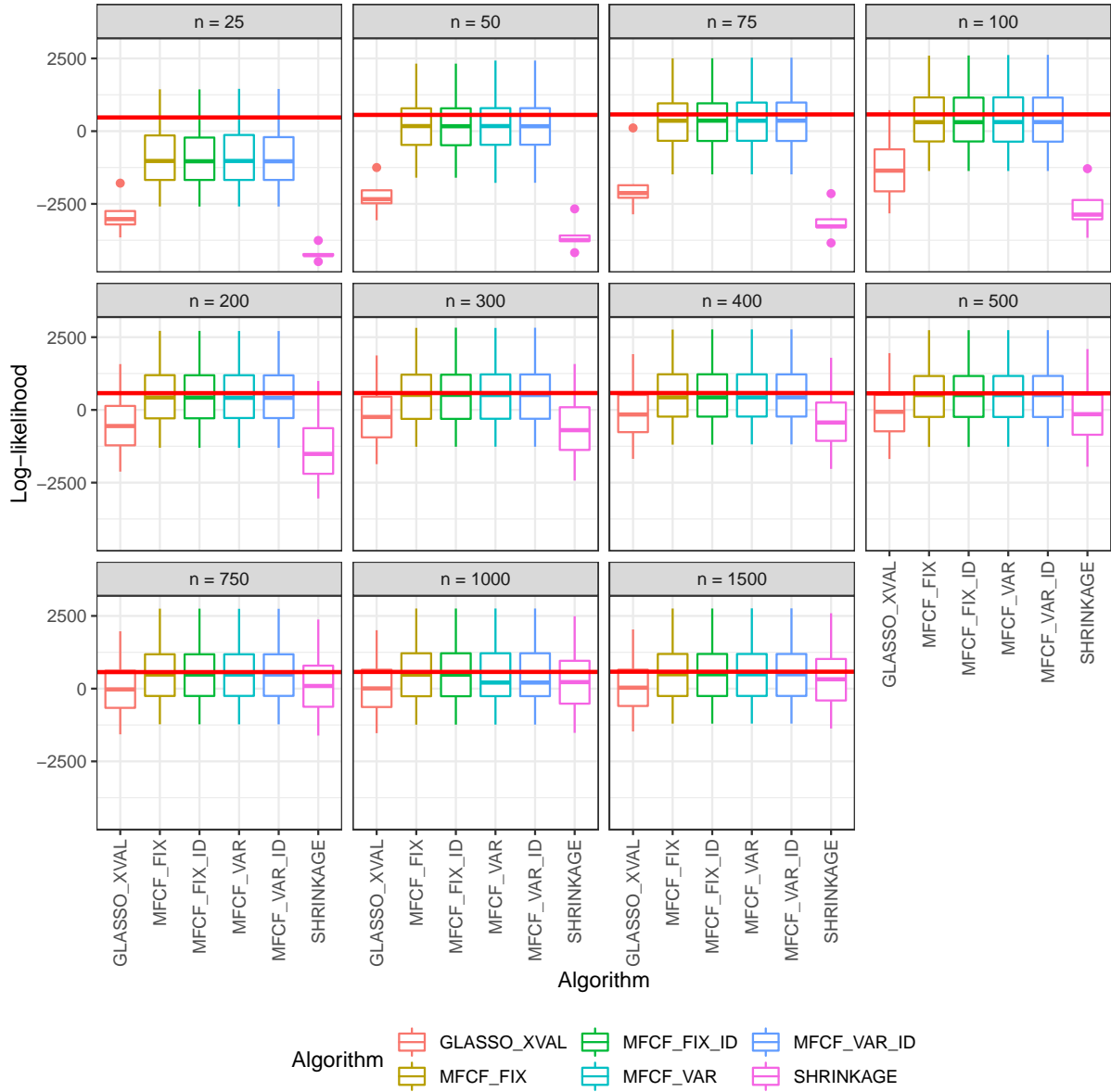


Figure 11: Box plot for the log-likelihood of the algorithms on synthetic data (sparse decomposable precision matrix) for different lengths of the series. The statistics is based on a total of 50 test sets (10 test sets for each of 5 different training / validation sets).

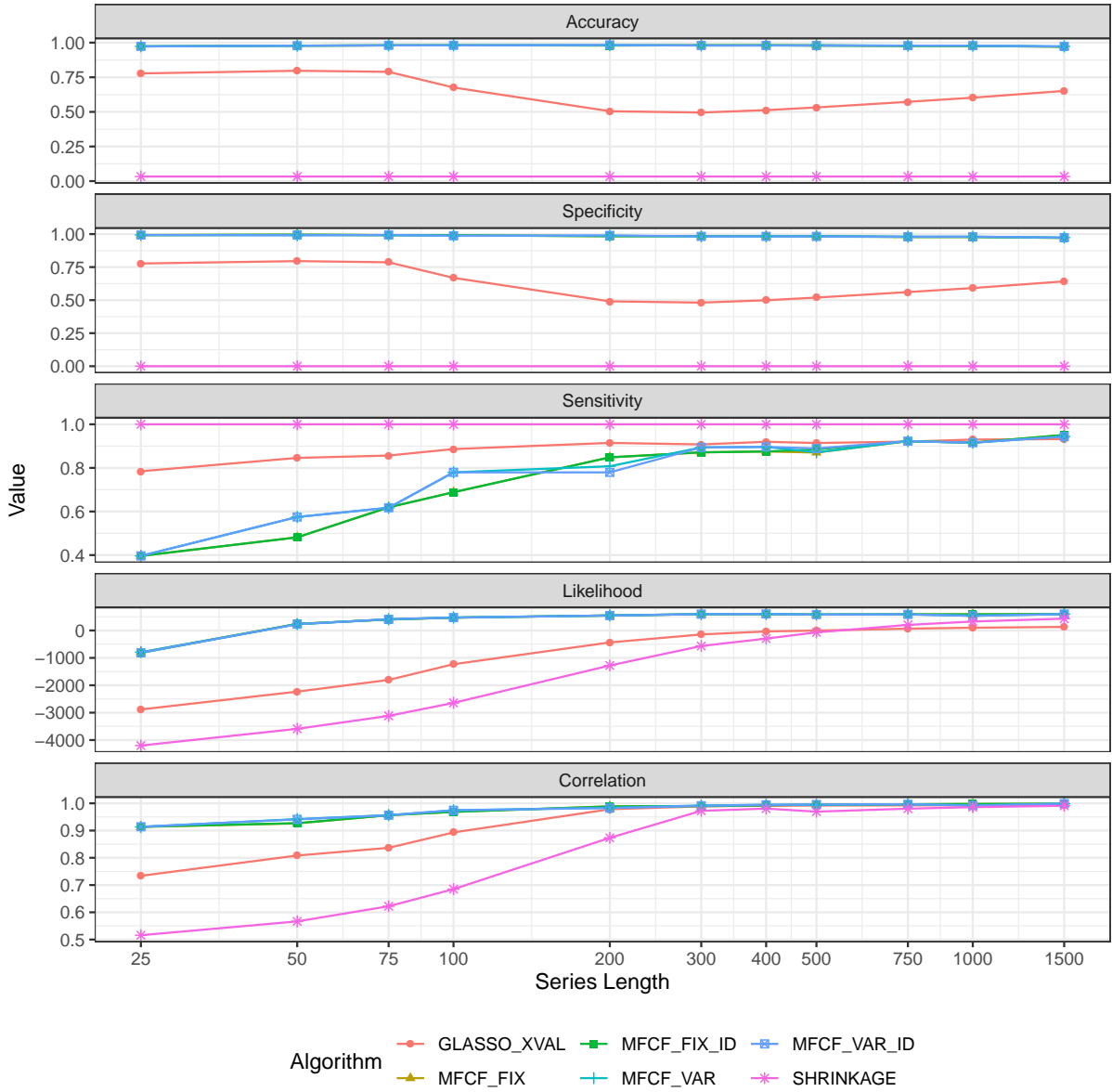


Figure 12: Performance measures of the algorithms on synthetic data (sparse decomposable precision matrix) for different lengths of the series. The statistics is based on a total of 50 test sets (10 test sets for each of 5 different training / validation sets).

Series length	GLASSO XVAL	MFCF FIX	MFCF FIX ID	MFCF VAR	MFCF VAR ID	SHRINKAGE
25	0.150	0.005	0.005	0.005	0.005	0.726
50	0.120	0.002	0.002	0.002	0.001	0.522
75	0.102	0.002	0.001	0.002	0.001	0.374
100	0.056	0.001	0.001	0.001	0.001	0.257
200	0.014	0.001	0.001	0.001	0.001	0.074
300	0.011	0.001	0.000	0.001	0.000	0.022
400	0.010	0.000	0.000	0.000	0.000	0.020
500	0.010	0.000	0.000	0.000	0.000	0.004
750	0.010	0.000	0.000	0.000	0.000	0.000
1000	0.010	0.000	0.000	0.000	0.000	0.000
1500	0.010	0.000	0.000	0.000	0.000	0.000

Table 3: Mean penalty (GLASSO_XVAL) or shrinkage parameters by length of time series. The statistics is based on 5 different calibrations (one per each training / validation set) of the shrinkage parameters per each length of the time series.

Series length	GLASSO XVAL	MFCF FIX	MFCF FIX ID	MFCF VAR	MFCF VAR ID	SHRINKAGE
25	1194	99	99	98	98	4950
50	1118	99	99	135	135	4950
75	1161	138	138	136	136	4950
100	1730	158	158	191	191	4950
200	2586	216	216	195	176	4950
300	2632	216	216	231	231	4950
400	2549	216	216	231	231	4950
500	2451	216	236	213	231	4950
750	2254	255	255	246	246	4950
1000	2108	255	255	244	244	4950
1500	1867	294	294	281	281	4950

Table 4: Mean number of non-zero coefficient in the precision matrix by length of time series. The statistics is based on 5 different calibrations (one per each training / validation set) per each length of the time series.

and the performance improves for all methods as the time series length increases, with the exception of the graphical lasso in the region where the penalty parameter is floored at 0.01.

Figure 14 shows the distance between the inverse spectra of the precision matrix (λ_i^{-1}) produced by the models and the ones for the true precision matrix. We observe that the MFCF algorithms perform slightly better than the graphical lasso and shrinkage but performance is very similar. Interestingly, in this case, the distance decreases with the time series length for all algorithms and there is no apparent effect due to the flooring of the graphical lasso penalty parameter.

Figure 15 shows the number of cliques of different size produced by the MFCF_VAR algorithm as a function of the maximum allowed clique size and of the time series length. We note that as the time series length increases the test becomes less stringent with a

values between the first quartile hinge and 1.5 times the interquartile range below the hinge. The remaining points are considered outliers and plotted individually.

15. The comparison of penalty and shrinkage parameter is purely indicative, as the two parameters are not directly comparable.

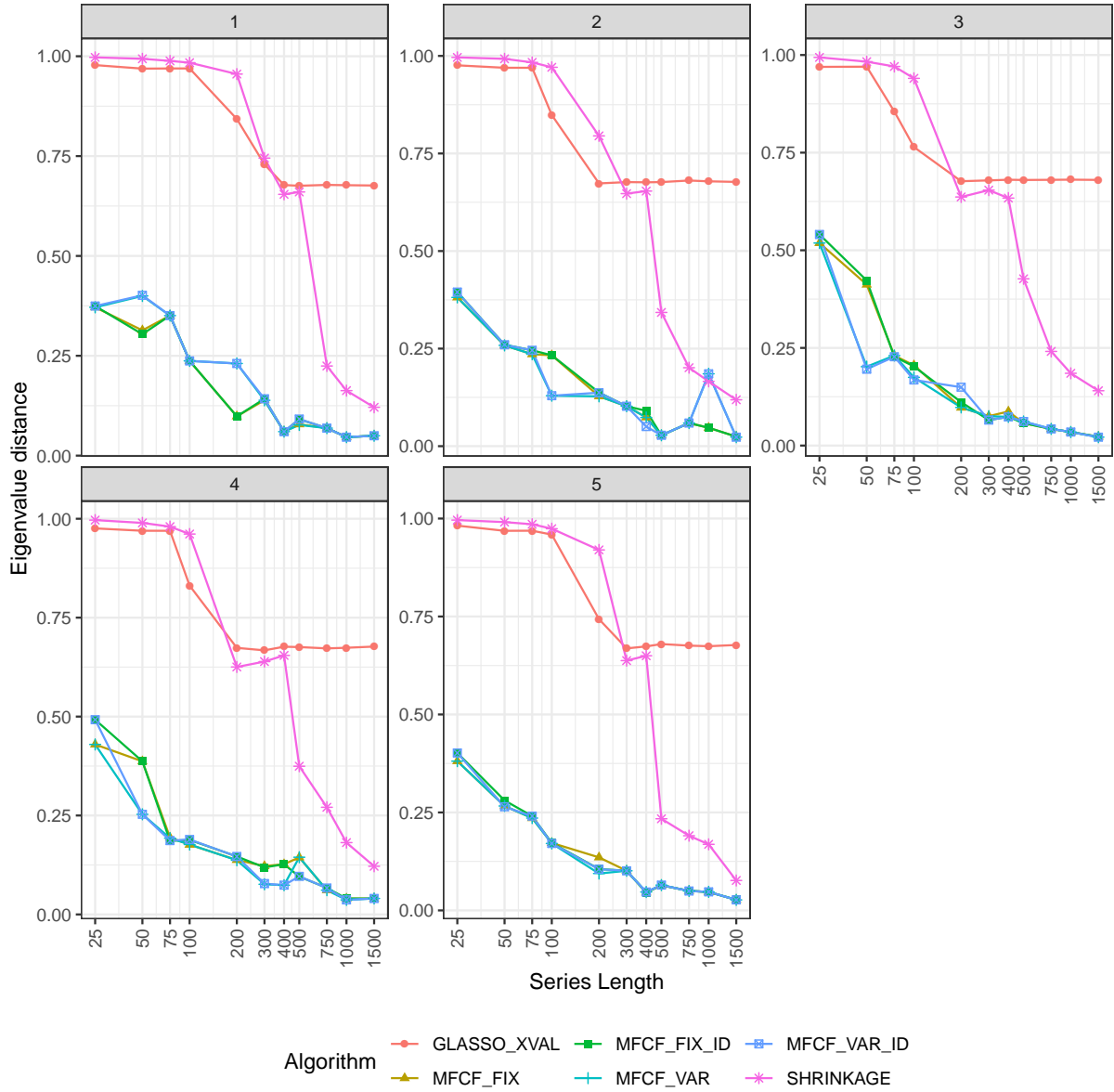


Figure 13: Eigenvalue distance for synthetic data (sparse decomposable precision matrix). The five panels show the values at different time series lengths for 5 training / validation datasets.

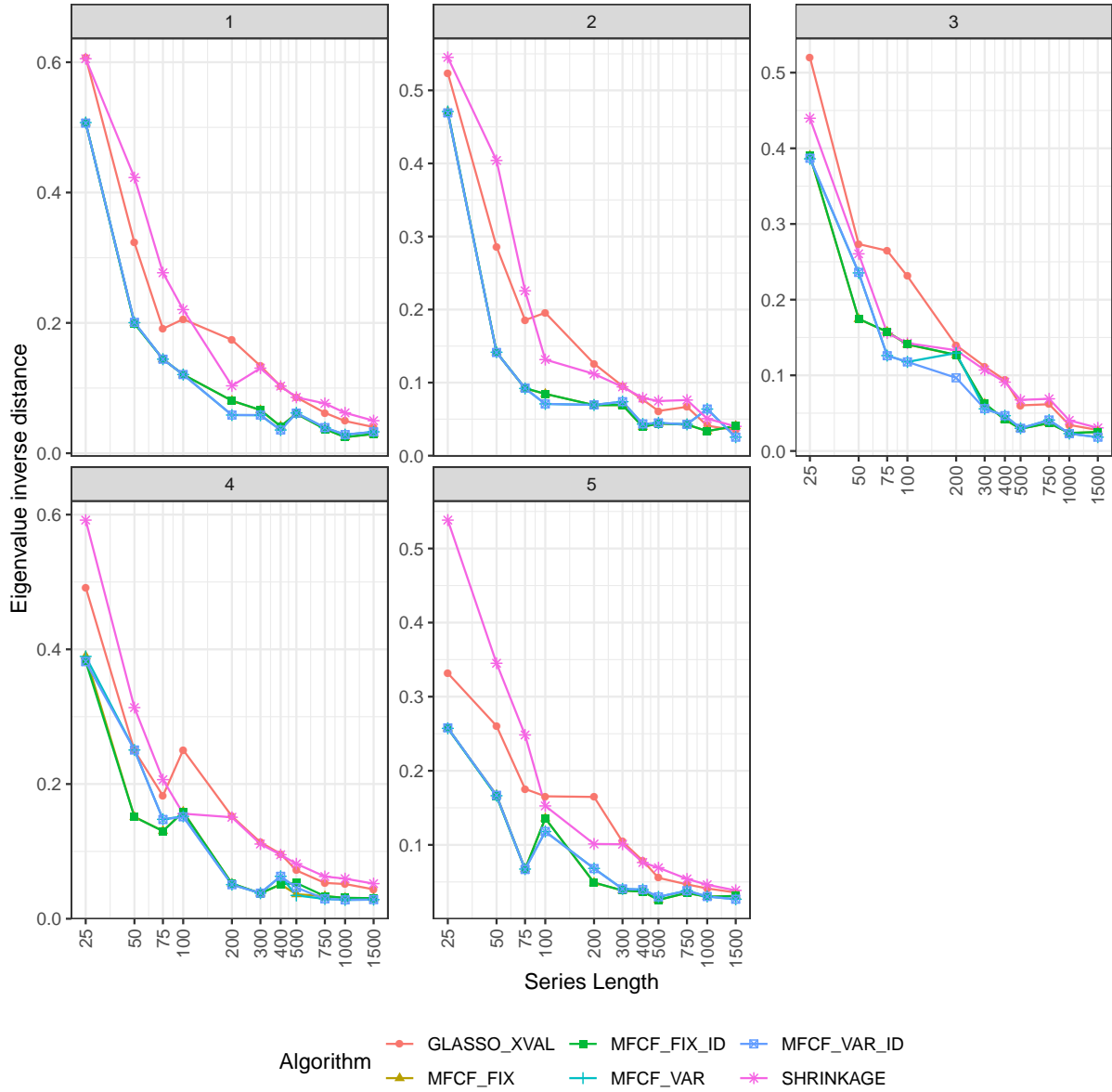


Figure 14: Inverse eigenvalue distance for synthetic data (sparse decomposable precision matrix). The five panels show the values at different time series lengths for 5 training / validation datasets.

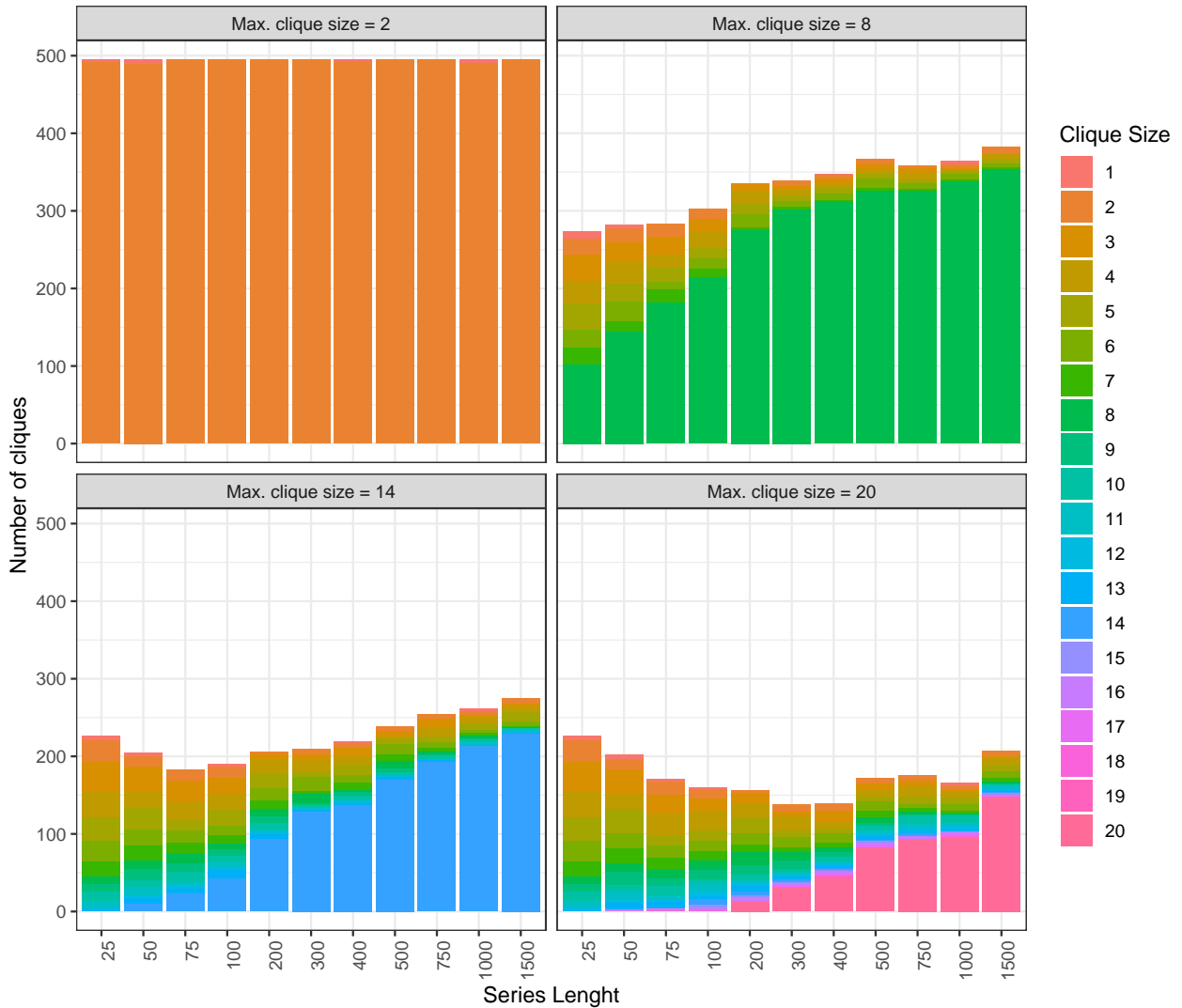


Figure 15: Composition of cliques from MFCF_VAR for synthetic data (sparse decomposable precision matrix). The statistics is based on a total of 5 different training / validation sets.

higher number of large cliques in the model; conversely, when the time series is shorter ($n < p$), the models produced are more parsimonious. The number of cliques of size smaller than the maximum is linked to the degree of sparsity of the model. We will see in Section 8.3.3 that in the case of systems that are inherently dense the vast majority of the cliques will have the maximum allowed clique size.

8.3.2 SYNTHETIC DATA: FULL POSITIVE DEFINITE MATRIX FROM PACKAGE “CLUSTERGENERATION”.

In this sub-section and in the next two we repeat on different datasets all the analyses described in the previous subsection 8.3.1. Figure 16 displays the log-likelihood of the models. We observe that MFCF algorithms perform overall better than either GLASSO or SHRINKAGE, but is worth noting the overall low level of the log-likelihood for all models. In particular the GLASSO performs worse than the null hypothesis (which has log-likelihood of 5000) for short time series. From Table 5 we observe that the penalty

or shrinkage parameters decrease but they retain higher overall values than in the other examples.

Series length	GLASSO XVAL	MFCF FIX	MFCF FIX ID	MFCF VAR	MFCF VAR ID	SHRINKAGE
25	0.33	0.97	0.95	0.99	0.99	0.99
50	0.24	0.97	0.89	0.97	0.91	0.99
75	0.22	0.94	0.88	0.95	0.87	0.95
100	0.17	0.88	0.83	0.90	0.83	0.93
200	0.12	0.85	0.75	0.86	0.77	0.89
300	0.12	0.73	0.64	0.72	0.62	0.86
400	0.12	0.63	0.55	0.63	0.54	0.84
500	0.12	0.56	0.48	0.54	0.46	0.80
750	0.10	0.40	0.36	0.39	0.38	0.76
1000	0.08	0.34	0.31	0.32	0.28	0.71
1500	0.05	0.20	0.18	0.20	0.18	0.62

Table 5: Mean penalty/shrinkage parameter by length of time series. The statistics is based on a total of 5 different training / validation sets per length of the time series.

Table 6 shows the number of non zero elements in the precision matrix for every length of the time series. We note that the statistically validated methods MFCF_VAR and MFCF_VAR.ID produce consistently sparser models, without significant deterioration on the performance in terms of log-likelihood or correlation.

Series length	GLASSO XVAL	MFCF FIX	MFCF FIX ID	MFCF VAR	MFCF VAR ID	SHRINKAGE
25	484	1062	1164	234	36	4950
50	459	465	679	250	276	4950
75	343	592	1129	255	353	4950
100	472	555	757	247	308	4950
200	472	351	687	238	301	4950
300	260	352	466	272	382	4950
400	155	331	369	272	343	4950
500	108	294	351	297	364	4950
750	165	370	408	330	428	4950
1000	171	313	427	292	336	4950
1500	922	313	313	282	349	4950

Table 6: Mean number of non-zero coefficient in the precision matrix by length of time series. The statistics is based on a total of 5 different training / validation sets per length of the time series.

The measures of performance are reported in Figures 16-20. We note that the MFCF_FIX and MFCF_FIX.ID are more accurate for short time series as they pick up many more matrix elements than the validated methods, but this does not translate in improvements for the other measures of performance. The MFCF methods seem to perform better than GLASSO and SHRINKAGE also when it comes to distance of the eigenvalues, especially with short time series. Interestingly, the composition of the clique structure produced by the MFCF_VAR shown in Figure 20 suggests that even for medium and long time series the algorithm produces a mostly small or large cliques with only a small fraction of cliques with intermediate sizes.

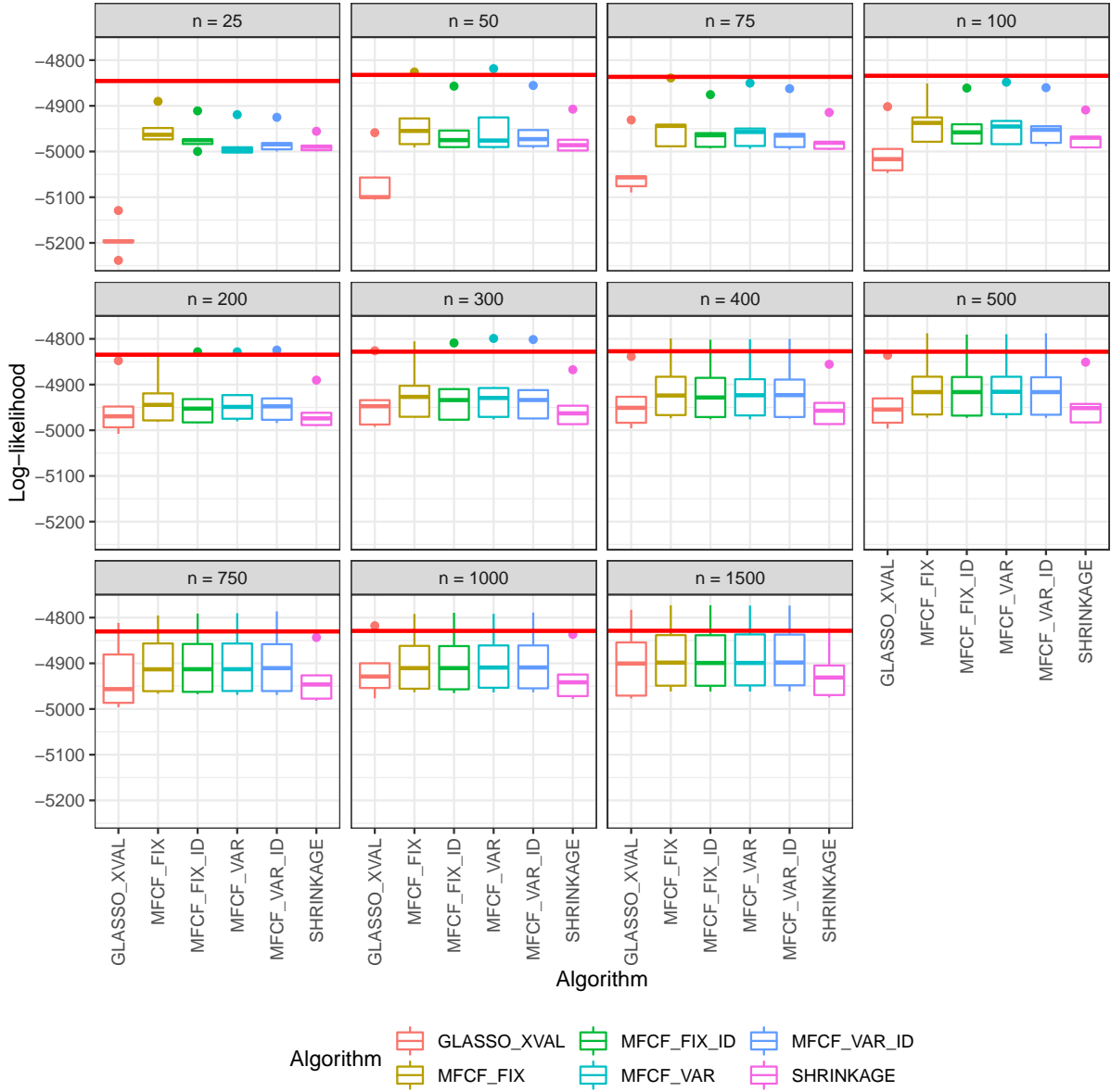


Figure 16: Box plot for the likelihood of the algorithms on synthetic data (random positive definite matrix generated by ClusterGen) for different lengths of the series. The statistics is based on a total of 50 test sets (10 test sets for each of 5 different training / validation sets) per length of the time series.

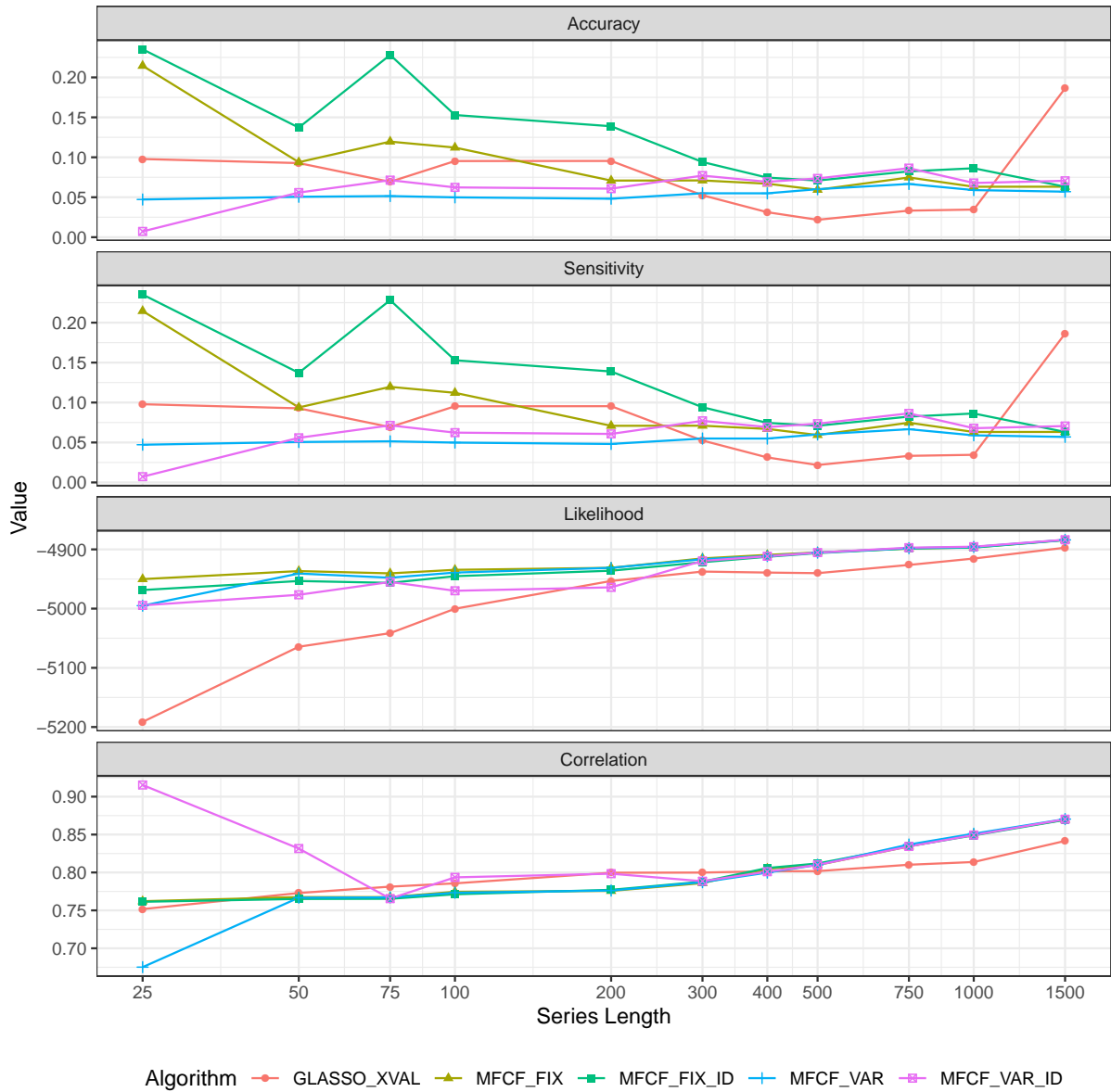


Figure 17: Performance of the algorithms on synthetic data (random positive definite matrix generated by ClusterGen) for different lengths of the series. The statistics is based on a total of 50 test sets (10 test sets for each of 5 different training / validation sets).

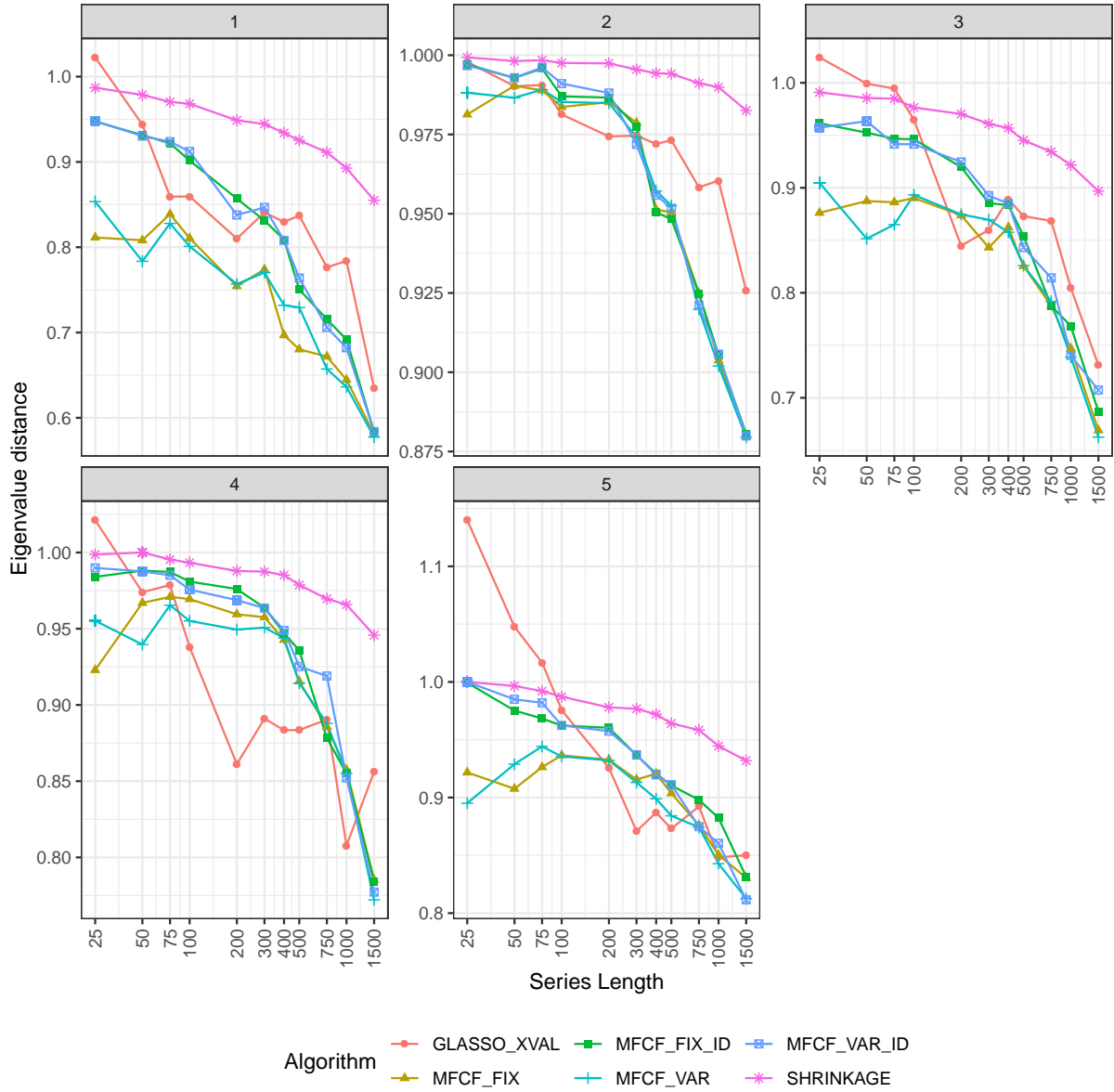


Figure 18: Eigenvalue distance for synthetic data (random positive definite matrix generated by ClusterGen). The five panels show the values at different time series lengths for 5 training / validation datasets.

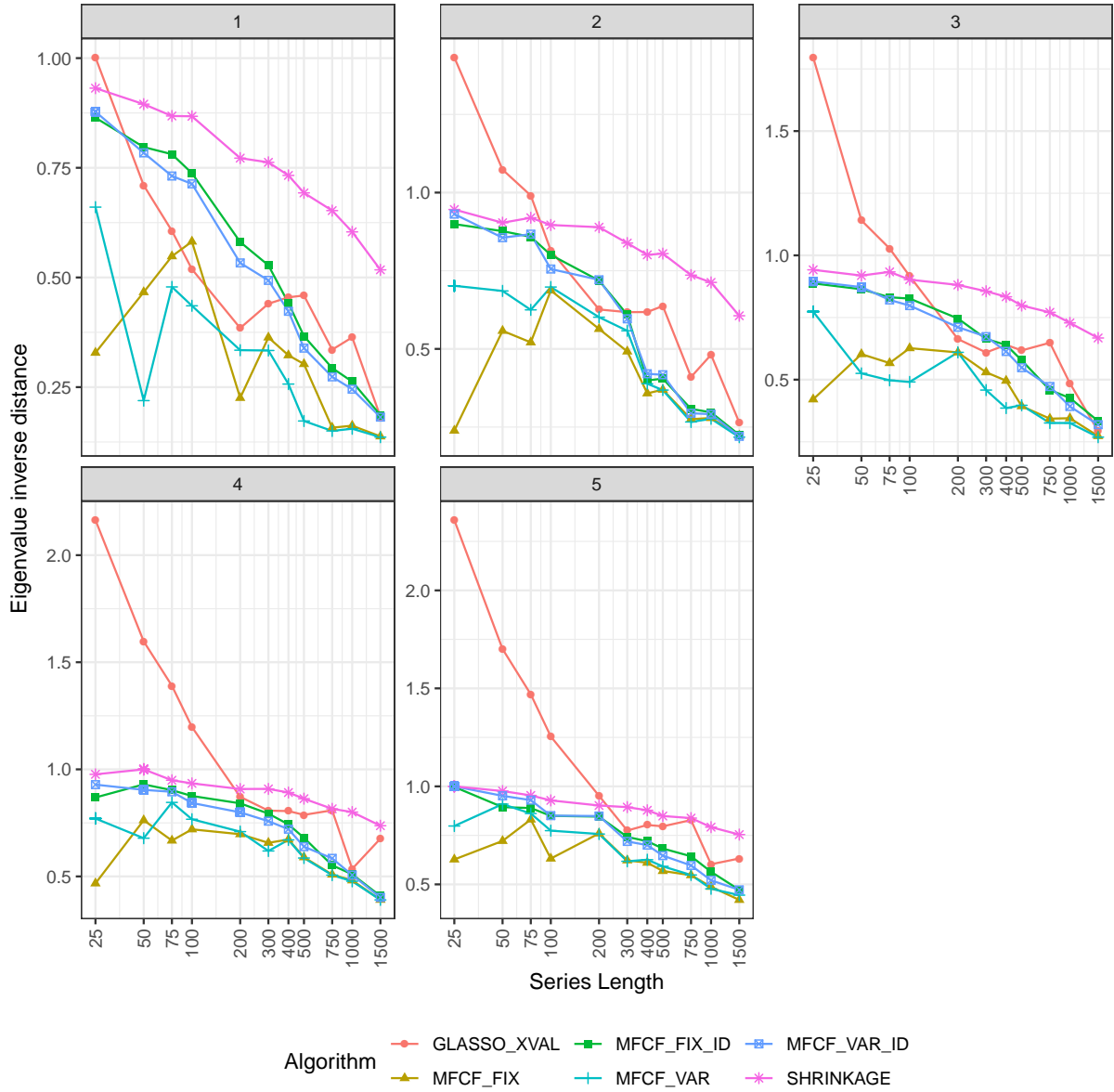


Figure 19: Inverse eigenvalue distance for synthetic data (random positive definite matrix generated by ClusterGen). The five panels show the values at different time series lengths for 5 training / validation datasets.

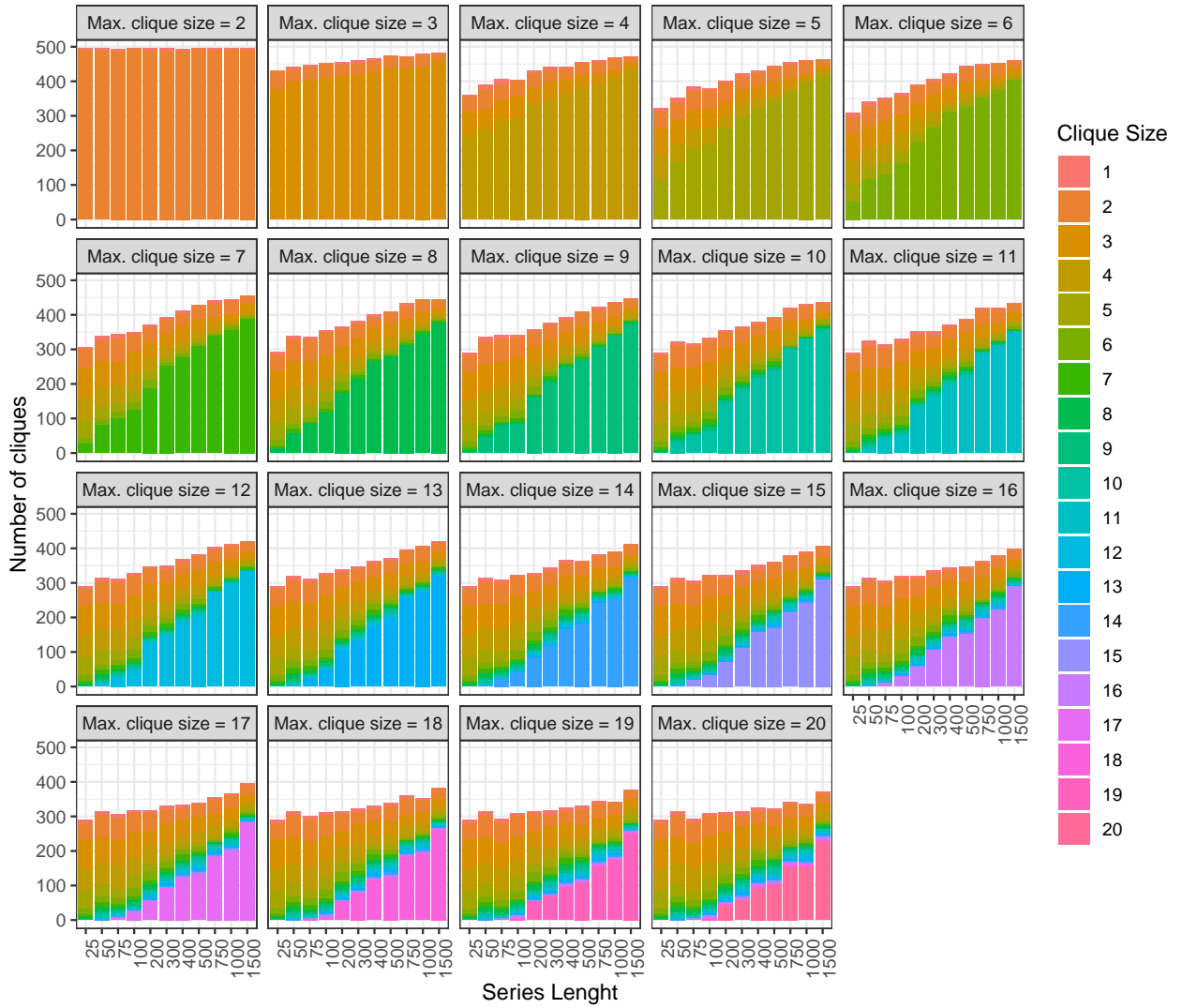


Figure 20: Composition of cliques from MF_{CF}_VAR for synthetic data (random positive definite matrix generated by ClusterGen). The statistics is based on a total of 5 different training / validation sets per length of the time series.

8.3.3 RANDOM FACTOR MODEL WITH NOISE

Performance measures are reported in Figures 21-25. As discussed in Section 8.1, the loadings to the 5 factors are different from zero for every time series, and therefore the model is not suitable for local algorithms such as the MFCF; this would probably explain why in this instance the GLASSO performs better in terms of almost all measures. Table 7 shows that the behaviour of the shrinkage or penalty parameters are decreasing with series length as expected. Table 8 highlights how all the models tend to use as many parameters as possible, consistently with the constraints imposed on penalty and clique size. Figure 25 supports the idea that the underlying model is non local, since the validated methods tend to use exclusively the largest cliques allowed by the constraints. This suggests that the analysis of the clique sizes might provide insight into the sparsity of the data set, when the data generation process is not known.

Series length	GLASSO XVAL	MFCF FIX	MFCF FIX ID	MFCF VAR	MFCF VAR ID	SHRINKAGE
25	0.12	0.27	0.26	0.25	0.25	0.30
50	0.12	0.19	0.18	0.18	0.18	0.23
75	0.09	0.15	0.14	0.15	0.15	0.20
100	0.06	0.13	0.13	0.12	0.12	0.18
200	0.02	0.08	0.08	0.08	0.08	0.14
300	0.01	0.06	0.06	0.06	0.06	0.11
400	0.01	0.05	0.05	0.05	0.05	0.09
500	0.01	0.04	0.04	0.04	0.04	0.08
750	0.01	0.03	0.03	0.03	0.03	0.06
1000	0.01	0.02	0.02	0.02	0.02	0.04
1500	0.01	0.01	0.01	0.01	0.01	0.04

Table 7: Mean penalty/shrinkage parameter by length of time series. The statistics is based on a total of 5 different training / validation sets per length of the time series.

Series length	GLASSO XVAL	MFCF FIX	MFCF FIX ID	MFCF VAR	MFCF VAR ID	SHRINKAGE
25	1168	1694	1661	1582	1597	4950
50	1206	1677	1661	1694	1694	4950
75	1308	1661	1661	1678	1678	4950
100	1648	1710	1710	1645	1645	4950
200	2143	1710	1710	1678	1694	4950
300	2426	1710	1694	1694	1694	4950
400	2568	1710	1710	1710	1710	4950
500	2814	1694	1694	1694	1694	4950
750	2760	1694	1694	1694	1694	4950
1000	2755	1710	1710	1678	1678	4950
1500	2761	1694	1694	1710	1710	4950

Table 8: Mean number of non-zero coefficient in the precision matrix by length of time series. The statistics is based on a total of 5 different training / validation sets per length of the time series.

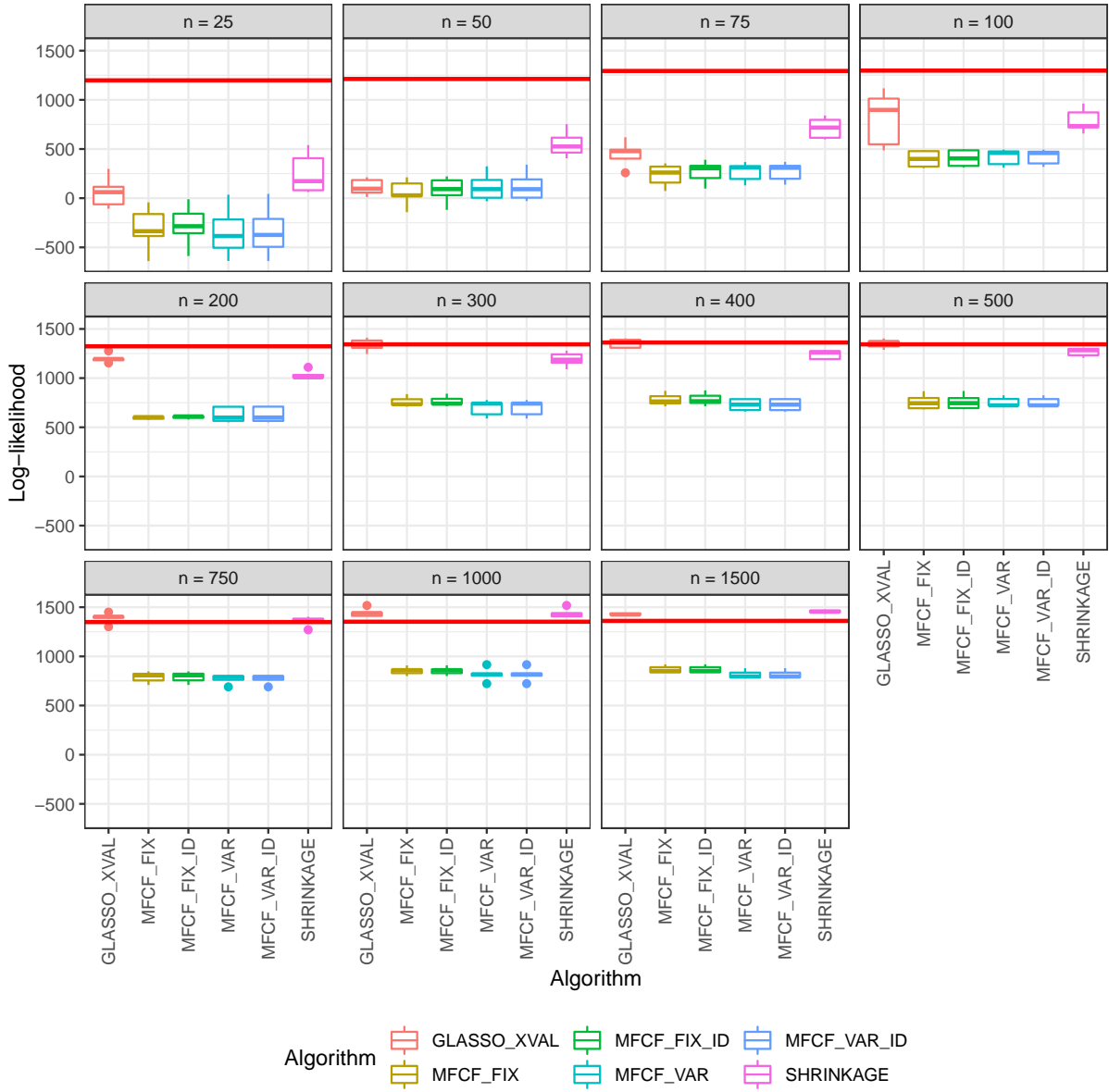


Figure 21: Box plot for the likelihood of the algorithms on synthetic data (factor model) for different lengths of the series. The statistics is based on a total of 50 test sets (10 test sets for each of 5 different training / validation sets) per length of the time series.

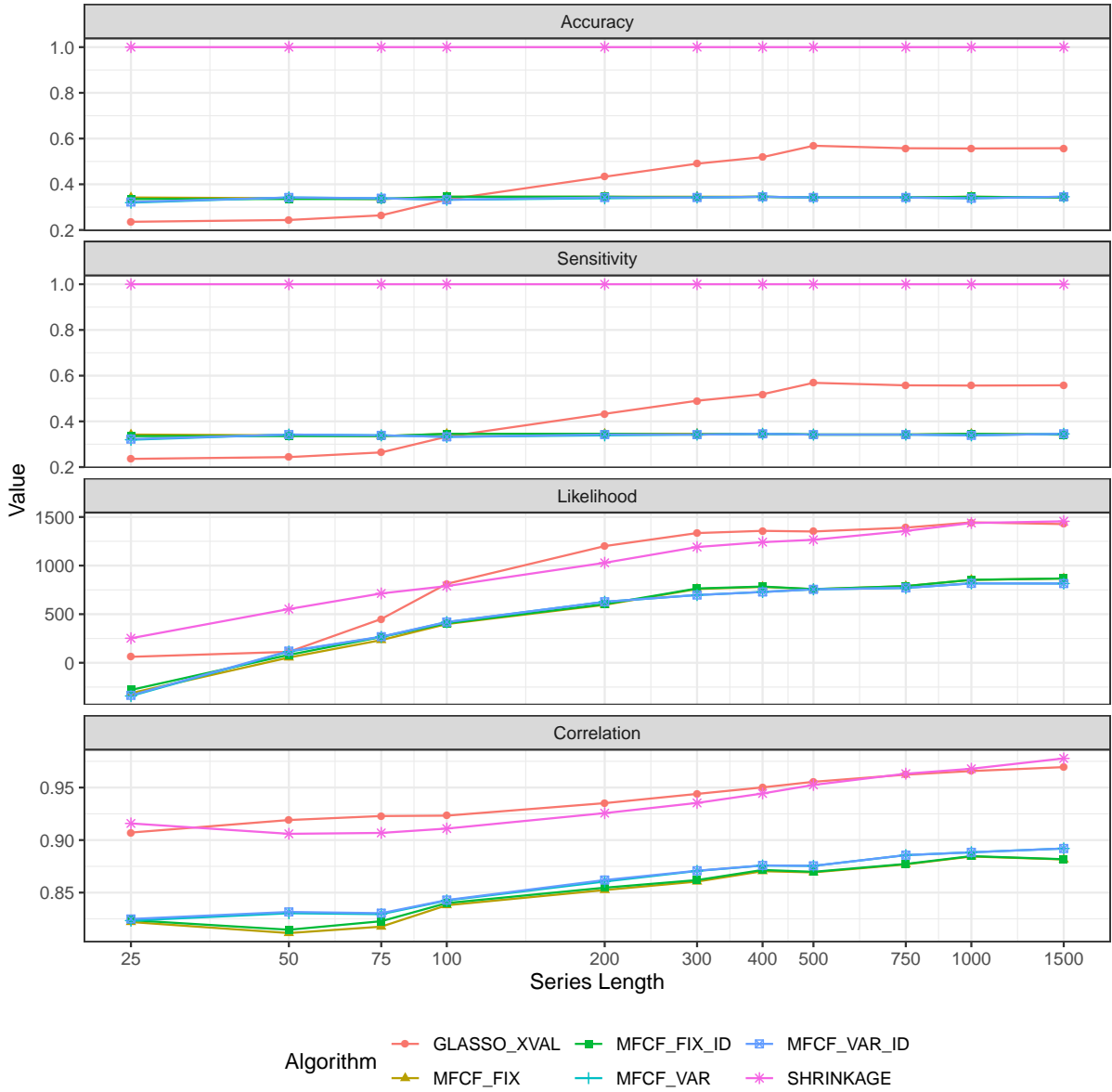


Figure 22: Performance of the algorithms on synthetic data (factor model) for different lengths of the series. The statistics is based on a total of 50 test sets (10 test sets for each of 5 different training / validation sets) per length of the time series.

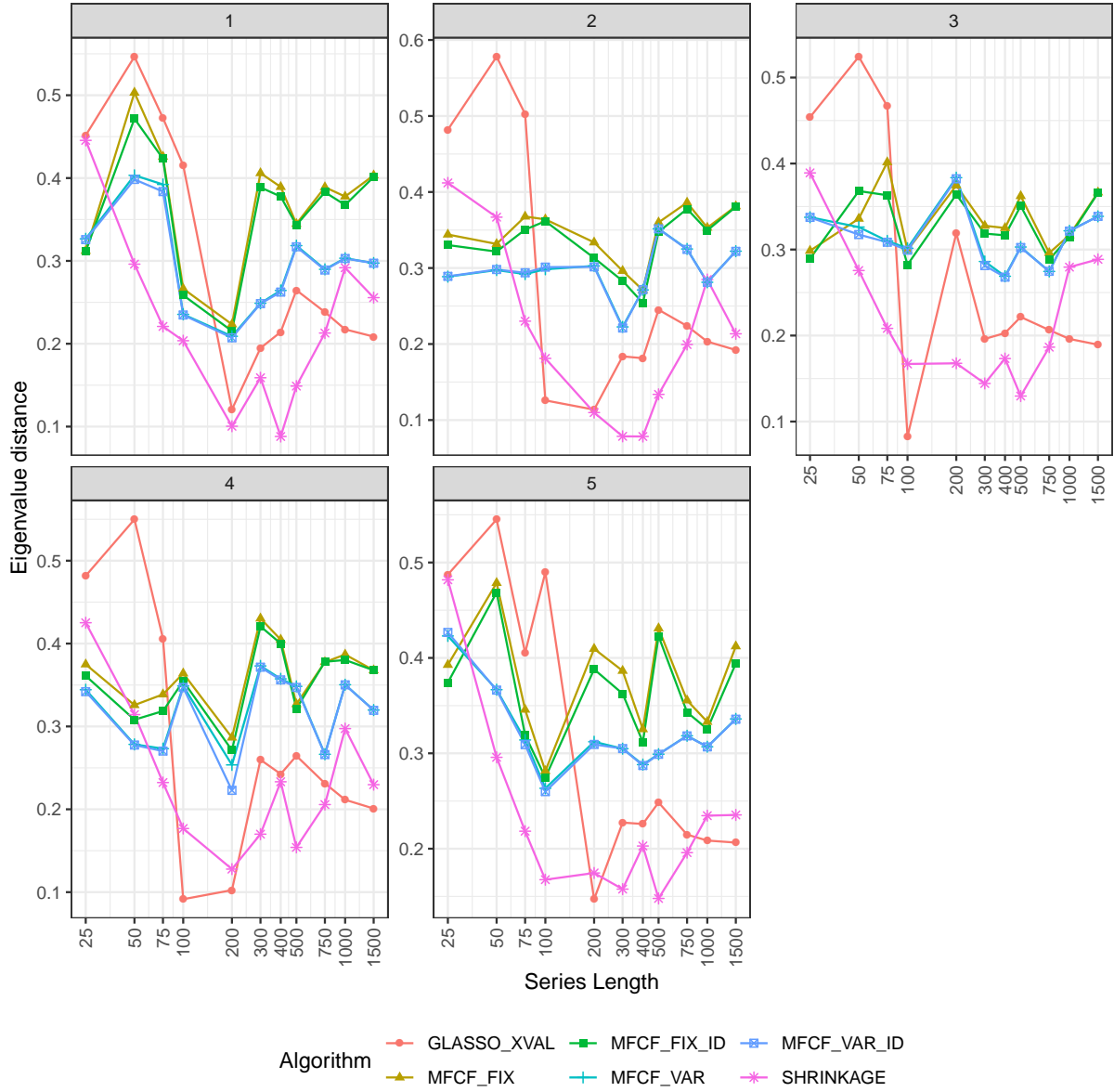


Figure 23: Eigenvalue distance for synthetic data (factor model). The five panels show the values at different time series lengths for 5 training / validation datasets.

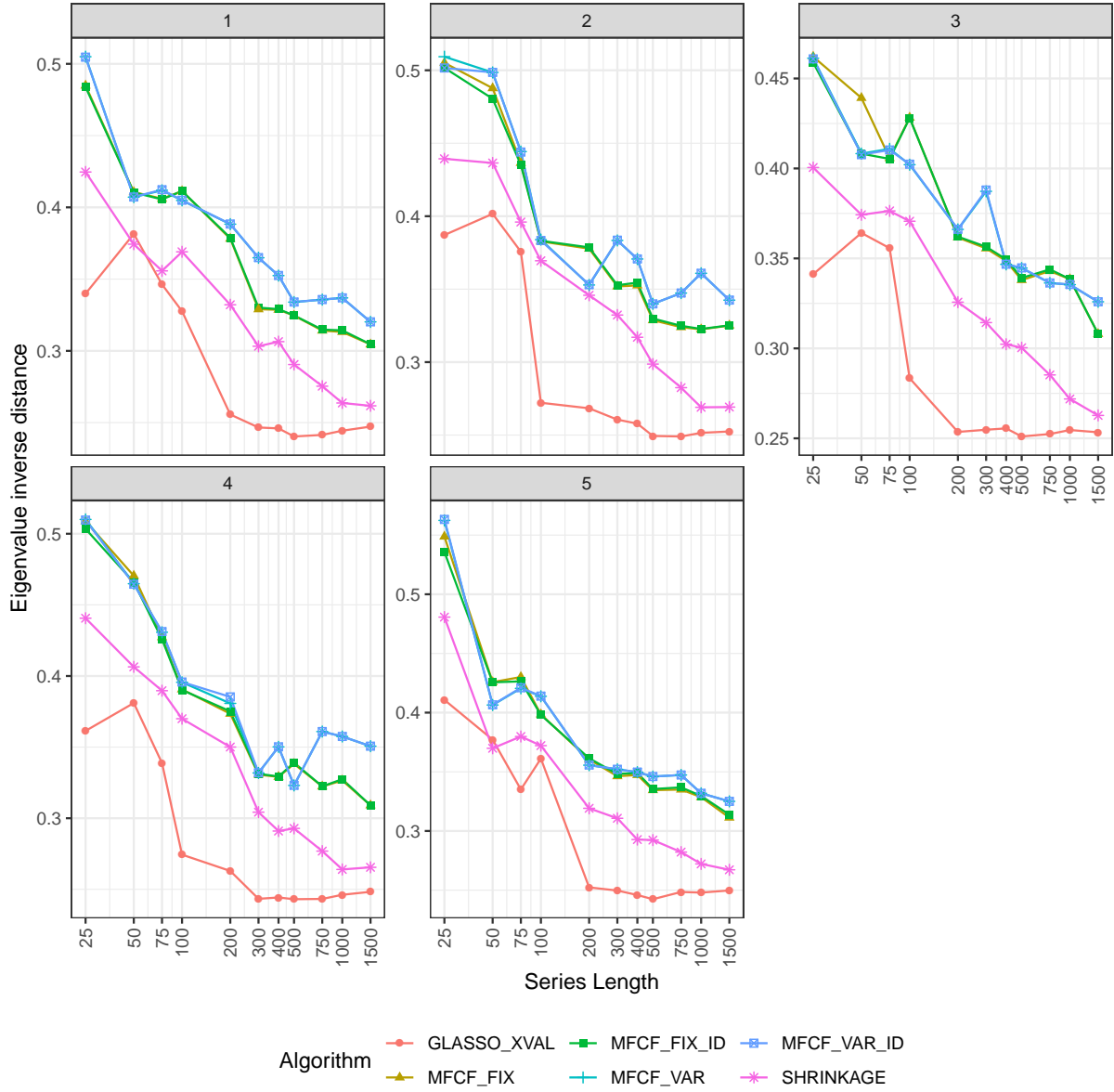


Figure 24: Inverse eigenvalue distance for synthetic data (factor model). The five panels show the values at different time series lengths for 5 training / validation datasets.

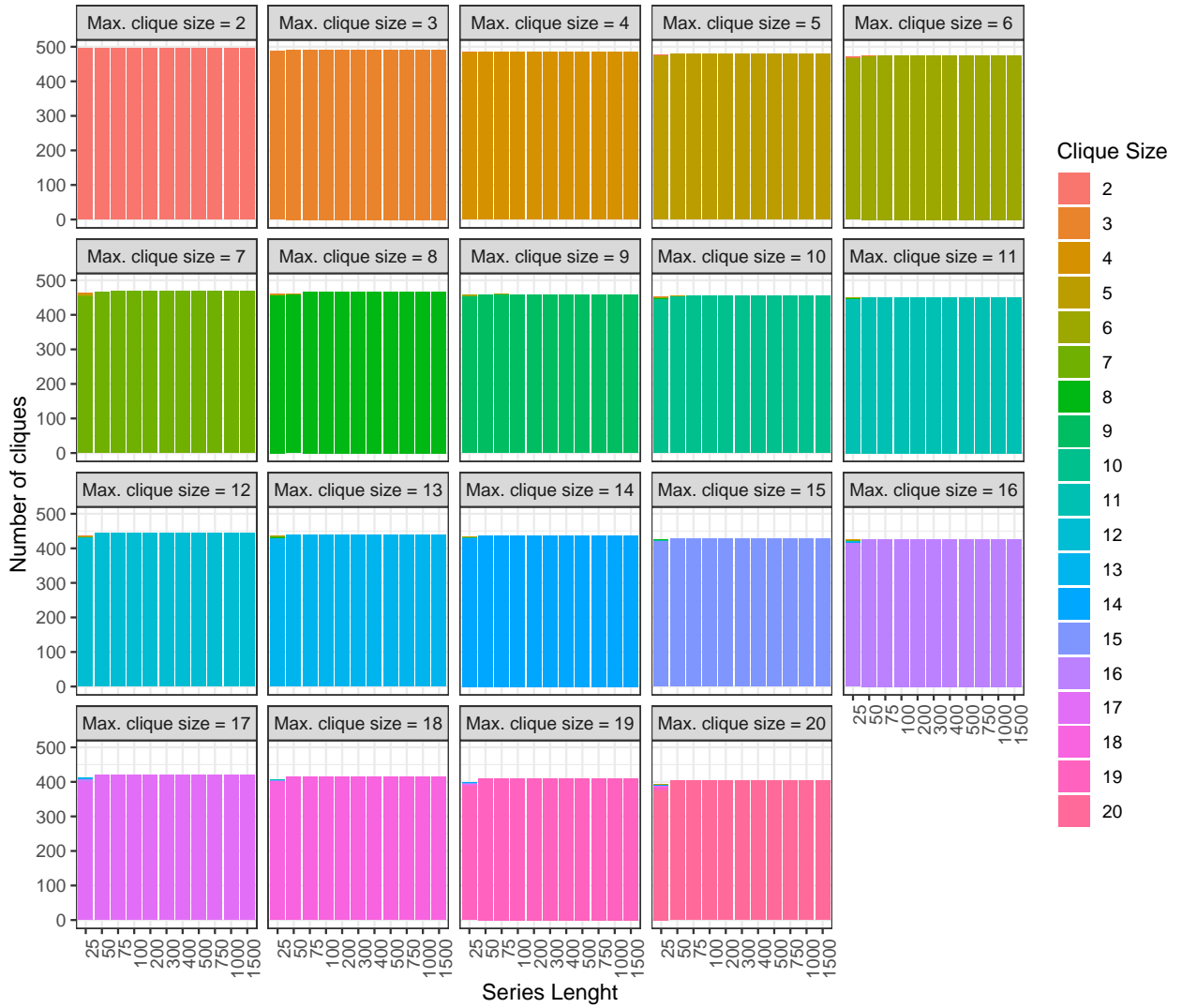


Figure 25: Composition of cliques from MFCF_VAR for synthetic data (factor model). The statistics is based on a total of 5 different training / validation sets per length of the time series.

8.3.4 REAL DATA

Performance measures are reported in Figures 26-30. We see from the inspection of Figures 26 and 27 that with real data the log-likelihood is comparable across all models, with slight better values for MFCF_FIX and MFCF_VAR for shorter time series. It is worth noting that, in the family of the MFCF algorithms, the two that use the clique tree shrinkage target described in Equation 19 (MFCF_FIX and MFCF_VAR) perform significantly better, for short time series, than the models with the same structure but the simpler identity matrix (MFCF_FIX_ID and MFCF_VAR_ID) as a shrinkage target. Table 9 shows that the penalty and shrinkage parameters decrease, as expected, with the length of the time series. Table 10 shows that from time series lengths above 500 the GLASSO produces matrices with a significantly higher number of parameters different from zero, including almost 50% of the total number of elements. The growth in performance for MFCF family of algorithms is in this case constrained by the maximum clique size. As Figure 28 shows the MFCF algorithms performs better in the approximation of the eigenvalues of the precision matrix, and slightly worse (Figure 29 in the representation of the eigenvalues of the inverse precision matrix. In this experiment, since we don't know the "true" correlation matrix we have used the maximum likelihood estimate of the correlation matrix over the full time series. Overall the results for this dataset demonstrate that MFCF_FIX and MFCF_VAR are the best performer. The analysis in Figure 30 showing the composition of the cliques of different sizes shows that the synthetic model closest to the real data is the factor model (see 8.3.3).

Series length	GLASSO XVAL	MFCF FIX	MFCF FIX ID	MFCF VAR	MFCF VAR ID	SHRINKAGE
25	0.21	0.81	0.57	0.80	0.54	0.67
50	0.15	0.73	0.47	0.70	0.47	0.63
75	0.12	0.62	0.35	0.61	0.36	0.55
100	0.12	0.56	0.31	0.54	0.33	0.54
200	0.12	0.43	0.26	0.44	0.26	0.44
300	0.10	0.32	0.20	0.34	0.18	0.39
400	0.08	0.28	0.17	0.28	0.17	0.34
500	0.07	0.25	0.15	0.24	0.15	0.30
750	0.03	0.18	0.12	0.19	0.13	0.24
1000	0.02	0.13	0.08	0.13	0.08	0.17
1500	0.01	0.11	0.07	0.11	0.07	0.14

Table 9: Mean penalty/shrinkage parameter by length of time series. The statistics is based on a total of 5 different training / validation sets per length of the time series.

Figure 30 shows that, excepting for the shortest time series, the MFCF_VAR algorithms almost always use the largest allowed clique size.

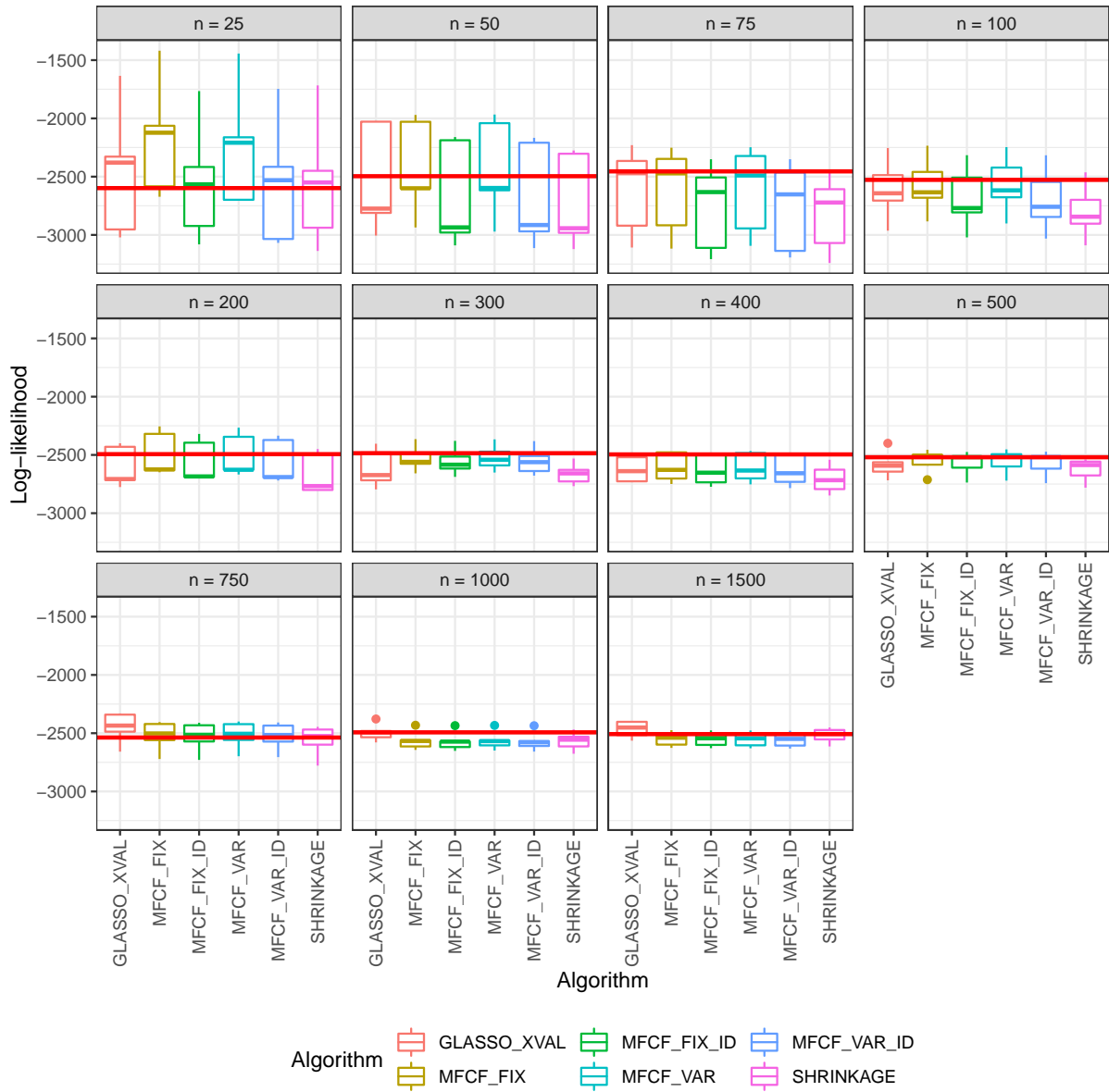


Figure 26: Log-likelihood of the algorithms on real data (stock returns) for different length of the series. The statistics is based on a total of 50 test sets (10 test sets for each of 5 different training / validation sets) per length of the time series.

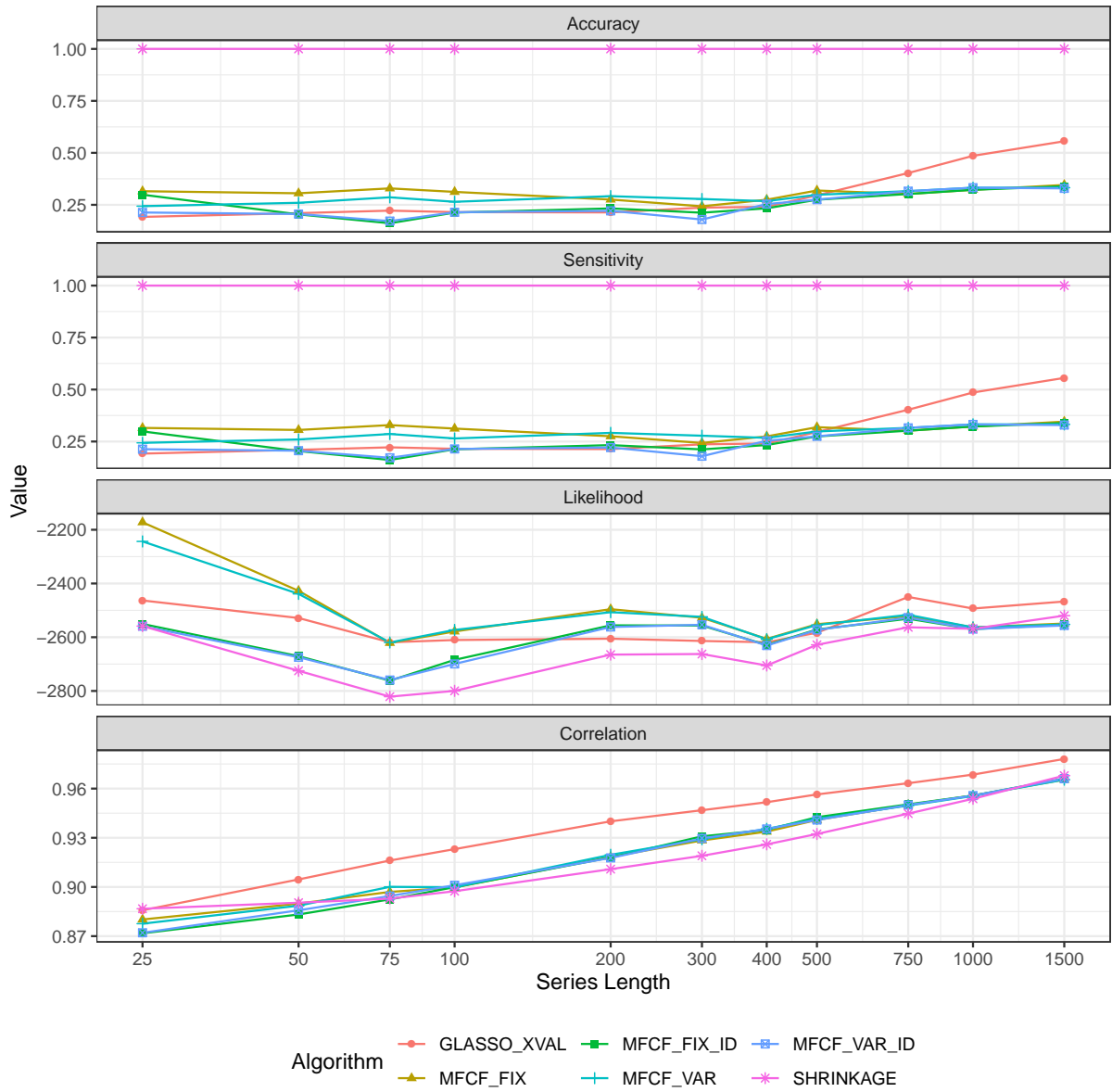


Figure 27: Performance of the algorithms on real data (stock returns) for different lengths of the series. The statistics is based on a total of 50 test sets (10 test sets for each of 5 different training / validation sets) per length of the time series.

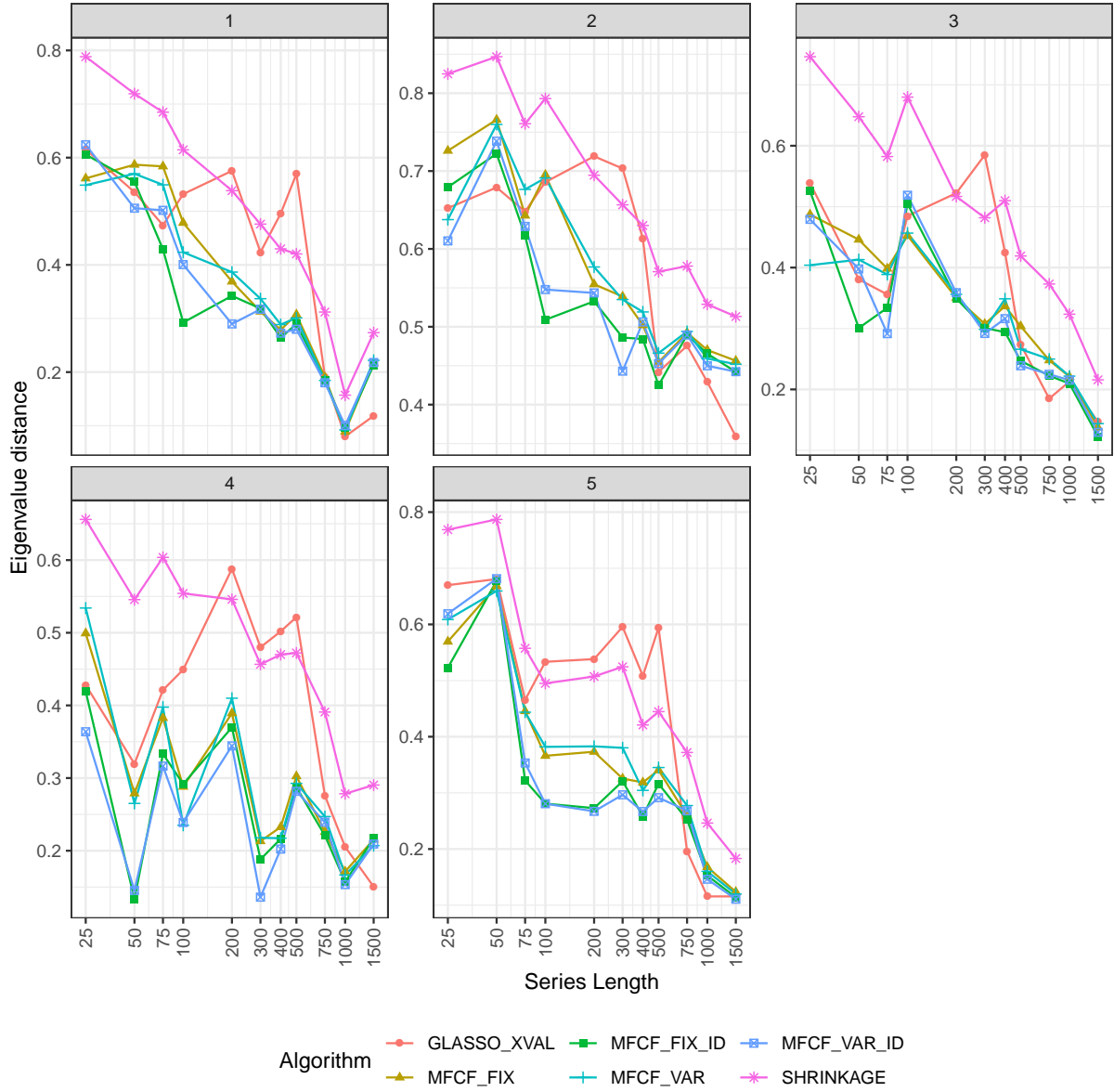


Figure 28: Eigenvalue distance for real data (stock returns) for 5 training sets. The five panels show the values at different time series lengths for 5 training / validation datasets.

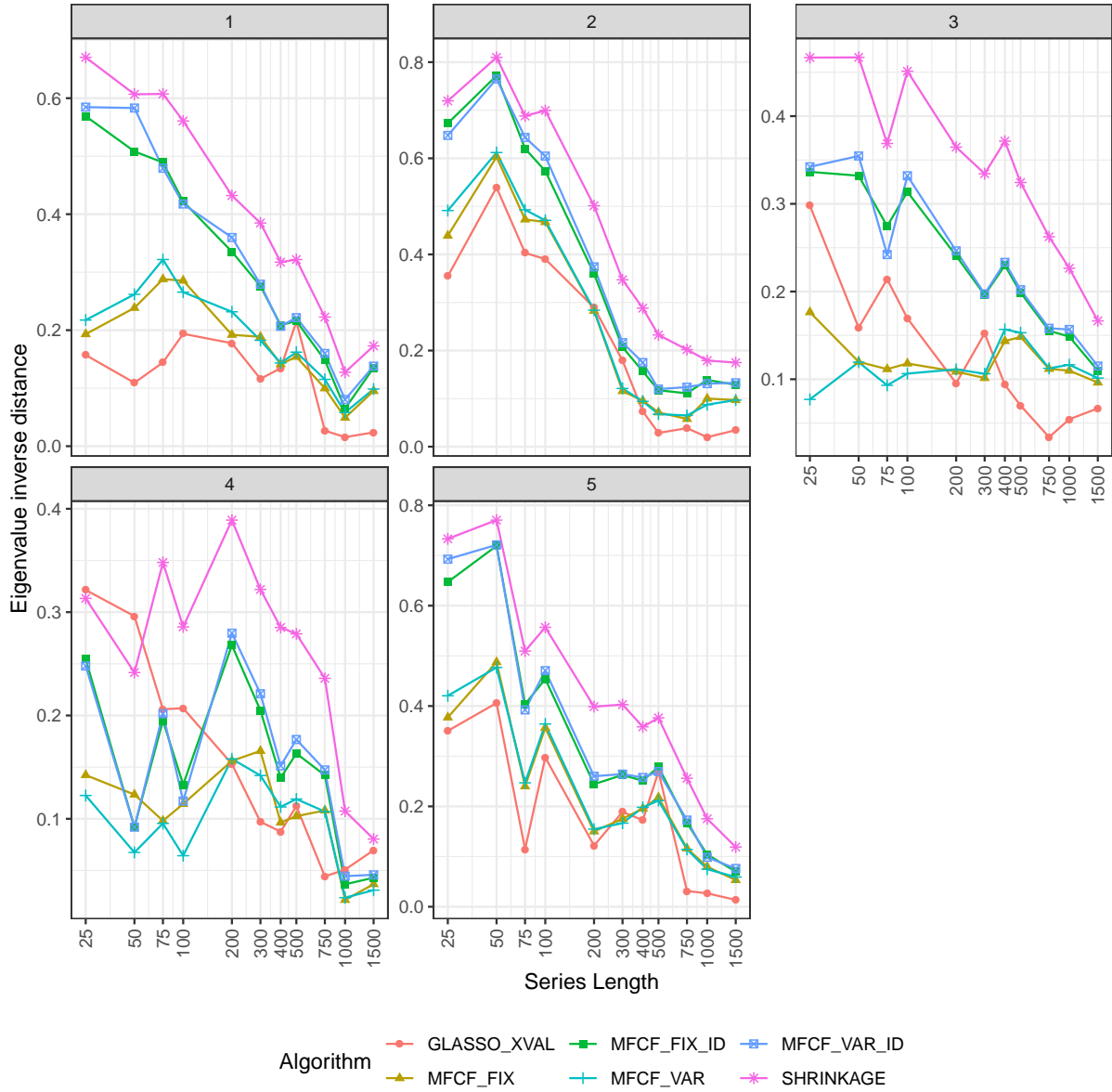


Figure 29: Inverse eigenvalue distance for real data (stock returns) for 5 training sets. The five panels show the values at different time series lengths for 5 training / validation datasets.

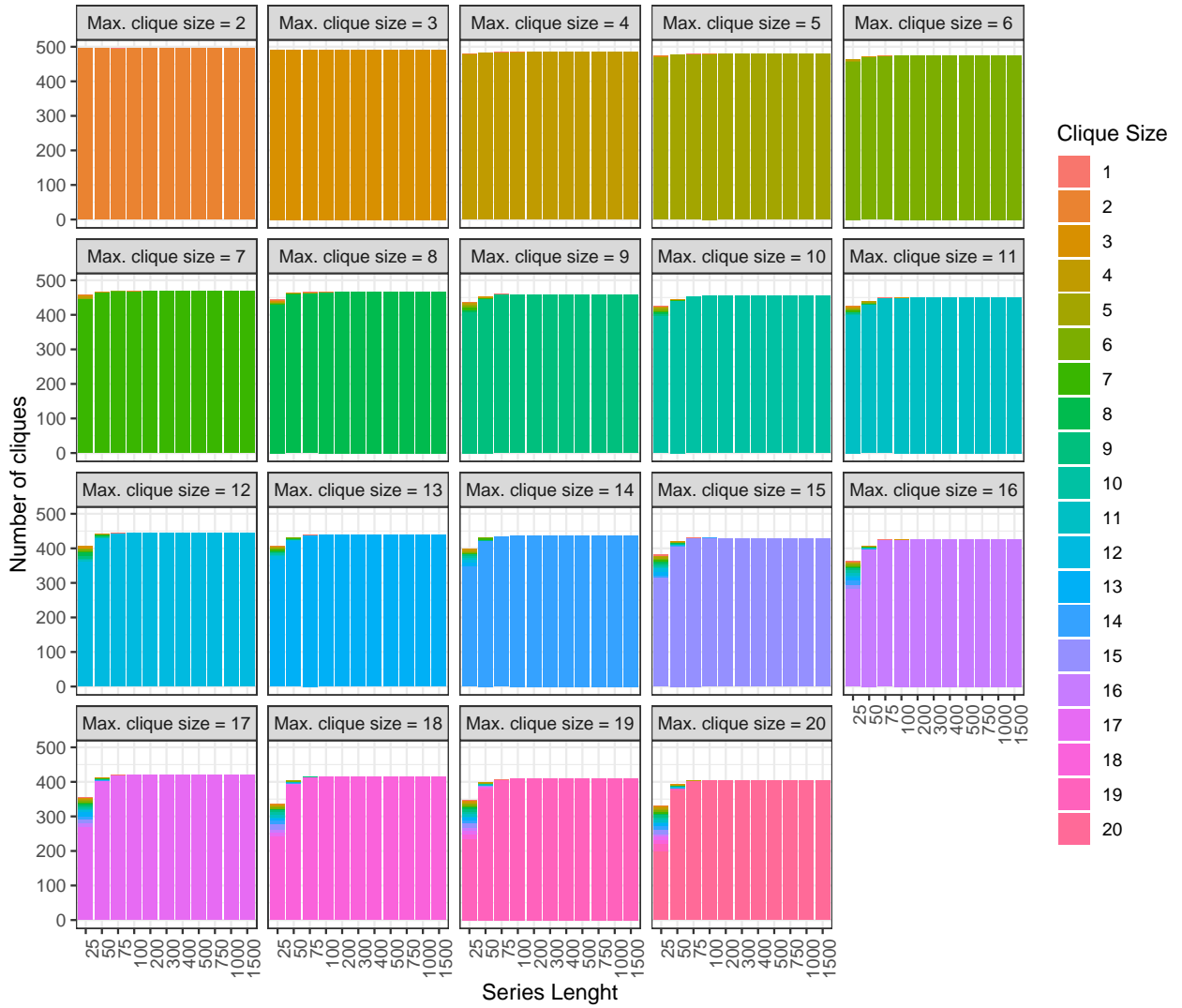


Figure 30: Composition of cliques from MFCF_VAR for real data (stock returns). The statistics is based on a total of 5 different training / validation sets per length of the time series.

Series length	GLASSO XVAL	MFCF FIX	MFCF FIX ID	MFCF VAR	MFCF VAR ID	SHRINKAGE
25	950	1561	1478	1206	1055	4950
50	1039	1512	1010	1286	1018	4950
75	1099	1628	798	1416	850	4950
100	1063	1545	1053	1310	1060	4950
200	1057	1363	1152	1443	1094	4950
300	1170	1202	1049	1375	888	4950
400	1191	1359	1154	1325	1255	4950
500	1464	1578	1358	1477	1360	4950
750	1994	1495	1495	1562	1562	4950
1000	2404	1595	1595	1645	1645	4950
1500	2752	1710	1677	1645	1629	4950

Table 10: Mean number of non-zero coefficient in the precision matrix by length of time series. The statistics is based on a total of 5 different training / validation sets per length of the time series.